MANUFACTURING PROCESSING AND PROPERTIES MANIPULATIONS OF THICK ADVANCED PERFORMANCE PEEK POLYMER AND COMPOSITES FOR BIOMEDICAL AND EXTREMELY HARSH ENVIRONMENTS

A Dissertation

by

RUAA YASEEN HAMMOUDI AL-MEZRAKCHI

Submitted to the Office of Graduate and Professional Studies of
Texas A&M University
in partial fulfillment of the requirements for the degree of

DOCTOR OF PHILOSOPHY

Chair of Committee,	Terry Creasy
Co-Chair of Committee,	Hung-Jue Sue
Committee Members,	Karl T. Hartwig
	Sivakumar Rathinam
Head of Department,	Andreas A. Polycarpou

May 2019

Major Subject: Mechanical Engineering

ABSTRACT

This study's aim is to investigate manipulating the compression molding manufacturing process to influence morphology and mechanical properties of thick wall and tall advanced performance thermoplastic polymers, as well as to highlight the mechanisms that cause property deterioration in those products. Two advanced performance polymer systems, neat poly(etheretherketone) (PEEK) and its composite (CF/PEEK), were considered as model systems to fundamentally understand structure-property relationships in thick wall advanced polymeric materials.

An instrumented compression molding setting with thermal control and 3D embedded thermocouples is designed and fabricated to produce thick polymer parts and investigate how altering processing procedures influences properties. A novel hybrid sealing method is invented to enhance compression molding quality and avoid leaking issues associated with this process.

The temperature distribution profiles throughout the compression molding and the bushing are collected during heating and cooling processes. The resultant temperature profiles are analyzed to further understand the compression molding process behavior, and thus adjust the processing procedure to enhance products morphology and properties.

Crystal structure formation is controlled via templating material manufacturing cooling process. The influence of holding temperature at the crystallization temperature while increasing the hold time is examined by characterizing samples throughout bushings processed using various strategies. Manipulating the cooling is expected to guide the polymer amorphous arrangement toward a uniform crystal structure and grow this structure equivalently throughout the thick cross-section and the extended length of the final product. Remarkable crystallinity improvement with

adequate consistency was achieved throughout thick wall and tall compression molded PEEK bushing that improved the compression molding product properties. Carbon fiber reinforcement's influence on crystal morphology and mechanical properties of thick products is addressed in this dissertation.

Different techniques and tests are used to investigate the bushings produced using different processing strategies such as dynamic scanning calorimetry (DSC), dynamic mechanical analysis (DMA), scanning electron microscopy (SEM), wide angle x-ray scattering (WAXS), polarized optical microscopy (POM), compression test, and 3-point bending test. Those techniques assisted in establishing correlation between the morphology modification and the material properties response.

Predictive numerical models are developed to simulate the compression molding heating process. Experimental validations provide beneficial tools to predict the heating time required for various thick compression molded materials. The predictive models established in this study can substitute building an expensive thermal control system and performing compression molding with embedded thermocouples to estimate material processing time. These models can provide a great assist for industrial applications.

This study highlights an intelligible processing procedure for developing thick compression molding bushing with consistent crystallinity and enhanced mechanical properties. The processing protocol introduced in this study acquired based on analyzing compression molding temperature profiles and studying the possibility of using different methods to control the process during the cooling stage to produce neat and composite polymers with better properties. The produced products can be used for many applications such as aerospace, biomedical, automotive, food processing, oil and gas industry, etc.

DEDICATION

*To my husband **Ahmed** for his consistent support, love, and motivation.*

*To my lovely children, **Noor** and **Ali**.*

*To my **parents, grandparents,** and **aunt** for their love and encouraging.*

Having you in my life truly a blessing.

ACKNOWLEDGEMENTS

I would like to express my sincerest gratitude to my committee chair Professor Terry Creasy, my committee co-chair Professor Hung-Jue Sue, and my committee members Professor Karl T. Hartwig and Professor Sivakumar Rathinam for their guidance and support throughout the course of this research.

I extend my deep appreciations and thanks to Dr. Tim Bremner, Vice President of Materials Technology at Hoerbiger Corporation of America, for his continuous assistance and guidance throughout the entire project period. I am indebted to the support provided by Dr. Bremner. Thanks also go to my friends and colleagues and the department faculty and staff for making my time at Texas A&M University a great experience.

I highly acknowledge the research funding support from Advancing Performance Polymers in Energy Applications (APPEAL) consortium through Polymer Technology Center (PTC) at Texas A&M University. I am grateful to Prof. Terry Creasy and Prof. Hung-Jue Sue, the director of the Polymer Technology Center, for their support and for giving me the opportunity to involve in the APPEAL consortium and present my research achievements in the semi-annual consortium review for four years respectively. I highly appreciate the support and the comments that I received from all industrial companies' representatives, who are leaders and experts in the polymer science field, during the semi-annual APPEAL consortium meetings. Their valuable discussions and comments assisted me to acquire more knowledge and critical thinking to solve realistic engineering problems, as well as helped in providing the right path for this research work. I would also like to thank Hoerbiger Corporation of America for providing the materials required for the experiments.

During my study period, I was very fortunate to get the opportunity to involve in several interdisciplinary research projects with multiple departments as well as interact and exchange ideas with a number of professors from different fields, such as Aerospace Engineering, Architecture, Material Science & Engineering, and Mechanical Engineering. Thus, I would like to personally thank Prof. Ergun Akleman in Departments of Visualization & Computer Science and Engineering, Prof. Tahir Cagin in Material Science & Engineering Department, Prof. Zofia Rybkowski in Department of Construction Science - Center for Health Systems & Design, and Prof. Negar Kalantar in College of Architecture for giving me the opportunity to lead a graduate and undergraduate research group of a multidisciplinary research project.

I would also like to thank Prof. Christopher Quick in Biomedical Engineering, Physiology, & Pharmacology and the director of Aggie Research Leadership Program to give me the opportunity to practice my leadership abilities by leading a group of undergraduate students from different fields through Aggie Research Leadership Program.

I was very fortunate to serve as a Co-Director of the CIRTL Academy of Future Faculty program for two years under the guidance of Dr. Ra'sheedah Richardson, Assistant Director of Center for Teaching Excellence. I am thankful to the support provided by Dr. Ra'sheedah Richardson.

Thanks to my parents, grandparents, and aunt for inspiring me in many ways but most importantly raise me and taught me to be myself. It is because of their love and care, I had the motivation and inspiration to set and reach the goals in my life.

Finally, I don't know how to express my deep grateful to my husband and children for their patience and love when I needed it the most. Without their significant love and support, the scope of this dissertation would not have been possible. You are the sunshine and brightness of my life.

CONTRIBUTORS AND FUNDING SOURSES

This work was supervised by a dissertation committee with these members:

- Dr. Terry Creasy, Associate Professor [Chair]
- Dr. Hung-Jue Sue, Professor [Co-Chair]
- Dr. Karl T. Hartwig, Professor [Member]
- Dr. Sivakumar Rathinam, Associate Professor [Member]

All the work conducted for this dissertation was completed independently by the student. This work was partially supported by the research funding from Advancing Performance Polymers in Energy Applications (APPEAL) consortium through Polymer Technology Center (PTC) at Texas A&M University.

NOMENCLATURE

AFM	Atomic Force Microscopy
APPEAL	Advancing Performance Polymers in Energy AppLications
b	Width at Specimen Midpoint
BC	Boundary Conditions
CF	Carbon Fiber
CNC	Computer Numerical Control
cp	Specific heat at constant pressure
d	Depth at Specimen Midpoint
D	Deflection at Specimen Midpoint
DSC	Differential Scanning Calorimetry
DMA	Dynamic Mechanical Analysis
E	Modulus of Elasticity in Compression
E_b	Modulus of Elasticity in Bending
FEM	Finite Element Method
g	Acceleration by Gravity
G’	Storage Modulus
G’’	Loss Modulus
Gr	Grashof Number
H_c	Crystallization Enthalpy
H_f	Enthalpy of Fusion for 100% Crystallized Polymer
ID	Inner Diameter

IR	Infrared Spectroscopy
k	Thermal Conductivity
L	Surface Length
m	Slope of Initial Straight-Line Portion of Load - Deflection Curve
Nu	Nusselt Number
OD	Outer Diameter
P	Load at specimen midpoint.
PAEK	PolyArylEtherKetone
PEEK	PolyEtherEtherKetone
POM	Polarized Optical Microscopy
Pr	Prandtl Number
PTFE	PolyTetraFluoroEthylene
Ra	Reynold Number
SEM	Scanning Electron Microscopy
TAMU	Texas A&M University
T	Temperature
Td	Time Delay
T_f	Film Temperature
Tg	Glass Transition Temperature
Tc	Crystallinity Temperature
TC(s)	Thermocouple(s)
Tm	Melting Temperature
WAXS	Wide Angle X-ray Scattering

ρ	Density
μ	Air Viscosity
β	Expansion Coefficient

TABLE OF CONTENTS

Page

ABSTRACT ii

DEDICATION iv

ACKNOWLEDGEMENTS v

CONTRIBUTORS AND FUNDING SOURSES vii

NOMENCLATURE viii

TABLE OF CONTENTS xi

LIST OF FIGURES xiv

LIST OF TABLES xix

1 INTRODUCTION 1

1.1 Background 1

1.2 Objectives and Significance 2

1.3 Layout of the Dissertation 6

2 LITERATURE REVIEW 8

2.1 Overview 8

2.2 Advanced Performance Polymer PAEK Structure 8

2.3 Mechanical and Thermal Properties 9

2.3.1 Effect of Stereoisomers and Molecular Weight 11

2.3.2 Effect of Processing Conditions 13

2.3.3 Effects of Post Processing Treatment 18

2.3.4 Fillings and Additives 21

2.4 Processing Methods of Advanced Performance Polymers 23

2.5 Concluding Remarks 24

3 DEVELOPMENT OF COMPRESSION MOLDING EQUIPMENT SUPPORTED WITH THERMAL CONTROL SYSTEM 25

3.1 Design and Build Compression Molding with Embedded Thermocouples 25

3.2 Special Components Fabrication for Lab Compression Mold Setting 27

3.3 Gasket Processing and Novel Hybrid Sealing Method 30

3.4 Thermal Control System Setting 33

4 COMPRESSION MOLDING OPERATING PROCEDURE AND PROCESSING STRATEGIES 37

4.1 Complete System Setting and Thermocouples Insertion 37

4.2 Compression Molding Processing Procedure 39

4.3 Processing Strategies for Producing Compression Molded Bushings 41

5 MATERIALS AND METHODOLOGIES 43

5.1 Materials and Bushing Production 43

5.2 Slicing Bushings and Preparing Specimens 44

5.3 Characterization 47

5.3.1 Differential Scanning Calorimetry (DSC) 47

5.3.2 Compression Test 48

5.3.3 Flexural (Three-Point Bend) Test 48

5.3.4 Dynamic Mechanical Analysis (DMA) 49

5.3.5 Wide Angle X-ray Scattering (WAXS) 50

5.3.6 Scanning Electron Microscopy (SEM) 50

5.3.7 Polarized Optical Microscopy (POM) 51

6 EXPERIMENTAL RESULTS AND DISCUSSION 52

6.1 Holding Temperature of Compression Molding Process 52

6.2 Compression Molding Temperature Profiles of Neat PEEK and CF/PEEK 53

6.3 Process Melting Time and Holding Time at Crystallization Temperature 59

6.4 Thermal Analysis 62

6.4.1 Neat PEEK 62
6.4.2 PEEK Filled Carbon Fiber Composite (CF/PEEK) 69
6.5 Polymer Morphology Distribution 74
6.6 Crystal Microstructure 78
6.10 Dynamic Mechanical Behavior 86
6.7 Compression Behavior 98
6.7.1 Neat PEEK Behavior at Room Temperature and Elevated Temperature 98
6.7.2 Crystallinity and Morphology Influences on Modulus 106
6.7.3 CF/PEEK Behavior at Room Temperature and Elevated Temperature 111
6.8 Flexural Behavior 114
6.9 Mann-Whitney analysis 117
7 COMPUTATIONAL ANALYSIS METHODS 119
7.1 Developing Finite Element thermal models 119
7.2 Parametric Study of Numerical Simulation 123
8 COMPUTATIONAL ANALYSIS RESULTS AND DISCUSSION 125
8.1 Time Required for Compression Molding Heating Process 125
8.2 Influence of Processing and Mold Manufacturing Imperfections (Tooling Quality) 128
9 SUMMARY AND FUTURE WORK 132
9.1 Summary of Research 132
9.2 Concluding Remarks and Future Works 138
REFERENCES 140

LIST OF FIGURES

Page

Figure 2.1. Chemical structure composition of PAEK: (left) PEEK and (right) PEK (adopted [17]). 9

Figure 2.2. Storage modulus of PAEKs as function of molecular weight (Redrawn from reference [36]). 12

Figure 2.3. Effect of quench rate on spherulite size and degree of crystallinity (Redrawn from reference [47]). 14

Figure 2.4. (a) Hold Temperature for 10 min. (b) Hold Temperature at crystallization for different times (Redrawn from reference [50]). 16

Figure 2.5. Effect of holding temperature at different values for 1h and 24h (a) on crystallinity and (b) Young's modulus (Redrawn from reference [62]). 20

Figure 3.1. schematic of compression molding experimental setup. 26

Figure 3.2. (a) Shell, (b) mandrel, and (c) end-rings of compression molding with thermocouples and compression fitting ports. 27

Figure 3.3. Special components added to Compression molding lab setting. (a) Glass-mica ceramic insulation base machined using lab CNC. (b) Base heater lab manufacturing procedure. 29

Figure 3.4. Producing Steel/PTFE composite gaskets. (a) Process gaskets using compression molding. (b) Slice and machine gaskets using lathe. (c) Drill holes for thermocouples to pass through the gasket to top and bottom polymer surface. 30

Figure 3.5. Schematic of hybrid sealing method for compression molding process. 32

Figure 3.6. (a) Schematic and (b) lab heating zones setup of the compression molding system. 34

Figure 3.7. (a) Schematic and (b) optical image of control system setting used to monitor the compression molding processing. 36

Figure 4.1. Instrumented compression molding system showing the system overview on the left and the system with insulation prior to an experiment on the right. 37

Figure 4.2. Schematic and lab thermocouples setup of the compression molding system. 38

Figure 4.3. Schematic of pressure and temperature profiles during compression molding processing procedure. 40

Figure 4.4. Schematic drawing of stripping the bushing from the compression molding tools. 40

Figure 4.5. Process control strategies flowchart of compression molding experiments. 42

Figure 5.1. Processing steps to produce thick and tall CF/PEEK composite products. 43

Figure 5.2. Optical images of slicing compression molded (a) neat PEEK bushing and (b) CF/PEEK bushing using lathe. 45

Figure 5.3. Schematic of samples positions within the sliced pieces of compression molding bushing. (a) PEEK bushing (b) DSC samples (c) Flexural samples (d) Compression samples. 46

Figure 6.1. Temperature profiles of (a) shell and (b) mandrel during processing compression molded neat PEEK bushings. 55

Figure 6.2. (a) Temperature profiles of neat PEEK polymer during compression molding process. Thermocouple positions along bushing cross-section at (b) mid-height and (c) top-height. 56

Figure 6.3. Temperature profiles of CF/PEEK polymer composites during compression molding process. 58

Figure 6.4. Temperature profiles of neat PEEK middle height bushing during (a) heating process and (b) cooling process of compression molding. 60

Figure 6.5. Temperature profiles of CF/PEEK middle height bushing during (a) heating process and (b) cooling process of compression molding. 61

Figure 6.6. Crystallinity distributions of neat PEEK bushings along bushing radius for different processing strategies. (a) strategy A and (b) strategies B, C, and D. 63

Figure 6.7. Neat PEEK bushings crystallinity distributions throughout bushing length for different processing strategies. (a) strategy A and (b) strategies B, C, and D. 64

Figure 6.8. The influence of changing time of holding temperature at crystallization during compression molding process on average crystallinity and variability of thick wall neat PEEK bushings. 66

Figure 6.9. DSC curves of neat PEEK bushing top section processed using (a) traditional free convection cooling method vs. (b) holding temperature at crystallization for 15 hours. 68

Figure 6.10. Crystallinity distributions of CF/PEEK composite bushings along (a) bushing radius and (b) bushing height for different processing strategies. ID: bushing inner diameter, MD: bushing middle diameter, OD: bushing outer diameter. 71

Figure 6.11. Crystallinity distributions of neat PEEK vs. CF/PEEK composite bushings for (a) free convection cooling process and (b) holding temperature at crystallization for 15 hours. ID: bushing inner diameter, MD: bushing middle diameter, OD: bushing outer diameter. 72

Figure 6.12. WAXS patterns throughout neat PEEK bushing length for (a) traditional free convection cooling method (b) holding temperature at crystallization for 15 hours. TM: Top height and Middle diameter of bushing, MM: Middle height and Middle diameter of bushing, BM: Bottom height and Middle diameter of bushing. 75

Figure 6.13. Neat PEEK WAXD patterns at bushing (a) top height, (b) middle height, (c) bottom height of different processing strategies. 77

Figure 6.14. Crystal morphology distributions throughout neat PEEK bushings processed using traditional free convection cooling method without holding temperature at crystallization. 79

Figure 6.15. Crystal morphology distributions throughout neat PEEK bushings processed with holding temperature at crystallization for 15 hours. 80

Figure 6.16. SEM images of CF/PEEK composites before compression molding process. 81

Figure 6.17. Polarized Optical Microscopy (POM) images of CF/PEEK composites after compression molding process. 82

Figure 6.18. CF/PEEK composite microstructure distributions throughout bushings processed using traditional free convection cooling method without holding temperature at crystallization. (a) Top bushing height. (b) Middle bushing height. (c) Bottom Bushing height. 83

Figure 6.19. CF/PEEK composite microstructure distributions throughout bushings processed with holding temperature at crystallization for 15 hours. (a) Top bushing height. (b) Middle bushing height. (c) Bottom Bushing height. 84

Figure 6.20. Temperature dependence of (a) storage moduli and (b) tan δ throughout PEEK bushing processed using traditional free convection cooling without holding temperature at crystallization. 88

Figure 6.21. Temperature dependence of (a) storage moduli and (b) tan δ throughout PEEK bushing processed holding temperature at crystallization (309 °C) for 4 hours. 89

Figure 6.22. Temperature dependence of (a) storage moduli and (b) tan δ throughout PEEK bushing processed holding temperature at crystallization (309 °C) for 15 hours. 90

Figure 6.23. Temperature dependence of (a) storage moduli and (b) tan δ for top height PEEK bushing processed using various strategies. 95

Figure 6.24. Temperature dependence of (a) storage moduli and (b) tan δ for middle height PEEK bushing processed using various strategies. 96

Figure 6.25. Temperature dependence of (a) storage moduli and (b) tan δ for bottom height PEEK bushing processed using various strategies. 97

Figure 6.26. Compression Modulus of Elasticity at room temperature of neat PEEK bushings for different processing strategies. (a) strategy A and (b) strategies B, C, and D throughout bushing radius. 99

Figure 6.27. Neat PEEK compression Modulus of Elasticity at room temperature throughout bushing length for different processing strategies. (a) strategy A and (b) strategies B, C, and D. 101

Figure 6.28. The influence of changing time of the hold temperature at crystallization during compression molding process on average bending modulus and variability of thick wall bushings at room temperature. 102

Figure 6.29. Neat PEEK compression Modulus of Elasticity at 225 ºC elevated temperature throughout (a) bushing radius and (b) bushing length for different processing strategies. 104

Figure 6.30. The influence of changing time of the hold temperature at crystallization during compression molding process on average bending modulus and variability of thick wall bushings at 225°C elevated temperature. 105

Figure 6.31. PEEK morphology images at the location of compression Modulus of Elasticity at 225 ºC elevated temperature along (a) bushing thickness and (b) bushing height for traditional free convection cooling process. 108

Figure 6.32. PEEK morphology images at the location of compression Modulus of Elasticity at 225 ºC elevated temperature along (a) bushing thickness and (b) bushing height for the process of hold temperature at crystallization (309 °C) for 15 hours. 109

Figure 6.33. Neat PEEK storage modulus and compression Modulus of Elasticity vs. crystallinity at middle bushing height for various processing strategies 110

Figure 6.34. CF/PEEK compression Modulus of Elasticity found at (a) room temperature and (b) 225ºC elevated temperature throughout bushing length for different processing strategies. 113

Figure 6.35. Modulus of Elasticity in bending found at room temperature throughout PEEK bushing length for different processing strategies 114

Figure 6.36. Modulus of Elasticity in bending found at 225ºC elevated temperature throughout PEEK bushing length for different processing strategies. 115

Figure 6.37. The influence of changing time of hold temperature at crystallization during compression molding process on average bending modulus and variability of thick wall and tall bushings. 116

Figure 7.1. Finite Element Analysis model for bushing compression molding system. 120

Figure 8.1. Temperature profile locations on numerical model of compression molding system. 126

Figure 8.2. Comparing experimental temperature profiles with numerical FEA model profiles throughout (a) top, (b) middle, and (c) bottom bushing heights during compression molding process. 127

Figure 8.3. Temperature distributions after 5 hours for different cases of numerical compression molding models. (a) Heating outer shell to 400 ºC. (b-e) Heating outer shell and inner mandrel to 400 ºC with (b) Top convection surface, (c) Top insulated surface, (d) 1.27 mm gap between end-rings and shell, (e) extended gasket between end-rings and shell. (f) Heating outer shell and mold top surface with sold mandrel (simulate convection oven)..... 131

LIST OF TABLES

Page

Table 2.1. Molecular weight (Mw) and crystallinity of PEEK in Figure 2. (Redrawn from references [36, 37]). 12

Table 2.2. PEEK crystallinity before and after thermal treatment by holding temperature at 420C for 30min in dry air (Redrawn from references [36, 37]). 18

Table 6.1. Melting temperatures, crystallization temperatures, and crystallinity% of pre-processed CF/PEEK composites and neat PEEK at different heating/cooling rates..... 53

Table 6.2. Average and variability of PEEK compression Modulus of Elasticity at room temperature and 225 ºC elevated temperature for bushings processed using different strategies. 106

Table 6.3. Average and variability of Modulus of Elasticity in bending found from 3-point-bend tests at 225 ºC elevated temperature for bushings processed using different strategies. 117

Table 6.4. Mann-Whitney outcomes of Modulus of Elasticity at room temperature (RM) and 225 ºC elevated temperature found from flexural tests and compression tests for bushings processed using strategy A and strategy D. “NO” means Mann-Whitney indicates no changes in modulus, “YES” means Mann-Whitney shows significant changes in modulus. 118

Table 7.1. Finite Element Analysis model for bushing compression molding system. 121

Table 7.2. The conditions of different Finite Element Analysis case studies of compression molding system. 124

1 INTRODUCTION

1.1 Background

In recent decades, polyayrletherketones (PAEKs) have become a major interest for academic research and industrial applications because of their outstanding mechanical, thermal, and chemical properties. The chemical composition of these polymers gives them special properties such as high temperature stability, high strength, low density, high melting temperatures, and resistance to chemical and radiation damage. These properties allow them to support many industry applications, especially in aerospace because their higher strength to weight ratios enhance fuel efficiency, performance, and maneuverability.

Despite PAEK's substantial properties and applications, their typical crystal structure inhomogeneity and low crystallinity have led to an apparent plateau in the final product properties. These low crystallinity and inhomogeneity are length and cross-section scale dependent and are related to the heat diffusion gradient through the cross-section and the product's length during the cooling stage.

At the manufacturing level, compression molding is usually used to produce thick PAEK polymer parts. Although those materials are considered high performance polymers, understanding their manufacturing process parameters effects on the final product properties is at primitive levels. PAEK polymers are insulating thermoplastic materials that often suffer from high temperature gradient during processing because they naturally acquire and diffuse heat slowly. Cooling rate influences polymer crystal structure morphology, where relatively fast cooling produces fine crystals while slow cooling produces large crystals. Making thick products from this material using free convection cooling will trigger the crystal structure inhomogeneity because the surfaces will

be first and fastest layers to cool much faster than the material deep within the cross-section. The same reasoning applies along the product's length, where increasing thick part length leads to faster cooling at the ends and slow cooling at mid height. As material thickness and length get larger, there is a higher temperature gradient that significantly compromises the crystal distribution. This crystal inhomogeneity could negatively impact the mechanical properties. On the other hand, the part produced from fast cooling usually has low crystallinity because there is not enough time for the polymer to build its crystal structure from the amorphous region. Moreover, fast cooling builds up huge internal stresses in the final product that could be expressed in structure inhomogeneity throughout the final part.

Recent studies suggest incorporating some filling, such as carbon fibers, to alter the crystal structure in the final product. Despite the cost increase coming from adding fillers, carbon fibers can play a significant role nucleating crystals that speed the crystallization process and increase the final crystallinity percentage in most polymers. However, other studies highlighted reinforcements providing a negative influence on composite crystallinity and properties depending on the filler and matrix in addition to other factors. Moreover, it is not clear how those additives behave in thick high-performance polymer products and when they are accompanied with manipulating processing parameters that suggest further investigations to analyze those effects and find new methods to manipulate them. Thus, it is crucial to understand how additives affect the crystal structure, morphology, and mechanical properties in the final product.

1.2 Objectives and Significance

This dissertation aims to explain structural behavior in advance performance polymers and their composites in order to develop improved materials with enhance properties and longer

lifetimes. The extended research objective is to fundamentally understand the physical relationships that manipulating the compression molding process might impart on the mechanical properties and the crystal structure in thick PAEK polymer bushings with and without fillings. This study unravels the processing procedures and the parameters that strongly influence the advanced polymer properties. Moreover, the dissertation target is set to maintain uniform crystallinity and mechanical properties throughout thick compression molded components as well as maximize those components. Another aspect is to develop a validated model to replace expensive experiments required to establish optimum procedures for processing advanced performance polymer products.

Controlling the cooling process is primarily intended to enhance crystal structure uniformity by holding the temperature at crystallization to allow the polymer to build its crystal structure uniformly throughout the bushing length and thickness. In addition, sufficient time will be provided for the polymer to reach maximum crystallinity that can be produced as it passes through its crystallization zone. As a result, the interest is in uniform, highly crystalline structure as well as enhanced mechanical properties. Acquiring the final target needed four steps:

1. Design and build a special compression mold with embedded thermocouples and develop a thermal control system to monitor and manipulate the polymer process as well as collect data during heating and cooling. A good heating system needs to be designed and selected carefully to assist the heat distribution applied on the compression molding.
2. Produce compression molded PEEK bushing (neat and composite) with controlled thermal history and analyze the temperature profiles during heating and cooling to further understand this process and develop it.

3. Investigate the effect that changing the processing parameters during cooling have on morphology, crystallinity, and mechanical properties (at room temperature and elevated temperature up to 225 °C and 300 °C) in neat and composite PEEK products.
4. Develop experimentally validated Finite Element model for thick compression molding system with the ability to adjust basic model characteristics in the molded polymer to estimate the time required for heating.

A thermal control compression molding system with embedded thermocouples was designed and built, in Approach 1, as well as suitable heating elements and effective controlling methods were identified for this mold. Then, the system was used to produce thick bushing with internal thermal history, through Approach 2. The temperature changes during compression molding were recorded via data acquisition system. Analyzing the thick, compression molded bushing's temperature profile helped to further explain process effects and guide adjusting the cooling procedure to enhance the final product. The adjustment was focused on holding the temperature at polymer crystallization point until it become stable everywhere through the bushing. Then the effect that increasing the temperature holding time beyond the stabilization period has was evaluated. Basically, four processing strategies were used to produce the bushings. In the first strategy, called free convection cooling, the bushing was heated above melting point then convection cooling to room temperature was allowed. This strategy is widely used in industry. The second strategy focused on modifying cooling through hold temperature at crystallization and wait until it becomes stable throughout the polymer then allowed convection cooling to room temperature. The third and fourth strategies followed the same procedure used in strategy two with additional hold time added before cooling to investigate the effect that increasing hold time has on

the final product. Those strategies were used to produce neat and composite PEEK bushings. Properties including crystallinity and mechanical properties were explored in Approach 3. Bushing properties produced from all four strategies were evaluated and compared to understand the effect that tuning the cooling step has on thick, high performance polymers. Moreover, the effect that additives have in the polymer were investigated to realize how manipulating cooling could affect the final product and what property was affected mostly. On the other hand, predictive models were developed in Approach 4 to acquire insights on the time required for heating as well as the instant temperature profile in compression molding. This model can substitute the experiments required to estimate the system heating time as the molded polymer properties change. This can set a foundation for expanding compression molding for different, thick high-performance polymers.

The main premise for this research is that controlled cooling thick high performance polymers can induce uniform crystal structure throughout the bulk bushing as well as improve the bushing's properties and crystallinity to enhance performance and reduce cracks that happen when extracting the bushing from the mold or while slicing the bushings into wafers.

This research study is unique in its focus on producing consistent and enhanced thermal and mechanical properties throughout thick wall and tall advanced performance polymers parts that are used for high temperature operating conditions and extremely harsh environments. It is highly expected for this work to contribute significantly to fundamental understanding of an advanced performance polymer's structure-property relationship. It also provides new information and guidance to industry that can bring tremendous impact to high performance applications in aerospace, oil and gas industry, and biomedical applications.

1.3 Layout of the Dissertation

Chapter II presents a brief literature review regarding advanced performance polymer structure-property relationships. The effects that processing conditions, fillings and additives, and post processing treatments have on the final product properties are also presented in that chapter. The current processing methods used to produce high performance polymer parts and the issues associated with those methods are highlighted.

Chapter III introduces the design and the fabrication of compression molding equipment instrumented with embedded thermocouples and driven with an advanced thermal control system. A novel hybrid sealing method and gasket processing procedure are explained in details. The compression molding operating procedure and processing strategies are presented in chapter IV. The procedures for slicing the bushings and preparing test samples are described in Chapter V. Methodologies and characterization used in the research are included in this chapter as well. Chapter VI investigated the compression molding temperature profiles obtained from neat PEEK and CF reinforced PEEK to show the minimum time required for the system to reach steady state and to determine the minimum time required for holding the temperature at crystallization to obtain a steady state temperature distribution. CF influences on changing the process behavior and temperature profiles are discussed in this chapter. Chapter VI focused on gaining fundamental insight into PEEK and CF/PEEK compression and flexure behaviors at room and elevated temperature. Moreover, chapter VI explores microstructural mechanisms associated with the remarkable increase detected in modulus of PEEK polymer at different conditions and the reasons behind the absence of this behavior by involving CF in the PEEK matrix.

Computational models through Finite Element Analysis method are developed in chapter VII to simulate thermal behavior during compression molding and relevant temperature profiles.

Thus, the validated models can substitute the expensive experimental procedures that used to extract the temperature profiles for future applications. Chapter VIII discusses computational analysis outcomes from the numerical models. The time required for compression molding heating is found and compared with the experimental findings to validate the analytical models. In addition, chapter VIII traced outside parameters that may impact the process and observed the optimum heating methodologies that can be used to enhance the process. Thus, processing parameter and mold imperfections influences on the thermal profile throughout the compression mold are discussed in this chapter.

Chapter IX presents a detailed summary and conclusions as well as future research suggestions are provided. Finally, the references citation is documented at the end of this dissertation.

2 LITERATURE REVIEW

2.1 Overview

Polyaryletherketones PAEK is a thermoplastic family used in many different industries because its mechanical, thermal, and chemical properties are superior. PAEK, specifically polyetheretherketone PEEK type, and its composites have higher strength to weight ratios than most conventional metals, epoxy composites, Al–Cu and Al–Li alloys. High strength-to-weight ratio makes PAEKs suitable choices in aerospace applications [1-4]. This high strength to weight ratio also makes PAEK polymers ideal for use in turbine blades and other aircraft parts [5, 6]. Because they tolerate high temperature and pressure, PAEK polymers have found much use in different energy applications such as flywheel [7], centrifugal compressors and steam turbine seals [8], ultra-high vacuum (UHV) [9], bearings [10], shape memory alloy wire coatings [11], and thermal spray coating [12]. Their high strength, high melting points, and corrosion resistance make them good candidates for use in high stress drilling areas and other harsh environments. PAEKs are also being used in the biomedical industry to make implants for hips, spinal, orthopedic, knees, and other medical devices [13-16].

2.2 Advanced Performance Polymer PAEK Structure

Increasing PAEKs use in industry must be associated with acquiring more information about their properties. These properties are determined individual polymer compositions. PAEK polymers contain repeating strings of monomers with ketone and ether groups as backbone. Altering these groups creates different polymer compositions with unique mechanical properties [17], where ether groups/ketone groups ratio added to benzene rings has a big influence on the

polymer's properties. Adding ketone groups to polymer structure creates a more rigid chain. This rigidity causes an increase in glass transition temperature and a decrease in polymer crystallinity [18]. To this end, PAEK chemical structure can be modified to accommodate different applications and fit desired properties; this is considered a key contribution to PAEKs diversity. Different polymers within PAEK class can be produced such as PEEK, PEKK, PEK, PEKEKK, etc [19]. Poly (etheretherketone) PEEK is among the most commonly used polymers. A sketch showing the PEEK's monomer backbone appears in **Figure 2.1** [17].

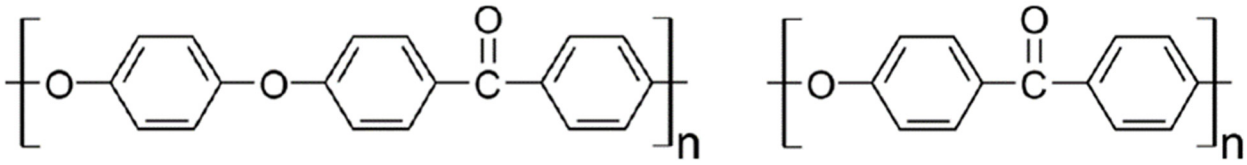

Figure 2.1. Chemical structure composition of PAEK: (left) PEEK and (right) PEK (adopted [17]).

2.3 Mechanical and Thermal Properties

PAEK polymers in general, and PEEK in specific, are gaining a huge attention as thermoplastics because their mechanical and thermal properties are attractive. PAEK compression properties are usually higher than its properties in tension. For example, PEEK compression yield limit is 30 – 40 % higher than tension limit [13, 20, 21]. Therefore, this advanced polymer is considered beneficial for ultra-high compression loading applications [1, 3, 4, 9, 20, 22] because of its outstanding compression properties at high temperatures and in harsh environments.

Those mechanical and thermal properties are highly attributed to crystallinity percentage and crystal structure morphology. Several approaches have been adopted to investigate the crystal

structure distributions and mechanical properties in thermoplastic polymers such as tension, compression, flexure, impact, fracture toughness, Dynamic Mechanical Analysis (DMA), Differential Scanning Calorimetry (DSC), X-ray scattering, infrared spectroscopy (IR), optical microscopy, Scanning electron microscopy (SEM) [23-26].

DSC, unlike other techniques, provides the ability to measure thermal properties and crystallinity in thermoplastic polymers while heating or cooling samples over temperature ranges. The test results are usually plotted as temperature vs heat flow. Crystallization density can be calculated from the heat of fusion peak and compared with the heat of fusion for fully crystalized polymer [27]. DSC has also been used widely to investigate PEEK crystallinity; however, some studies indicated DSC has limited accuracy because recrystallization may occur during the experiment [13], while other studies indicated no overestimation in the DSC crystallinity result when it compared with other techniques [28]. Thus, DSC might need additional investigation to validate its results [29]. X-ray and dynamic mechanical analysis (DMA) can be powerful tools to differentiate mechanical behavior and crystal structure distribution in samples [30-33]. Different X-ray techniques can be used to test the samples such as small-angle X-ray or wide-angle X-ray as well as diffraction or scattering signals collected from X-ray radiation applied to the samples [31, 34, 35]. While DMA tests are usually associated with applying force on samples and collecting their mechanical responses. Samples' structure evaluations can take place by comparing their mechanical responses [33, 36, 37].

The crystallinity percentage and crystal morphology of semi-crystalline polymer are influenced by several parameters such as polymer stereoisomers and molecular weight, processing conditions (cooling rate, holding temperature, and time for holding temperature), post processing

treatment, and involving additives and fillings. The effects of those parameters on PAEK polymer properties have been investigated and presented in the following section.

2.3.1 Effect of Stereoisomers and Molecular Weight

Polymer stereoisomers (tacticity) are usually decided when the polymer produced in the reactor. Those architectures influence the crystallinity of the polymer. Differences in molecular weight and chain branching can impact chain packing and affect the polymer ability to perform uniform crystal structure during thermal processing [35, 38, 39]. Several researchers highlighted those effects for different high performance polymers. For instance, Rueda et. al. [35] was able to observe those effects in poly-aryl(ether ketone ether ketone ketone) PEKEKK using X-ray scattering (WAXS and SAXS). While White et. al [36, 37] used thermal and rheological characterization and DSC to study the crystallization poly(ether ether ketone) PEEK and poly(ether ketone) PEK. They discovered the long-chain branching in PEEK for the first time, and they compared the effect of linear chains vs. long-chain branching of the PEEK on crystallization. It was found that PEEKs with long branching (PEEK-A5 and PEEK-B) achieve lower modulus because the molecular chains are unable to pack, and this produces low crystallinity as presented in **Table 2.1**. Moreover, they observed the inverse relation between molecular weight and storage modulus, as illustrated in **Figure 2.2**, because crystallinity decreases with increasing molecular weight. This was linked to reducing the ability of the high molecular weight chains to reorganize themselves in a uniform crystal structure during the melt state.

Table 2.1. Molecular weight (Mw) and crystallinity of PEEK in Figure 2. (Redrawn from references [36, 37]).

	Mw	Xc
PEEK-A1	66.2	50
PEEK-A2	76.1	48
PEEK-A3	114.4	42
PEEK-A4	143.6	41
PEEK-A5	123.6	37
PEEK-B1	85.1	38
PEEK-B2	119.2	37
PEEK-B3	118.5	35

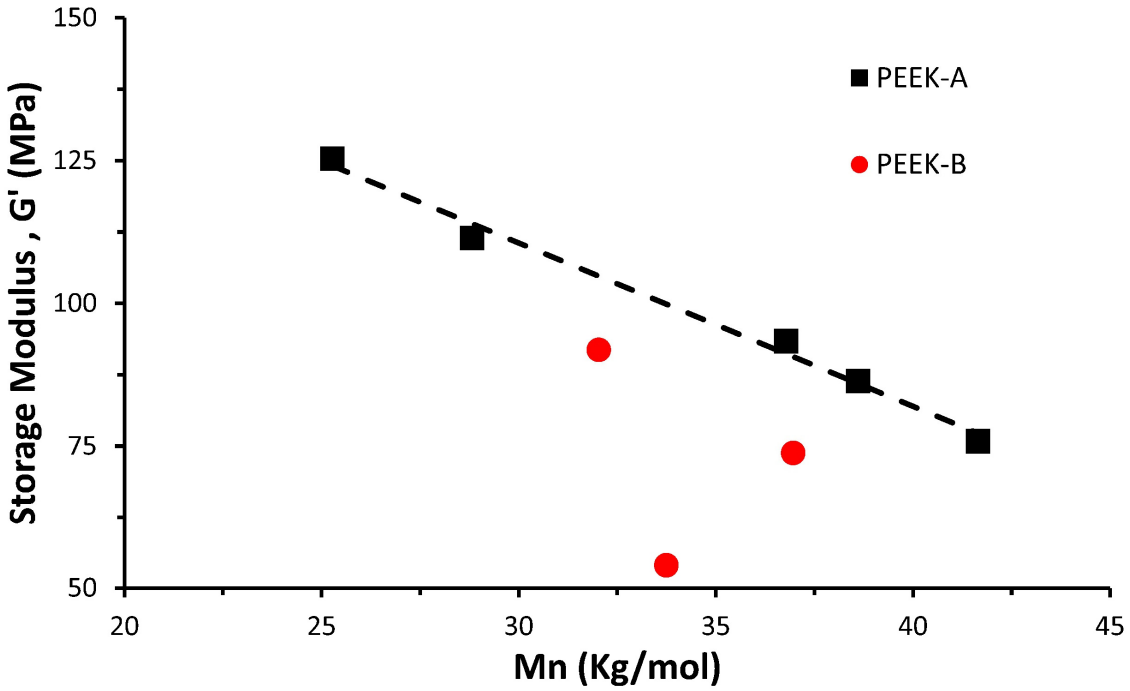

Figure 2.2. Storage modulus of PAEKs as function of molecular weight (Redrawn from reference [36]).

2.3.2 Effect of Processing Conditions

Although PEEK forms one crystal structure called spherulite [40], PEEK, as semi crystalline structure, acquires different degrees of crystallinity within same specimen that influences its mechanical properties. PEEK crystallization involves two competitive steps [41]. During initial stage, crystalline lamellae are formed through massive heterogeneous nucleation to develop spherulites. The next step involves a secondary process associated with inter-lamellar growth and/or enhancing crystalline structure perfection at slow rates [42-45].

Crystallinity percentage and crystal structure morphology can be affected by thermal processing procedure, such as cooling rates, holding at different temperatures, time of holding temperature, and thermal gradient [46]. For instance, Tung et. al. [47] proved that increasing cooling rate have a big influence on reducing spherulite crystal radius and deceasing crystallinity percentage as presented in **Figure 2.3**. Jin et. al. [48] studied the effect of cooling rate and holding temperature during processing on degree of crystalline perfection at different positions of thin film polymer under optical microscope. They used standard differential scanning calorimetry (DSC), flash DSC, X-ray scattering, optical microscopy, and atomic force microscopy (AFM) in their analysis. This study proved building different crystal structure throughout the sample and carried out a simplified model to explain this behavior.

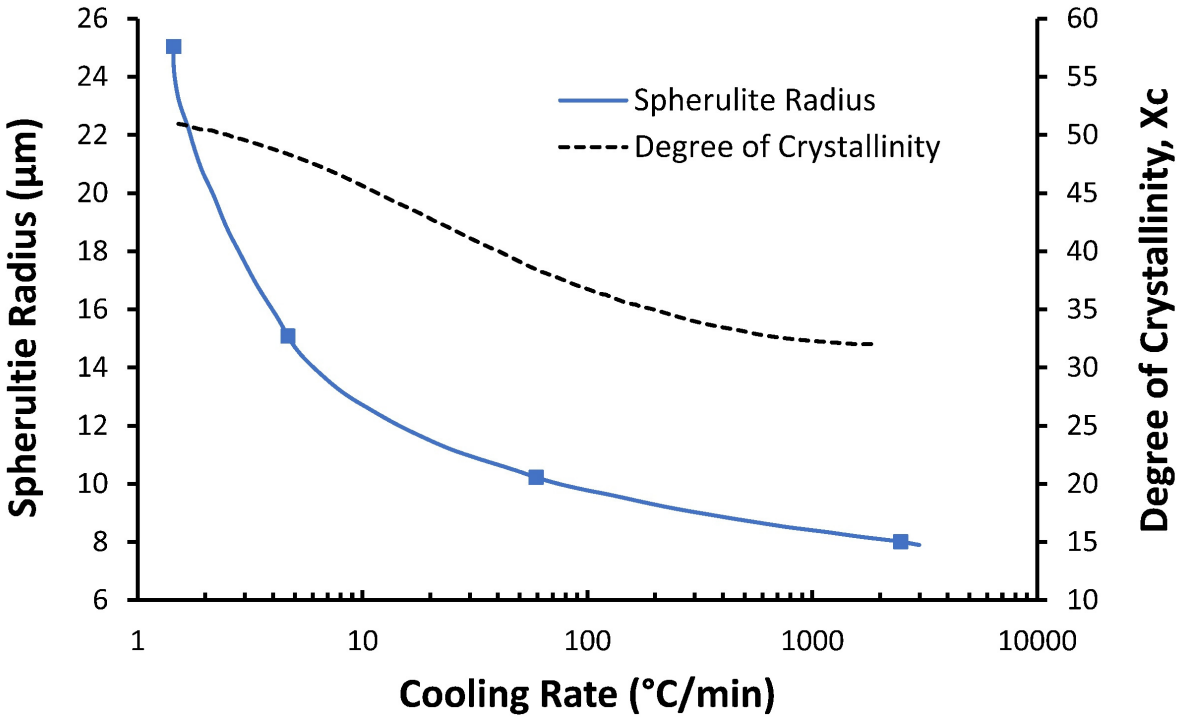

Figure 2.3. Effect of quench rate on spherulite size and degree of crystallinity (Redrawn from reference [47]).

The time of holding temperature at crystallization has a great impact on polymer morphology and thus mechanical properties. Increasing holding time at crystallization temperature assists in building polymer crystal structure and increase spherulite radius as indicated by Kumar et. al [49]. Several papers studied this effect extensively using thermal analysis and scanning electron microscopy (SEM) [48, 50-54]. They found that holding temperature at crystallization or slow cooling introduce double melting points. The second melting point disappeared after holding the temperature for enough time to make the crystallization peak to become narrower, as presented in **Figure 2.4**(a) and (b) [50].

Several explanations and models were proposed in the literature regarding double melting phenomena. The first model related this phenomenon to the physical aging in the amorphous part

of semi-crystalline polymer [12]. The physical aging reduces the molecular chain mobility, so part of the amorphous phase stays rigid above Tg and below Tm [55]. This rigid amorphous relaxes gradually above the polymer glass transition temperature without performing additional glass transition temperature [56]. Their hypothesis was based on the DSC overestimation of crystallinity compared with the density measurements. However, a following research compared the crystallinity of annealed polymer using wide angle X-ray vs DSC [28]. They proved there was no overestimation in the DSC measurements; this was evidence against the physical aging model. Other researchers explained the double melting phenomena by proposing dual lamellar thickness model [50, 51]. This model suggested the presentation of two crystal morphologies in isothermally crystallized PEEK. Those structures consisted of primary crystals and thick lamellae produced from the first nucleation and secondary crystals, which appeared between primary crystal structures as thinner lamellae while keeping temperature isothermal [48, 50, 52-54]. The third model, called melting-recrystallization, was based on melting the crystals that have low melting temperature then re-crystallizing to thicker and more perfect lamellae during heating or annealing treatment. They used scanning rate dependency as evidence to support this model [33, 34, 54, 57]; however, later studies showed that low temperature endotherm can perform after high temperature endotherm in the DSC depending on the polymer history and the heating/cooling rates capability of DSC; this suggests the invalidity of the third proposed model [50, 58]. An adequate model was proposed recently by Jin et. al. [48] based on the formation of lamellar layer with variation in crystal perfection. In this model, they assumed that the perfect part of the crystal related to the lamella middle structure; however, there is an imperfect portion because chains bend in the lamella boundaries that extend to the amorphous region.

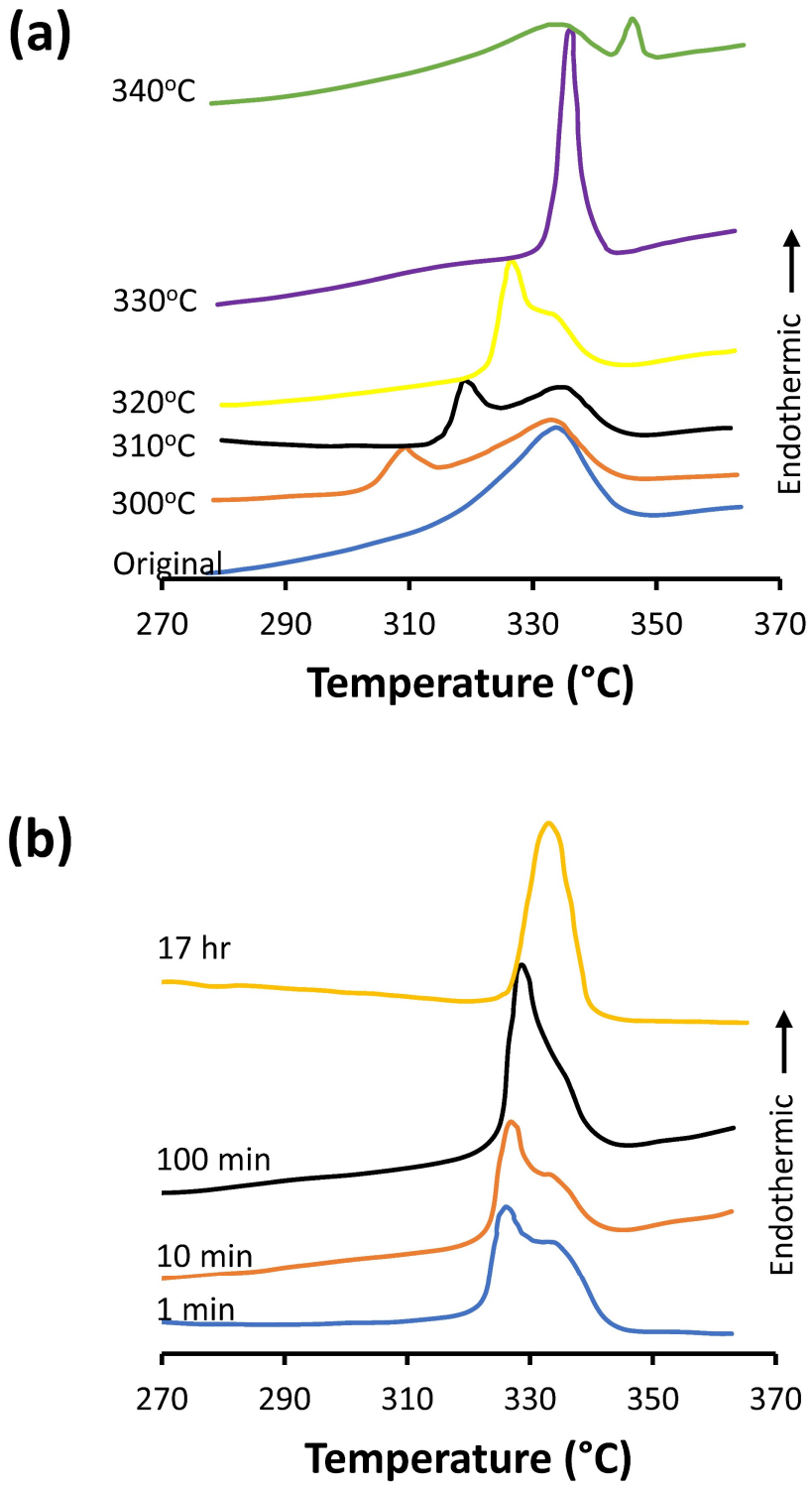

Figure 2.4. (a) Hold Temperature for 10 min. (b) Hold Temperature at crystallization for different times (Redrawn from reference [50]).

All previous studies showed that holding temperature during processing have positive influence on the high performance polymer properties; however, they have not consider the effect of holding temperature at higher ranges that can introduce negative impact of the polymer properties and thermal stability caused by structural modification following thermal treatment in PAEK polymers as proved by Reuda et.al. [35] , Jonas and Legras [59], and White et. al. [36, 37]. They also found that PAEK with higher molecular weight was most sensitive to thermal treatment at Tm, as presented in **Table 2.2** [36, 37]. Reducing the crystallization percentage by holding temperature around Tm is attributed to combined molecular viscosity increases from undesired crosslinking reactions, and from introduced structural defects along the polymer chains. The observations found by those researchers indicate that it may be impossible to manufacture the high performance PAEK polymers without introducing some percentage of irreversible structural modification.

Table 2.2. PEEK crystallinity before and after thermal treatment by holding temperature at 420C for 30min in dry air (Redrawn from references [36, 37]).

	Mw	Xc before holding	Xc after holding
PEEK-A1	66.2	50	36
PEEK-A2	76.1	48	36
PEEK-A3	114.4	42	31
PEEK-A4	143.6	41	25
PEEK-A5	123.6	37	22
PEEK-B1	85.1	38	28
PEEK-B2	119.2	37	24
PEEK-B3	118.5	35	26

2.3.3 Effects of Post Processing Treatment

Semi-crystalline polymer properties are highly related to crystallinity percentage and crystal structure morphology that are influenced by polymer thermal history during processing condition and post processing treatment. Several post treatments can be applied on PAEK polymers after processing to improve the products. Annealing, heating polymer parts above their glass transition point, is one of the post processes used currently to enhance crystallinity percentage and crystal perfection of the final part [50, 51, 60, 61]. As a result, mechanical properties including young modulus, yield stress, break stress, and flexural strength will be increased, while break strain and impact strength will be decreased [18, 62]. For instance, Arzak et. al [62] observed those behaviors during annealing process of small PAEK samples. They noticed an increase in the

crystallinity percentage and the young modulus with increasing the annealing temperature; while increasing the annealing time from 1 hr to 24 hrs enhanced the modulus values and reflected no effect on the crystallinity percentage, see **Figure 2.5**(a) and (b) [62]. They linked the reason for not changing the crystallinity percentage by changing the annealing time to restricting polymer chains mobility after reaching certain crystallinity percentage that prevents the polymer from building further crystal structure. While changing the modulus is manly attributed to increasing the crystal structure perfection by increasing the annealing time; however, in my opinion, they were supposed to perform further investigation to prove their claim considering the limited sensitivities of standard DSC in detecting the changes in the crystallinity percentages. I believe the best explanations for the crystallinity percentage and modulus responses to the annealing time could be attributed to the changes in lamellar layer structure perfection that was proved later by Jin model [48] through explaining differences between the linear crystallinity and bulk crystallinity.

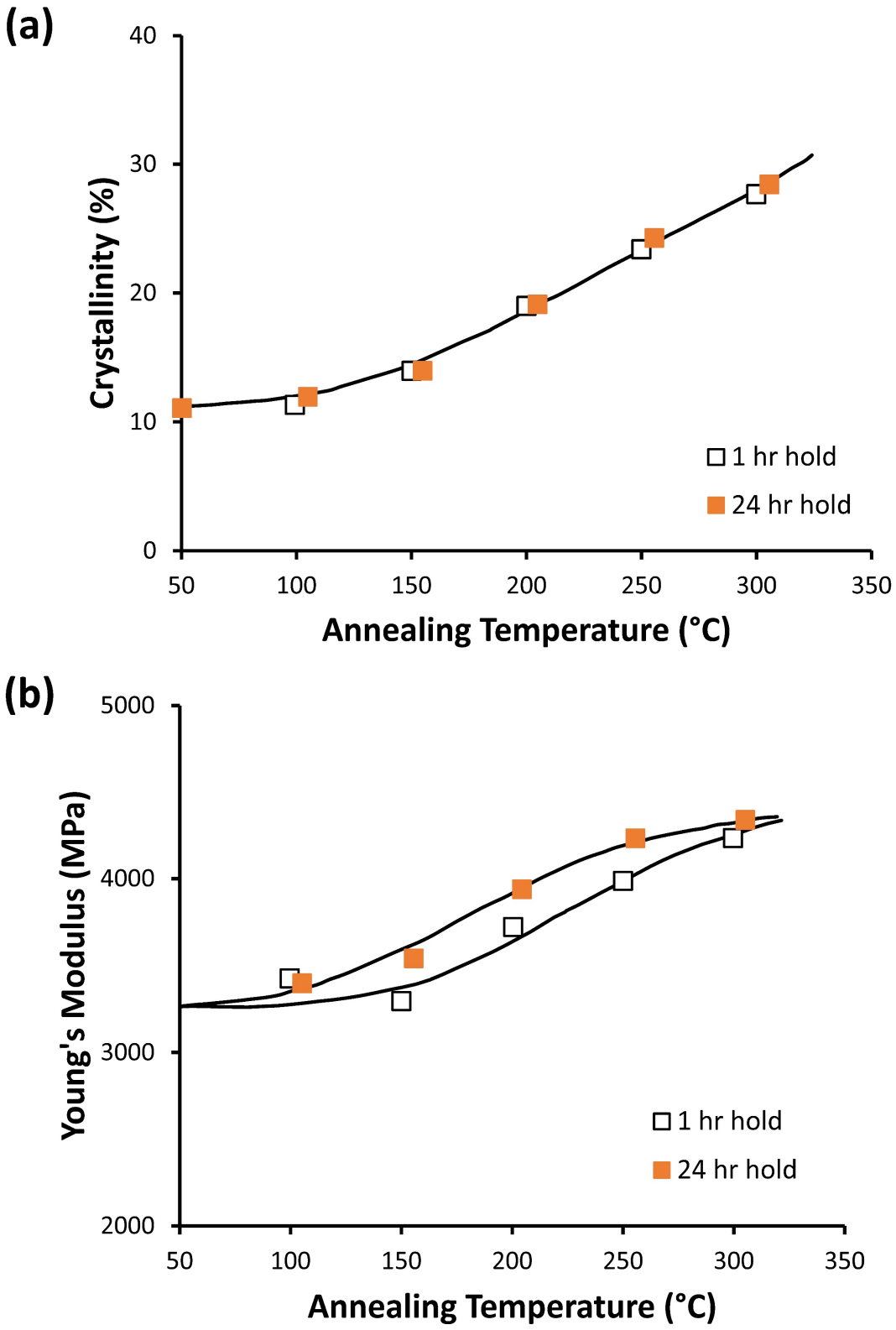

Figure 2.5. Effect of holding temperature at different values for 1h and 24h (a) on crystallinity and (b) Young's modulus (Redrawn from reference [62]).

Aside from using annealing to enhance crystallinity of thermoplastic parts, it can also be used to relief stresses built up during producing the products. Those stresses can cause distortion, cracks, lowering physical properties, and changing dimension of final product. Annealing method is meant to increase crystallinity by heating the polymer parts above their glass transition temperature that allows polymer chains, in amorphous region, to move and re-arrange themselves to build the crystal structure. This method can enhance the properties of small parts that have same crystal structure in all regions. Considering annealing post processing method to improve the properties of thick PAEK parts is challenging because of different crystal structure that is been formed during processing this material in the first place [18, 62]. Thermal aging and sterilization using gamma ray, steam (autoclave), or ethylene oxide (ETO) are other type of post processing procedures can be applied on PAEK polymers. However, those post processes have negligible effects on flexural strength, fatigue performance, and other polymer mechanical properties [18, 63].

2.3.4 Fillings and Additives

PAEK can be strengthened by adding filings to create different composites with various properties. Those additives play significant role in nucleating crystals and forming extended polymer chains [64] that influence polymer microstructure and thus its mechanical and thermal properties [24, 25, 47, 64, 65]. There are several types of fillers and additives that can be used with PAEK polymers such as carbon fibers, glass fibers, carbon nanofibers, and carbon nanotubes, etc.

Common processes for the preparation of thermoplastic composites include solution mixing, sonication and melt-compounding [66]. In the case of PEEK polymers, melt-blending is the most frequently used for the fabrication of their composites. Injection-molding is one of the

common tools, based melt-blending processing method, utilized to produce thermoplastic composites. During the process, fibers/nanofibers and nanotubes aligned along the flow direction of the matrix [67]. Moreover, the strong tendency of the fillers to aggregate and form bundles or micron-sized agglomerates could limit their uniform dispersion in thermoplastic composites. Ultrasonic treatment was used to avoid agglomerates of some filler types. This treatment assisted in inducing shorter and better dispersed fillers forming a network throughout the matrix [68].

Morphology, mechanical and thermal properties, and crystallization of composites are highly influenced by the way of incorporating the fillers into the matrix as well as the composite processing procedure. For instance, allowing composites to cool slowly during the process provides sufficient time for the polymer matrix to build more crystals in larger sizes [64]. Moreover, composites prepared by a pre-dispersion stage in an organic solvent showed narrower peaks compared with those obtained by direct mixing, indicating a higher degree of crystallinity and larger crystal size. On the other hand, low percentages of reinforcements in PEEK can enhance crystallinity and properties of this polymer. However, increasing the concentration of some fillers can negatively impact crystallinity and other composites properties [69, 70]. Those opposite behaviors relied on competitive influence of two factors. One factor is related to surface area increase by incorporating fillers in the polymer matrix that enhance crystal nucleation. While, the other factor associated with the filler influence on reducing polymer chains ability to move and build crystal structure [71-73]. At low reinforcement content, the filler nucleating effect prevails over mobility loss and crystal packing limits; this results in an increase in the overall crystallization rate. However, strong restrictions of chain mobility imposed by the intense fillers-matrix interactions because higher concentrations hinder polymer crystallization [74, 75].

Enhancing PEEK crystallinity and mechanical properties by introducing fillers and additives requires considering multiple factors such as filler type, purification method, concentration, and pre-treatments. Selecting the right processing method for producing PEEK composites with good properties and minimum filling damages and aggregations is a huge challenge.

2.4 Processing Methods of Advanced Performance Polymers

PAEK polymers, pellets or powder, can be processed into final products via three major methods: extrusion [76], injection molding [77], and compression molding [78]. Although both extrusion and injection processes involve same series of steps (melting polymer, pumping polymer, forming molten polymer into required shape, and solidifying), the biggest distinction from a monetary perspective is that extrusion process is material intensive while injection process is labor intensive [79-81]. Among these processing methods, compression molding is an effective and commonly used method for manufacturing thick high performance polymer products that can eliminate issues associated with the other processing methods such as inability to produce 3-dimensional parts by extrusion because dies are 2-dimensional, unable to create large complex parts, limitation in predicting shrinkage, warpage issues during solidification, and stress cracking when two melted bodies bind together and solidify. Moreover, an advantage that recognize compression molding process from other processing methods is the ability to process reinforced polymers because the lowest levels of deformation and stress are involved in this particular processing method. As a result, the reinforcing fibers are not damaged. This makes it possible for high fiber concentrations and longer fibers to be included in compression molded products [80].

To this end, compression molding processing method provides a platform for adding fillings to enhance thick thermoplastics products.

2.5 Concluding Remarks

Although they have higher strength, advanced polymers represent only a small portion of the market because better performing polymers cost more. Therefore, further investigation and development are required for manufacturing thick advanced performance polymers to enhance their yield and affordability. The main focus in this study will be given to compression molding process because it is the best method to produce thick parts and add different reinforcements types with minimal stresses and without deformation.

Despite considerable studies on PAEK polymers that focused on injection molding and extrusion processing methods and properties of those semi-crystalline polymers and their composites, those studies were mostly focused on thin film PAEK polymer while thick polymer parts are highly unexplored. That is partly rooted to experimental limitations in producing those thick polymers, measuring temperature inside those thick parts during processing, and providing temperature profile of the overall processing to predict the behavior and the mechanical properties of those polymer. Moreover, compression molding processing strategies need to be revisited to address and solve the difficulties associated with this process. Solving those issues and enhancing the thick advance polymer properties are the primary focus of my research that can set a foundation for the next generation of advance performance polymers and their composites for different applications especially the ones associated with aerospace, biomedical, and harsh environments.

3 DEVELOPMENT OF COMPRESSION MOLDING EQUIPMENT SUPPORTED WITH THERMAL CONTROL SYSTEM

Designing and fabricating an instrumented compression molding with embedded thermocouples lab equipment are essential for this research. This system requires developing a special thermal control system to monitor polymer processing during heating and cooling. The methods and procedures used to develop the entire system are introduced in this chapter.

3.1 Design and Build Compression Molding with Embedded Thermocouples

I developed a lab compression molding system to investigate the effect of manipulating thick semi-crystalline polymers processing parameters on properties and crystal structure of final parts. Compression molding system comprised of an outer cylinder (usually called mold referred here as shell) and an inner cylinder (mandrel), see **Figure 3.1**. End-rings at the top and the bottom ensure that the polymer powder is filled in between the shell and the mandrel. A pressure is applied on the top end-ring resulting in the powder to be compacted to the final bushing height of 6”. A schematic of the lab equipment setup before and after applying pressure is illustrated in **Figure 3.1**.

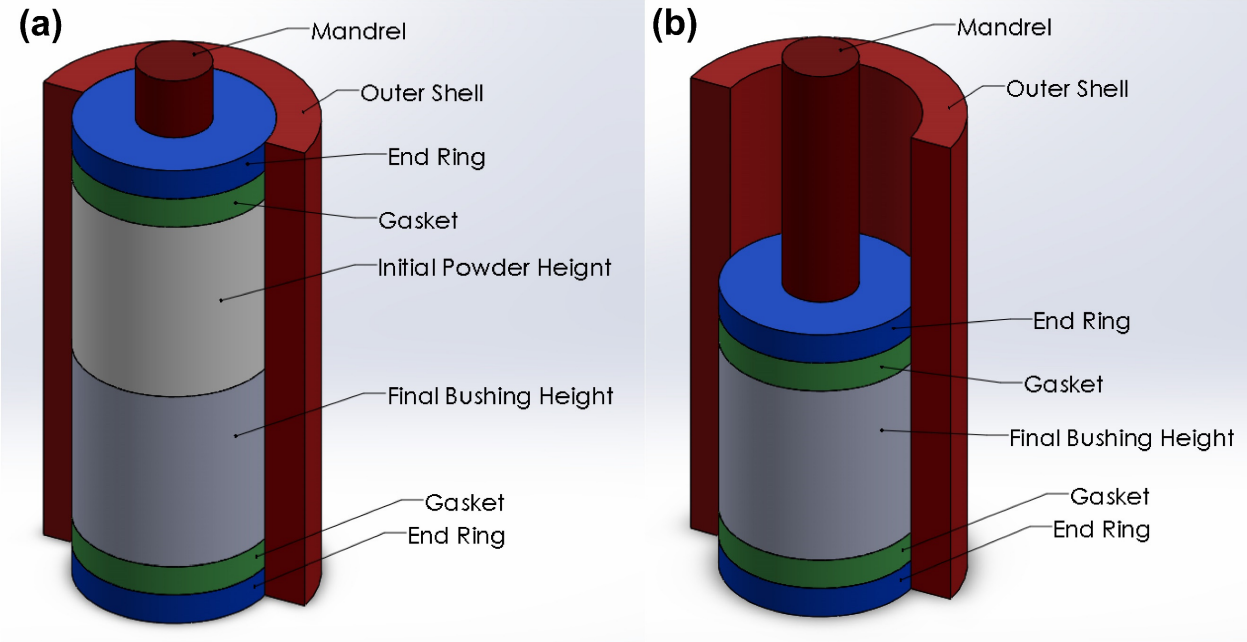

Figure 3.1. schematic of compression molding experimental setup.

This research focused on producing compression molded bushings with dimensions of 5.75” outer diameter, 1.5” inner diameter, and 6” length. The compression molding design used to produce this bushing consisted of shell (mold outer part) and mandrel (mold inner part). Pipe size 6 schedule 80 was used to make the shell mold with the following dimensions: 5.761” ID, 6.625” OD, and 12” length. While, mandrel pipe was fabricated to form 1.5” OD, 0.75” ID, and 12” length. SolidWorks software was used to design the compression molding setting. The final compression molding parts are presented in **Figure 3.2**. The shell part of the mold had 9 thermocouples ports with 0.25” depth though its thickness. Those ports were distributed through the shell length to measure and control the temperature throughout the outer surface of the mold. The positions of those thermocouples ports were as follow (2”, 3”, 4”, 5”, 6”, 7”, 8”, 9”, 10”) measured from the bottom of the shell. In addition, there were five thermocouples ports with

compression fittings placed around the shell at 5” height from bottom, see **Figure 3.2**. Those compression fittings used to embed thermocouples inside the polymer to measure temperature distributions, through polymer cross-sectional area at the middle height of the final bushing, during the process. Compression fittings were used to prevent leaking when polymer melted. Mandrel had three thermocouples ports with different depth (4”, 7”, and 10” measured from the top) to measure and control temperature through mandrel length. Two end-rings with three compression fittings ports in each end-ring used for embedding thermocouples to measure temperature at the top and the bottom polymer surface. End-rings with compression fitting ports are presented in **Figure 3.2**.

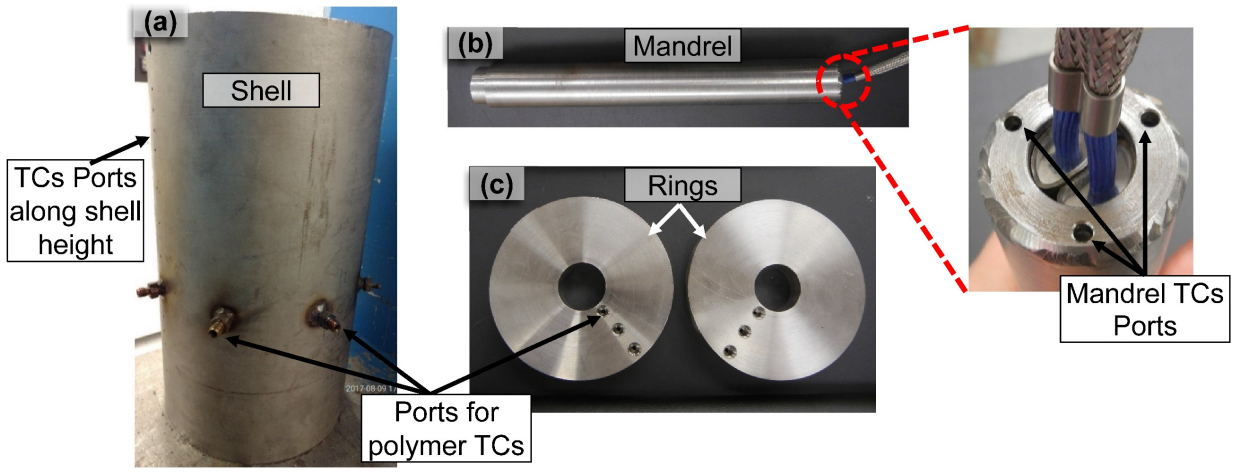

Figure 3.2. (a) Shell, (b) mandrel, and (c) end-rings of compression molding with thermocouples and compression fitting ports.

3.2 Special Components Fabrication for Lab Compression Mold Setting

Additional components were required to adjust the lab compression molding equipment setting. For instance, adding insulation base at the bottom setting to prevent heat leaking from the

bottom mold to the press frame. This base should be electrical and thermal insulation, and it can handle high pressure of 4000 psi. Different approaches were considered as a base for this system such as using high-temperature rigid mineral wool insulation sheets, cutting high compressive strength brick pieces with the band saw, and using electric and thermal insulation ceramic powder (Zirconium Oxide) with high compressive strength properties to custom build the base using 3D printed mold, and glass-mica ceramic sheet. Among all those methods, glass-mica ceramic was the only approach that could survive as a base for compression molding setting because of its favorable properties (high electrical and thermal insulation up to 930 ºF and high compressive strength up to 32000 psi). To this end, two base insulation rings with 1" thickness each were CNC machined from glass-mica ceramic sheet. Channels were CNC machined through the insulated base to adjust the end-ring compression fitting and thermocouples places as the end ring sits on the insulated base. Glass-mica ceramic base with compression fitting channels is presented in **Figure 3.3**(a).

The compression molding experiments indicated that there wasn't enough heat applied on the bottom section because heat rises to the top. To overcome this issue, a base heater was added to the compression molding lab setting to adjust the temperature profile on the bottom system. The base heater working conditions were above 400 ºC and 4000 psi. In addition, the base heater required having a channel to allow end-ring compression fittings and thermocouples to pass through it. There was no commercial heater available with those specifications; therefore, a special heater was custom made in the lab to satisfy those requirements. To this end, bar with 6" OD was machined, using lathe, to 5.5" OD and 1" length. A thermocouple hole with 0.125" OD was drilled at 0.5" from the top bar surface. Then CNC was used to machine the compression fittings channel. Another channel with 1" wide and 0.6" depth was machines at distance of 1.375" from the center

as presented in **Figure 3.3**(b). High temperature ceramic casting compound, Alumina based Al_2O_3, was used because its properties, such as electrical insulation, thermal conductivity, and compressive strength, are good. The two parts were mixed and placed as a thin layer along the channel surface and left 24 hours to cure at room temperature. A heater coil was cut and adjusted to fit in the channel. Non-insulated high-temperature ring terminals were crimped at the coil ends in order to connect the heating element with the electric wires. The channel was filled with the ceramic paste carefully and left to cure for 24 hours at room temperature. The base heater manufacturing procedure is presented in **Figure 3.3**.

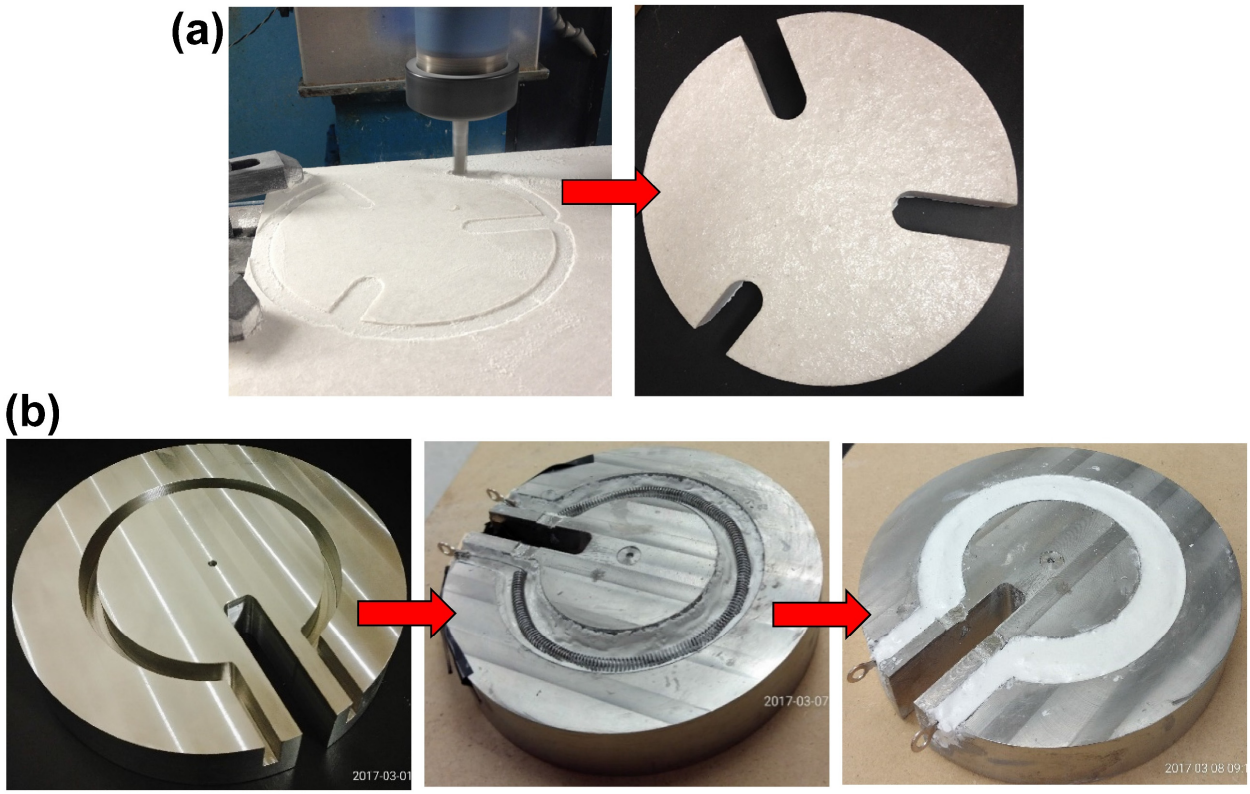

Figure 3.3. Special components added to Compression molding lab setting. (a) Glass-mica ceramic insulation base machined using lab CNC. (b) Base heater lab manufacturing procedure.

3.3 Gasket Processing and Novel Hybrid Sealing Method

The traditional compression molding process use special custom-made thick Polytetrafluoroethylene filled with steel (Steel/ PTFE) composite gaskets placed between the end-rings and the polymer. Those gaskets are rigid at room temperature. Applying heat on the system plays significant role in softening the gaskets and making them flow to close the gaps and act as seals.

Steel/ PTFE composite gaskets were custom made in the lab using a compression mold with slightly larger diameters than the one used for processing the polymer bushing in order to accommodate the shrinkage that happens in the processed gaskets. After processing the gaskets, a lathe was used to slice and machine them to final dimensions of 5.6” OD, 1.5” ID, and 1” thick. Then 3 holes were drilled in each gasket to allow thermocouples to pass through the gasket to top and bottom polymer surfaces. The gasket processing procedure is illustrated in **Figure 3.4**.

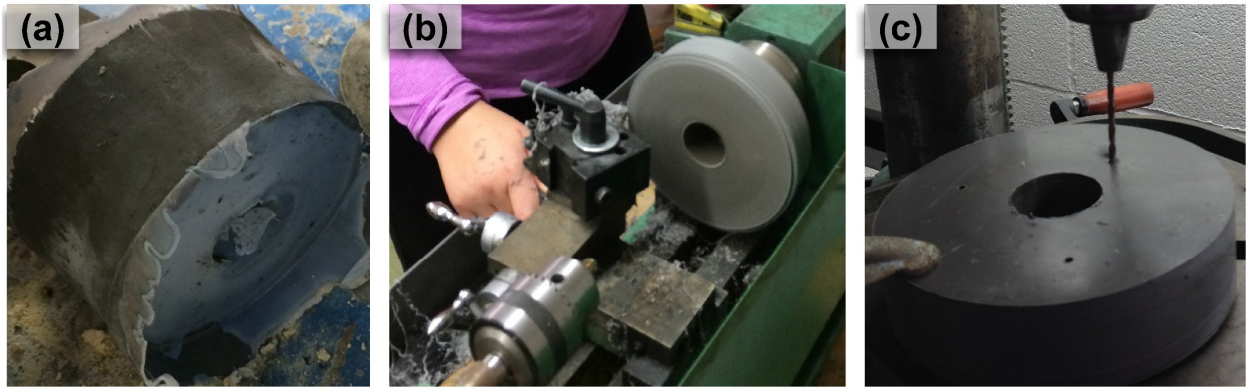

Figure 3.4. Producing Steel/PTFE composite gaskets. (a) Process gaskets using compression molding. (b) Slice and machine gaskets using lathe. (c) Drill holes for thermocouples to pass through the gasket to top and bottom polymer surface.

One of the biggest issues in compression molding process is polymer leaking from the mold end-rings that causes terminating the process and wasting the parts. The current industry practice uses a water hose to quench the material and stop the leak issue. However, using this method causes sudden temperature drop on one side of the mold that introduces a huge temperature gradient within the part (i.e. increase cooling rate differences throughout the polymer part). As it is well known, changing the cooling rate of semi crystalline polymer initiates significant property differences along the product resulted from forcing the material to build different crystal structure [47, 49]. As a result, unreliable parts with inconsistent crystallinity and mechanical properties are produced from the compression molding process.

It was crucial to find a permanent solution to stop the leak during compression molding process before further proceeding with the lab experiments to reduce the temperature gradient that happens when a quench gets applied during the process. The initial lab experiments showed gaskets degraded, during compression molding, because the process high temperature (400 ºC) exceeded PTFE's limits. Different gasket was required to proceed with compression molding process. The new gasket should satisfy the following conditions: (i) survive at high temperature > 800 ºF, (ii) hold high pressure > 4000 psi, (iii) be porous to allow air to escape, yet polymer cannot flow through it. Those combined properties were not available in any commercial or custom-made gaskets. To this end, a hybrid gasket was introduced as a sealing system for this compression molding process. In this invented hybrid sealing method, sand plays significant role because it can handle high pressure and high temperature, and its melting temperature is 1650 ºC (3002 ºF). In addition, this material is porous, which provides a path for the air to escape and doesn't allow the polymer to flow through it because the polymer has high viscosity and the path through the packed sand it torturous. A thin Steel/PTFE gasket was used as interface layer between the polymer and

the sand. Another thin gasket was added between the sand and the bottom ring to prevent sand leaking through the clearance between the ring and the shell. The schematic setting of hybrid sealing method in compression molding system is presented in **Figure 3.5**. Sand layer thickness used in this system was ~ 0.5" while Steel/PTFE gasket thickness was ~ 0.2". By utilizing the new high pressure and high temperature HPHT sealing method, much higher pressure was applied to the system without experiencing any leaking issues in order to remove all trapped air and collapse the remaining voids inside the melted material. Thus, the novel HPHT hybrid sealing method was able to eliminate all leaks and guaranteed producing all bushings without any quenching or voids. Moreover, this new method helped reducing Steel/PTFE gasket material by 80%; this would significantly reduce the compression molding processing cost.

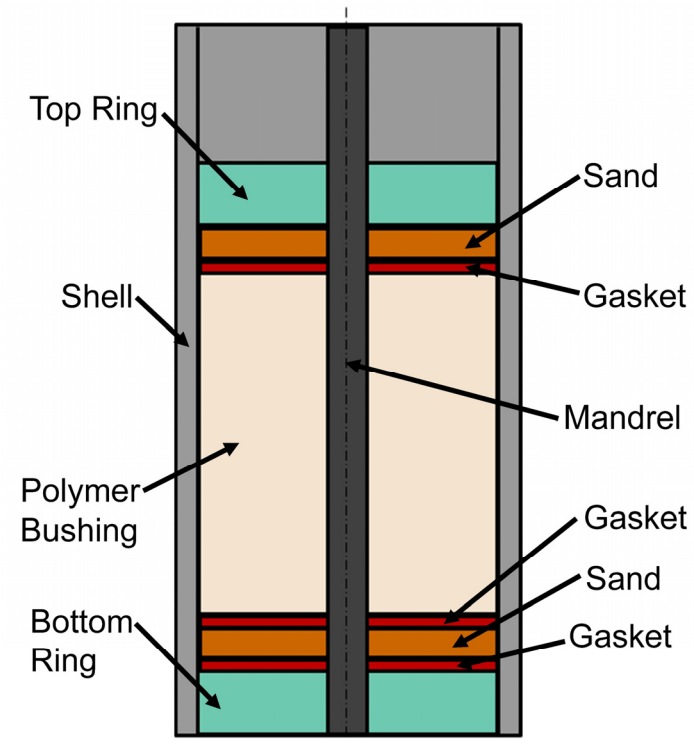

Figure 3.5. Schematic of hybrid sealing method for compression molding process.

3.4 Thermal Control System Setting

Different heating elements such as regular heater band, ceramic heater bands, and cable heaters were used to provide the heating source for the lab compression molding system setting. Several tests were made for those heaters to confirm the temperature distribution uniformity through their circumferential. Both regular and ceramic heater bands produced non-uniform temperature distribution through their circumferential; this burned the final bushing product from one side. Heater cables demonstrated best temperature distribution profile through their length; therefore, they were selected for heating the shell in this research. Moreover, different parameters were manipulated to optimize the effective heating zones and accomplish acceptable results, such as selecting effective areas for controlling the mold, changing the wiring methods of the heating elements (i.e. parallel and series wiring combination was selected), and adjusting the heating elements specifications (i.e. size, wattage, and number of heating elements needed). The final heating zones of the lab compression molding setup consisted of 6 heating zones, 4 heating zones for the shell, 1 heating zone for the base heater, and 1 heating zone for the mandrel, see **Figure 3.6**.

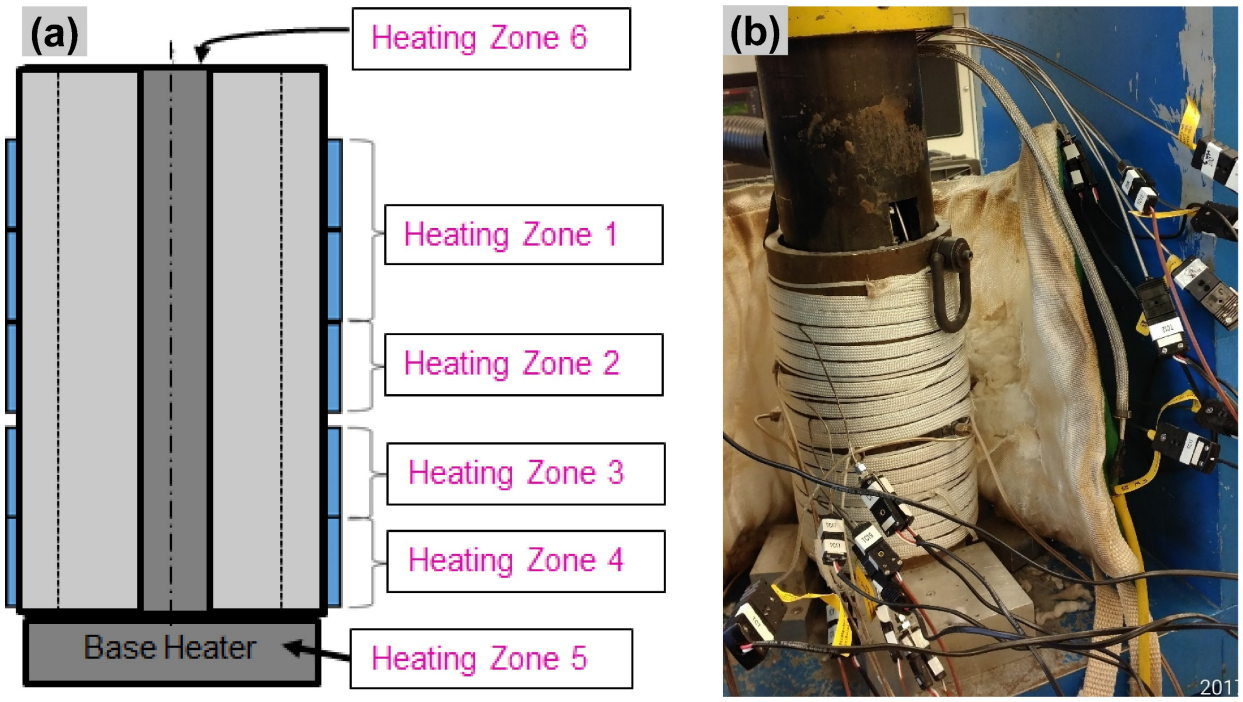

Figure 3.6. (a) Schematic and (b) lab heating zones setup of the compression molding system.

A control system was developed in this research to monitor the polymer heating and cooling process through 6 channels supported with Solid State Relays and fuses. The schematic drawing of the system circuit and the optical image of the control box are presented in **Figure 3.7**(a) and (b), respectively.

As explained previously, parallel and series wiring settings were used to connect heating elements in order to optimize the heating zones and produce best controlled temperature profile throughout the mold. As a result, six controlling zones have been identified, four control zones for shell though its length, one control zone for mandrel, and one control zone for base heater. A multi-zones controller from OMEGA with ramp/soak and manual PID setting was used to control this system. The manual PID tuning procedure, used for estimating the controlling parameter, can be

summarized by these steps: shell was wrapped with thermal blanket, to reduce heat losses, and loaded with fiber glass, insulation material to simulate the polymer in the real process. A full power was applied on the heaters and the temperature profiles were recorded, using data acquisition system, on selected control points throughout the shell, mandrel and base heater.

The maximum slope, in degree per minute, was found for each curve while Time delay Td, Proportional Band, Reset, and Rate were calculated using the following equations:

Td = time to max. slope – (temperature at max. slope – ambient temperature) / max. slope

Proportional Band = Td x max. slope x 100/span = % of span

Reset = 0.4 / Td = resets/minute

Rate = 0.4 x Td = minutes

Those parameters were founded for each controlling zone and placed in the controller. Several tests were carried out later to further tune those parameters to provide acceptable temperature profiles for all controlled zones. After optimizing and testing PID functionality on each part of the compression molding, experiments were carried over to test the control behavior and durability during real process by preparing all compression molding setting and adding polymer inside the mold. It was noticed that PID control method did not have significant effect, compared with using the on/off control setting, because the fact that polymer takes in heat slowly and allows time for the thermal control system to stabilize itself.

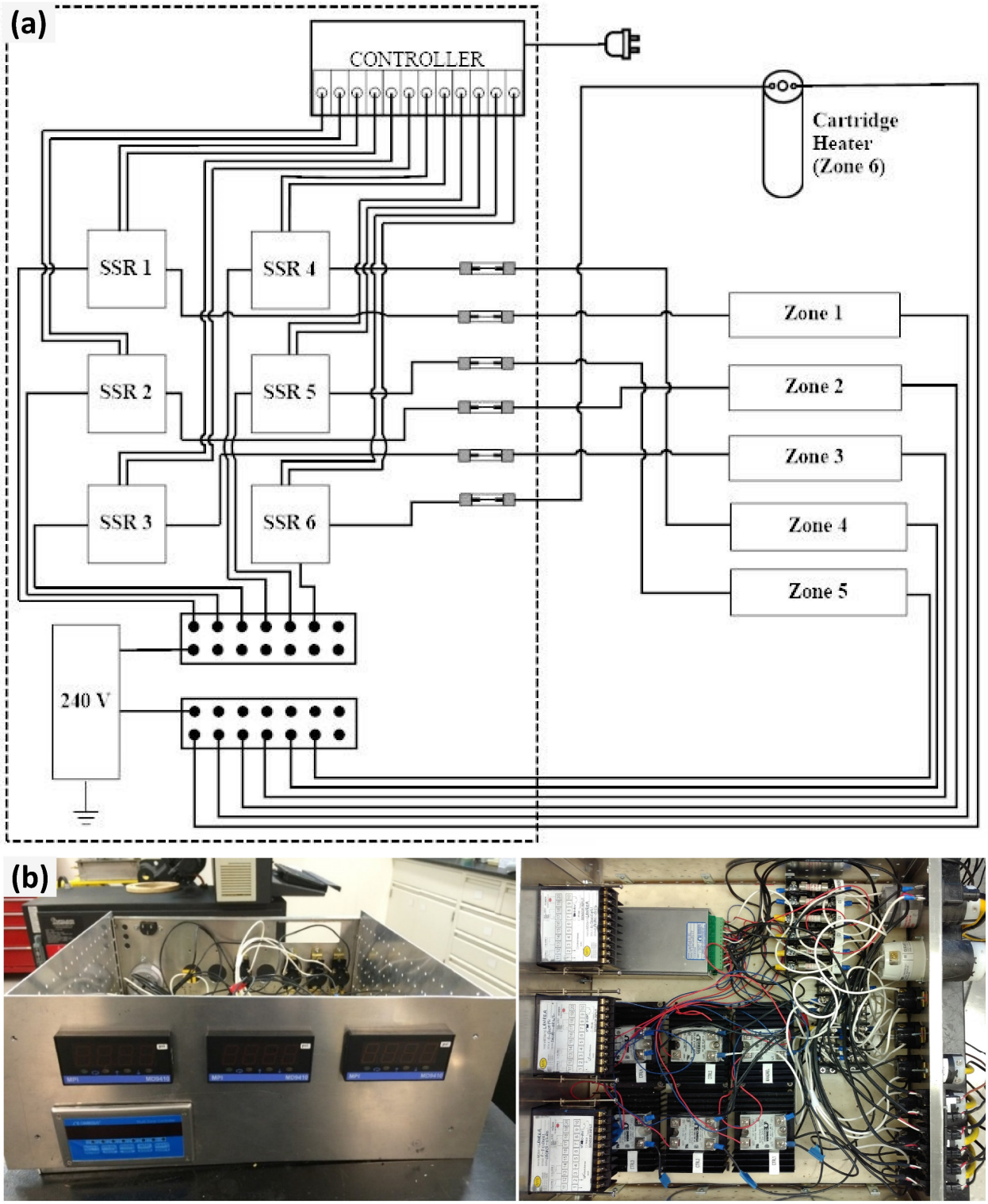

Figure 3.7. (a) Schematic and (b) optical image of control system setting used to monitor the compression molding processing.

4 COMPRESSION MOLDING OPERATING PROCEDURE AND PROCESSING STRATEGIES

4.1 Complete System Setting and Thermocouples Insertion

Final compression molding lab setting comprised of shell, mandrel, two end-rings, thermal control system with six heating zones, twenty-nine thermocouples to control and measure temperature throughout the mold, three data acquisitions connected with computer to collect the temperature profiles, heating cables wrapped around the shell, cartridge inserted in the mandrel, base heater, insulated glass- mica ceramic base, ram to press the polymer, and thermal blanket to reduce heat losses. The optical images of the final lab compression molding with embedded thermocouples sitting on the press is presented in **Figure 4.1**.

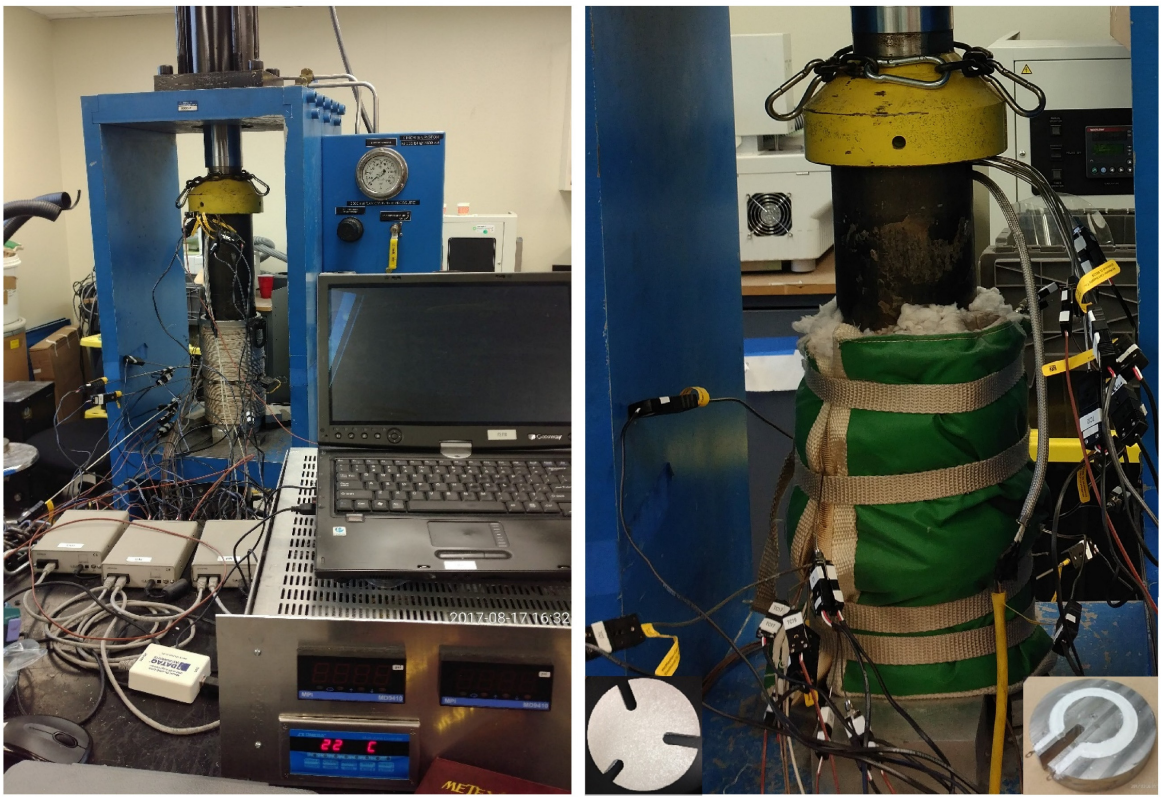

Figure 4.1. Instrumented compression molding system showing the system overview on the left and the system with insulation prior to an experiment on the right.

The system setting started with applying mold release on the shell inner surface and mandrel outer surface. Then polymer powder was loaded between end-rings and hybrid gaskets and pressed to 4000 psi using the ram; this resulted in compacting the polymer powder to ~ 6" final bushing height. While pressure was applied, thermocouples ports were opened and clearance holes were drilled. Five thermocouples were then inserted in the drilled holes to different depth (0.792", 1.151", 1.510", 1.869", and 2.227" measured from the shell outer surface) to collect the temperature profile in each position. Schematic and lab thermocouples setup of the compression molding system is presented in **Figure 4.2.**

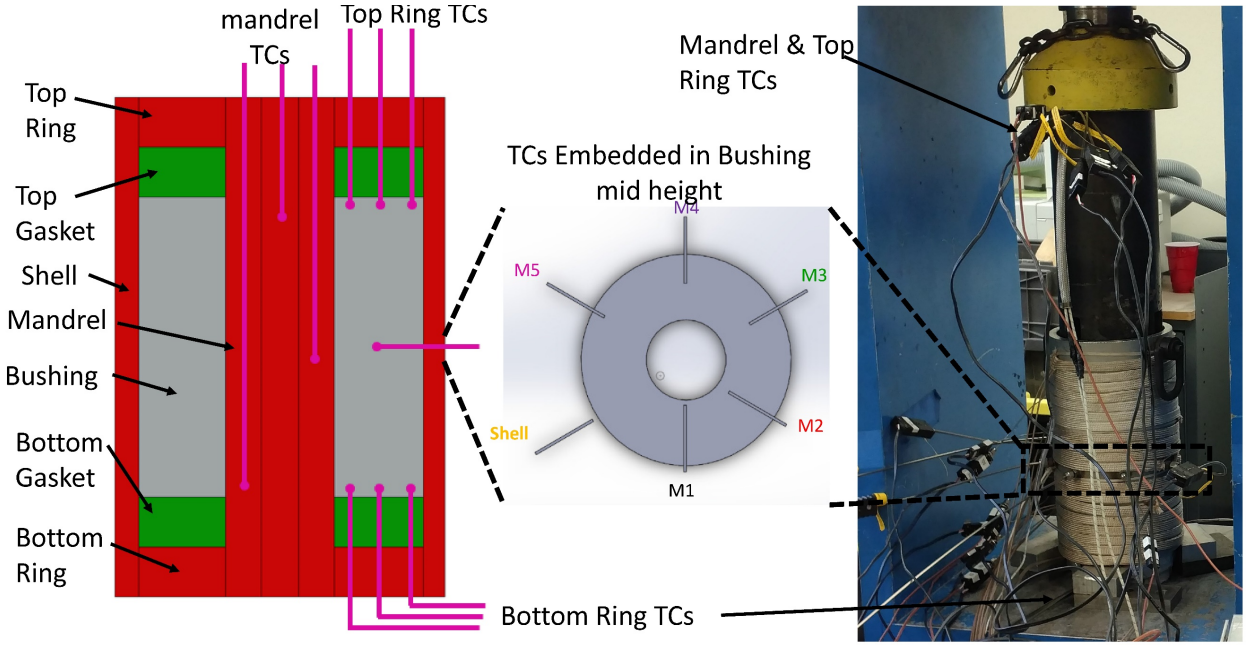

Figure 4.2. Schematic and lab thermocouples setup of the compression molding system.

4.2 Compression Molding Processing Procedure

The mold setting was prepared by pressing polymer powder to 4000 psi and inserting thermocouples at bushing mid height. This was the first step in the compression molding process that was explained in details in previous section. The shell was wrapped with thermal blanket and the control system set-points were programed to heat the compression molding to 400 ºC, above polymer melting temperature of 343 ºC to break all polymer crystal structures. Thermal control system power was turned on to start polymer melting process and data acquisitions collected the temperature profiles. Pressure and temperature profiles during processing steps are presented in **Figure 4.3**. The system was held on 400 C until temperature steady state was acquired throughout the bushing, processing step 3 in **Figure 4.3**. At the end of step 3, pressure was increased to 4000 psi and control set-points were reduced to crystallization temperature Tc. The system was held at crystallization temperature to allow reaching system steady state. Then the mandrel was striped at the end of step 5, see **Figure 4.4**, and the compression molding system left to cool to room temperature.

The proposed processing procedure unlike the traditional processing method by holding the temperature at crystallization and adjusting the holding time to obtain optimum results. To this end, it is important to determine PEEK powder crystallinity temperature Tc using Differential Scanning Calorimetry (DSC) in order to identify the holding temperature during the compression molding process.

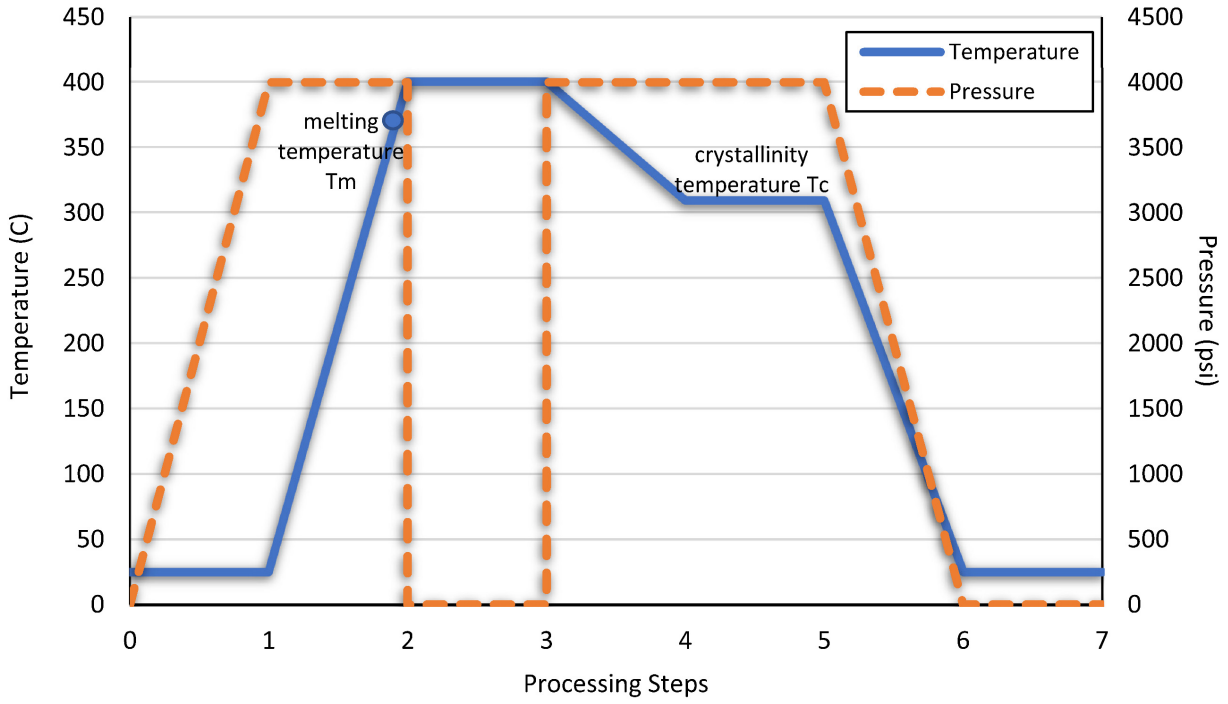

Figure 4.3. Schematic of pressure and temperature profiles during compression molding processing procedure.

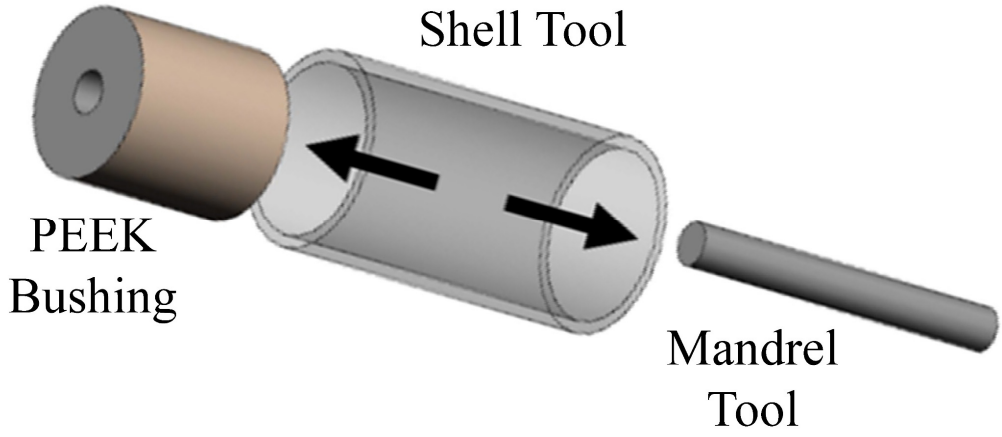

Figure 4.4. Schematic drawing of stripping the bushing from the compression molding tools.

4.3 Processing Strategies for Producing Compression Molded Bushings

Different control strategies were applied on compression molding process to investigate their effects on thick high performance polymer bushing properties. For all strategies, the process started with pressing the powder to 4000 psi followed by heating the mold to 400 ºC using lab compression molding setting. The heating temperature used in this process was above polymer melting temperature as explained in previously. The heating process followed by cooling process using four cooling strategies:

- **Strategy A (Free convection cooling):** Turn power off, remove insulation, allow free convection cooling to room temperature.
- **Strategy B (4 hours isothermal hold):** Reduce control temperature set point to crystallization temperature Tc and wait 4 hours to for the system to reach its steady state. Then, shut down as done in strategy A
- **Strategy C (10 hours isothermal hold):** Reduce control set point to Tc and hold temperature for 10 hours. After that, shut down as done in strategy A.
- **Strategy D (15 hours isothermal hold):** Reduce temperature to Tc and hold it for 15 hours, then shut down as done in strategy A.

The processing strategies flowchart is illustrated in **Figure 4.5**. Strategy A meant to simulate traditional compression molding procedure in producing bushings. While other strategies were modified to examine the effect of holding temperature at crystallization Tc. The holding time was a major concern for strategies B to D. Strategy B allowed holding temperature until steady state was acquired everywhere throughout the bushing. While strategies C and D explored the effect of increasing holding time beyond system steady state. Several bushings were produced in

order to investigate the effect of changing processing strategies on crystallinity and mechanical properties of thick high performance polymer bushing.

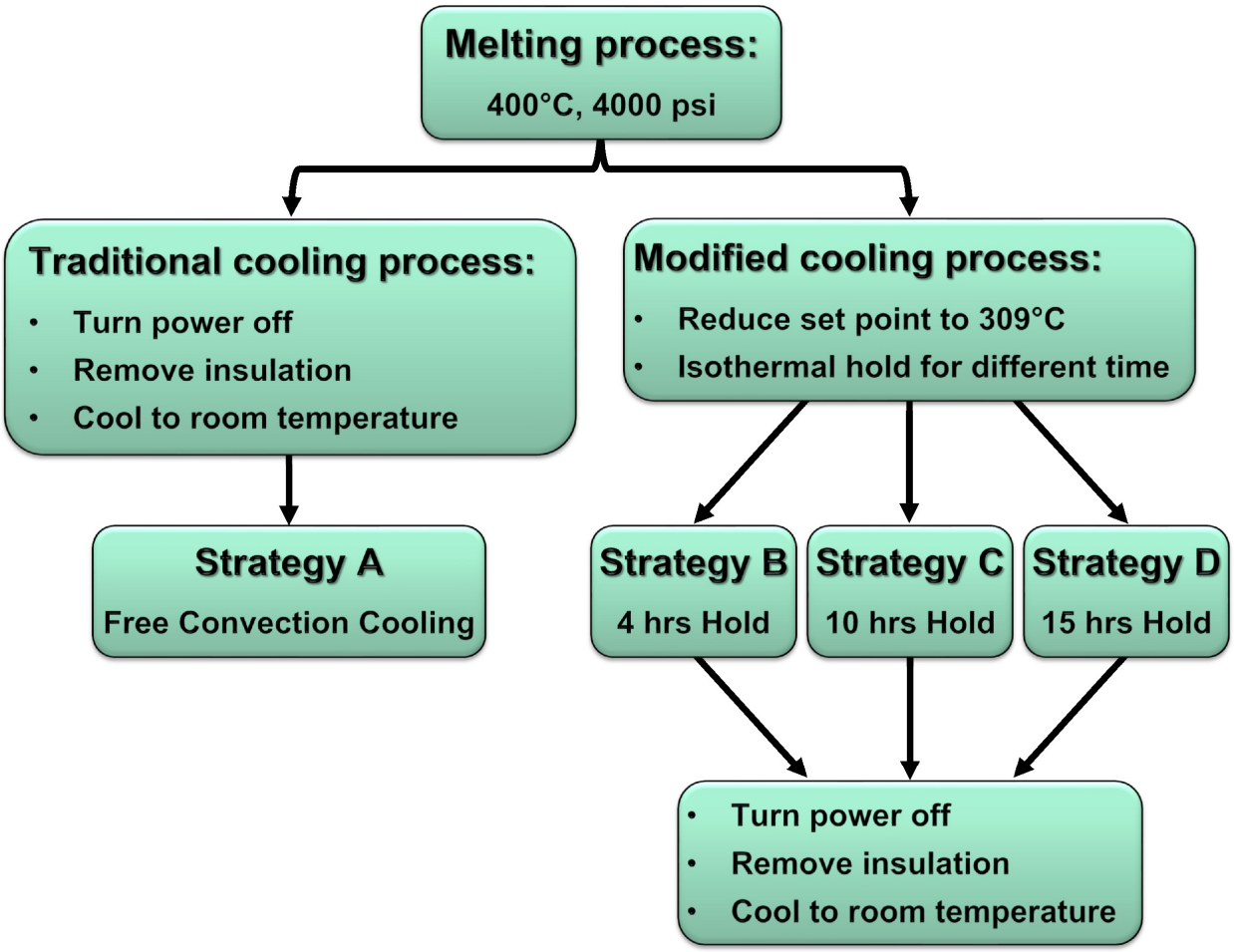

Figure 4.5. Process control strategies flowchart of compression molding experiments.

5 MATERIALS AND METHODOLOGIES

5.1 Materials and Bushing Production

Unfilled PEEK (KT820PF, Solvay) fine powder and PEEK filled Carbon Fibers composites (PEEK 450CA20) were donated by Hoerbiger Corporation of America (Hoerbiger Corp.) and used in this research. The CF/PEEK material was extruded and grinded into small chunks that could be used to produce large products via compression molding process. The summery of processing steps to produce CF/PEEK bushing are presented in **Figure 5.1**. Both neat and filled PEEK were compression molded into cylindrical bushings with 146.3 mm in OD, 38.1 mm ID, and 127 mm to 152 mm long. The four strategies explained in the previous section were used to govern bushing production.

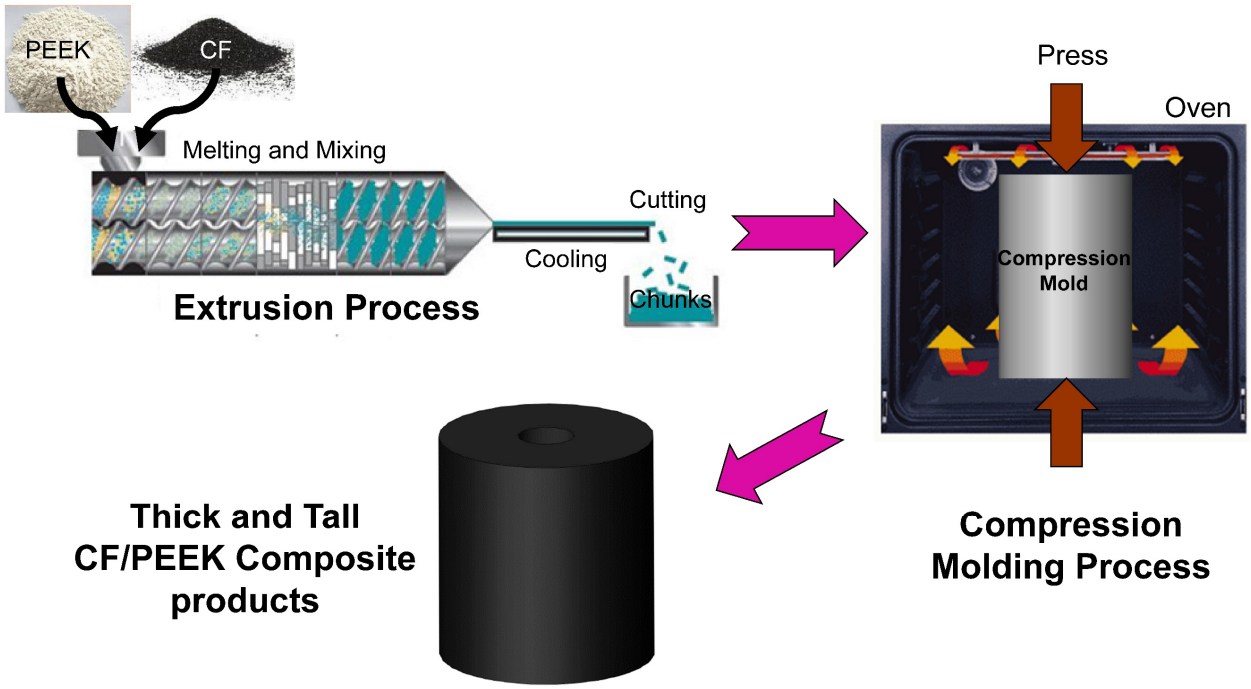

Figure 5.1. Processing steps to produce thick and tall CF/PEEK composite products.

5.2 Slicing Bushings and Preparing Specimens

The bushings fabricated through four different cooling strategies were sliced via a lathe into rings with ~ 6 mm thick as presented in **Figure 5.2**. A fluid was applied on the cutting area to prevent rising temperature and changing polymer properties caused by the local annealing that could happen with increasing temperature. Lathe speed and feed rate were adjusted to get a smooth cutting surface, avoid breaking the cutting tools, and prevent cracking the bushings during the cutting process.

Bushing slices were used to produce specimens for differential scanning calorimetry (DSC), Dynamic Mechanical Analysis (DMA), compression, and flexural tests. Specimens were taken from different places to reveal polymer properties throughout the bushings. To this end, for all tests, specimens were taken from top, middle, and bottom bushing length. For DSC and compression tests, three positions were considered for taking specimens from each slice; these were inner, middle, and outer diameters. While DMA and flexural test specimens were circumferential through the slice because those specimens are large, DSC, Flexure, and compression specimens' positions within the bushing are presented in **Figure 5.3**.

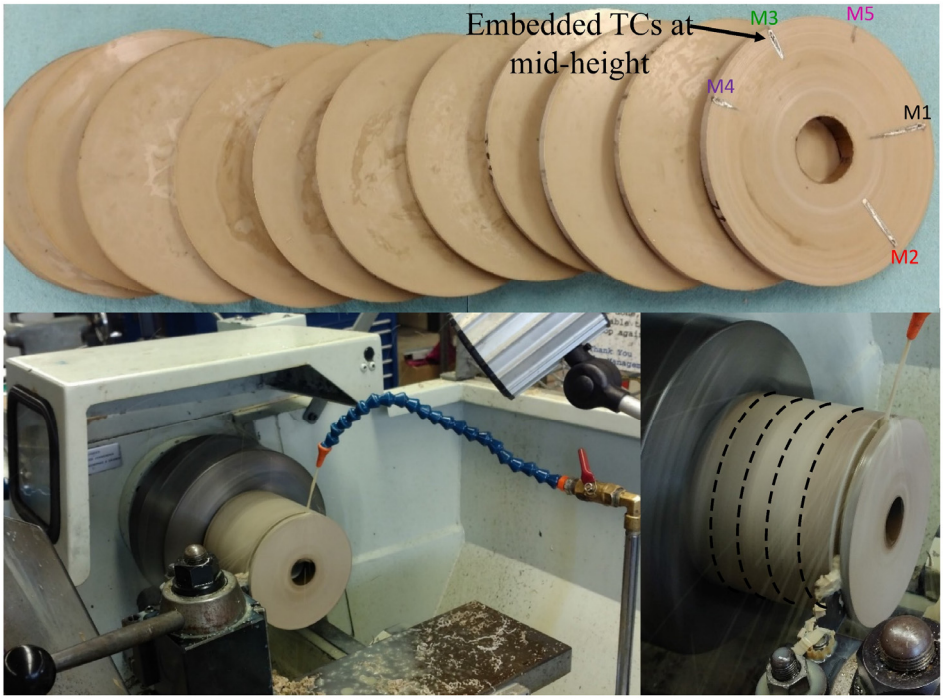

(a) Cutting neat bushing

(b) Cutting CF/PEEK bushing

Figure 5.2. Optical images of slicing compression molded (a) neat PEEK bushing and (b) CF/PEEK bushing using lathe.

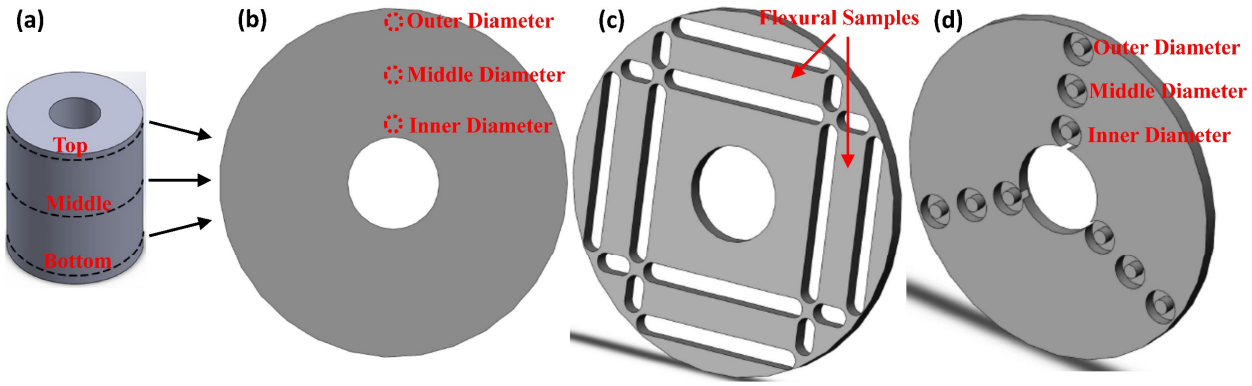

Figure 5.3. Schematic of samples positions within the sliced pieces of compression molding bushing. (a) PEEK bushing (b) DSC samples (c) Flexural samples (d) Compression samples.

DSC samples, 72 totals for neat PEEK and CF/PEEK, were prepared by cutting small pieces ~10 mg from the bushing, on the remarked areas in **Figure 5.3**, and hermetically sealing them in aluminum pans. SolidWorks software was used to design compression, DMA, and flexural specimens' patterns on bushing slices as shown in **Figure 5.3**. The final SolidWorks designs were used to program CNC to cut the specimens. Total of 72 flexural specimens were prepared according to ASTM D790 standard. Each specimen had rectangular prism shape with dimensions of (70 X 12.7 X 3) mm. DMA specimens had similar prismatic shape with smaller dimensions (30 X 10 X 3) mm according to ASTM D4065 standard. For neat PEEK compression tests, 216 cylindrical specimens with 6 mm diameter and 6 mm length were made from bushings processed using different strategies. While rectangular prisms with dimensions of (12.7 X 12.7 X 6) mm were used for CF/PEEK composites following ASTM D695 standard.

5.3 Characterization

5.3.1 Differential Scanning Calorimetry (DSC)

DSC - Q2000 (TA Instruments) provided with 50 mL/min nitrogen flow rate was used to analyze thermal behavior of as recieved neat PEEK powder (KT820) and CF/PEEK composites (PEEK 450CA20). Four samples with about 10 mg polymer were prepared and hermetically sealed in aluminum pans. Each sample was heated to 400 C at a rate of 20 C/min, isothermally held for 5 min, then fast cooled to room temperature at 75 C/min to clear thermal history. The next heating and cooling cycles indicated heating samples to 400 C, holding for 5 min, then cooling to 150 C at rates of 20 C/min, 10 C/min, 5 C/min, and 2 C/min.

Polymer melting temperatures Tm at different heating rates were found from second heating cycles, while second cooling cycles were used to identify the effect of changing cooling rate on crystallinity temperatures Tc and crystallization behavior. Crystallinity percentage was found from the following equation:

$$\text{crystallization}\% = \frac{\Delta H_c}{\Delta H_f} \text{ X } 100$$

Where ΔH_c = crystallization enthalpy found from area under peak of second cooling cycle. While ΔH_f = enthalpy of fusion for 100% crystallized PEEK = 130 J/g [37].

In addition, DSC-Q2000 was used to calculate the crystallinity of the compression molded neat PEEK and CF/PEEK composite bushings by extracting samples ~10 mg and hermetically sealing them in aluminum pans. The DSC samples were heated to 400 ºC at 20 °C/min to determine the enthalpy of fusion (ΔH_f) of the crystals and use it to find the crystallinity percentages of the processed polymers.

5.3.2 Compression Test

Compression specimens were prepared following ASTM D790 standard as explained previously. An electromechanical testing system (MTS Insight) was utilized to accomplish compression tests at room temperature and elevated temperature. During the test procedure, specimens were placed between two flat surfaces. Load was applied on specimen by moving top surface with speed rate of 0.006 mm/s and 0.026 mm/s for neat PEEK and CF/PEEK composites, respectively. Load vs. deflection data was collected during the test. Stress vs strain curves were calculated and used to obtain modulus of elasticity. Two environmental testing conditions were selected in investigate the manipulated polymer produced in this research. The first testing condition was at room temperature to evaluate the material behavior when they are applied for applications at room temperature environment. The other testing condition that was considered in this research was the elevated temperature. After consulting several industrial companies, the elevated temperature tests were performed at 225 ºC because it was the maximum temperature that PEEK products can be used and performed safely in high temperature applications. A convection oven with PID controlled was used to maintain the environmental testing conditions.

5.3.3 Flexural (Three-Point Bend) Test

Three-point bend test method was performed using MTS Insight Electromechanical Testing System to find flexural properties of PEEK bushings produced with different strategies. Flexural specimens were prepared as explained in previous section. In this test, specimens were placed upon two supports. According to ASTM D790 standard, span to depth ratio of 16:1 was needed as a distance between specimen's supports. Load was applied at the specimen top-middle surface using an indenter with an 0.5 mm curved end radius wedge. The indenter moved at 0.025

mm/s. Flexure tests were performed at room temperature and elevated temperature. Load vs. deflection data was collected during the test. Flexural stress σ_f, flexural strain ε_f, and modulus of elasticity in bending E_b were calculated using the following equations:

Flexural Stress $\sigma_f = \frac{3 * P * L}{2 * b * d^2}$ (MPa)

FLexural Strain $\varepsilon_f = \frac{6 * D * d}{L^2}$

Modulus of Elasticity in Bending $E_b = \frac{L^3 * m}{4 * b * d^3}$ (MPa)

Where

P = load at specimen midpoint (N).

L = support span (mm).

b & d = width and depth at specimen midpoint, respectively (mm).

D = deflection at specimen midpoint (mm).

m = slope of initial straight-line portion of load - deflection curve (N/mm).

Two environmental testing conditions, room temperature and 225 ºC, were selected for the 3-point-bend test as explained in previous section.

5.3.4 Dynamic Mechanical Analysis (DMA)

Dynamic mechanical analysis behavior was explored using an ARES-G2 rheometer (TA instruments). Torsional mode accompanied with strain amplitude of 0.05 % was applied to ensure remaining within the polymer linear viscoelastic region. A fixed frequency of 1Hz and a temperature ramp from 30 °C to 300 °C with 5 °C/min constant rate was implemented. Two vertical grips held the specimen ends. The grips and the specimen were placed inside a forced convection oven to monitor temperature and environmental conditions. A storage modulus G' and

loss modulus G'' as a function of temperature were obtained from this isochronal temperature sweep. Those values were used to find tan δ = G''/G' and plot it against temperature to estimate polymer glass transition temperature (Tg) from maximum peak.

5.3.5 Wide Angle X-ray Scattering (WAXS)

The compression molded PEEK bushings using different processing strategies were investigated via Bruker-AXS D8 Venture lμs CMOS kappa X-ray Diffractometer. Wide-angle X-ray scattering (WAXS) patterns were performed at a scanning steps size of 0.05° over a range of $4° < 2\theta < 49°$. The detector measured the total integrated intensity collected from the specimen. WAXS data was collected at detector distance of 50 mm. All scattering intensity measurements were corrected with respect to background scattering. X-ray specimens with thickness ~ 1.0 μm were sectioned from trimmed block specimens at various positions of the bushings processed using different strategies. LEICA EM UC7 ultramicrotome with diamond knife was used to prepare the ultra-thin sections. WAXS patterns were used to evaluate the morphology changes throughout the bushing for various processing strategies.

5.3.6 Scanning Electron Microscopy (SEM)

The morphology of CF/PEEK composites and carbon fiber diameters and dispersion within the matrix were studied via scanning electron microscopy [QUANTA 600 field emission-SEM (FE-SEM)]. The applied acceleration voltage and the spot size were 10 kV and 3 nm, respectively. The specimens were sputter coated with 10 nm layer of Iridium (Ir) to enhance the quality of the captured images. Over 50 measurements were collected to obtain a distribution of fiber diameters and confirm composite homogeneity.

5.3.7 Polarized Optical Microscopy (POM)

Crystal structure of the produced neat PEEK and CF/PEEK composite bushings using different strategies were studied via Zeiss Axiophot Polarized Optical Microscopy (POM). Microtome cut was used to prepare POM ultra-thin sections from trimmed block specimens at various positions of bushings processed using different strategies. Sections with thickness ~ 500 nm were prepared using a LEICA EM UC7 ultramicrotome with diamond knife. Ultra-thin section specimens of neat PEEK and CF/PEEK composite were placed on glass slides for POM observation. More than 20 specimens were made for each observed area to obtain the distribution of crystal morphology at different spots within that area.

6 EXPERIMENTAL RESULTS AND DISCUSSION

6.1 Holding Temperature of Compression Molding Process

The proposed compression molding processing procedure in this research is based on heating polymer above Tm, holding the temperature at Tc, and adjusting the holding time to obtain optimum results. Thus, it is important to determine melting temperature Tm and crystallinity temperature Tc of the pre-processed material in order to detect the required processing temperatures during the compression molding procedure.

Differential Scanning Calorimetry (DSC) was used to investigate thermal properties of as-received PEEK powder and CF/PEEK composites. Melting temperatures, crystallization temperatures, and crystallinity percentages at different heating/cooling rates are summarized in **Table 6.1**. It was noticed that decreasing the cooling rate would increase the melting temperature Tm, crystallization temperature Tc, and crystallinity percentage because slower cooling allows more time for the polymer to build its crystal structure. As mentioned previously, it is important to identify crystallization temperature value to apply it to step 4 of polymer processing procedure in **Figure 4.3**. Because Tc was sensitive to cooling rate, thick polymer bushing was compression molded using lab setting to evaluate lowest polymer cooling rate. The experimental data indicated that lowest cooling rate was ~ 0.5 C/min. Standard DSC didn't have the ability to control the cooling rate below 2 C/min; therefore, crystallization temperatures of neat PEEK and CF/ PEEK composite at cooling rate of 2 C/min was considered as a holding temperature of the proposed compression molding process in **Figure 4.3**.

Table 6.1. Melting temperatures, crystallization temperatures, and crystallinity% of pre-processed CF/PEEK composites and neat PEEK at different heating/cooling rates.

Heating/Cooling Rate (C/min)		Melting Temperature Tm (C)	Crystallization Temperature Tc (C)	Crystallinity (%)
Neat PEEK	20	341.1	286.8	31.2
	10	341	295.1	32.8
	5	343.3	301.5	34.6
	2	343.3	309.0	35
CF/PEEK	2	341.7	302.1	24.2

6.2 Compression Molding Temperature Profiles of Neat PEEK and CF/PEEK

Controlling semi-crystalline polymer process can have an essential influence on its crystal structure distribution [47-49], thus it can impact product properties and consistency throughout thickness and length. A compression molding setting with thermal control system was developed in this study, as explained in previous sections, to reveal the effects of manipulating compression molding processing parameters on properties and crystal structure of thick semi-crystalline polymers. Several experiments were conducted using lab compression molding setting to perform optimum temperature profile and demonstrate system stability during the process. A typical temperature profiles of shell, mandrel, and neat PEEK polymer during processing compression molded bushings are presented in **Figure 6.1**(a)-(b) and **Figure 6.2**(a), respectively. Thermocouples positions throughout polymer bushing cross-section and height are presented in **Figure 6.2**(b) and (c). Heat was applied on the mold to melt the polymer. The controllers set-points were programed to 400 C, which is above polymer melting temperature, and to 434 C to ensure melt all polymer crystal structures so that new and uniform crystal structure would grow during

the cooling process. Once the polymer melted, the control set points were reduced to crystallization temperature (309 °C) and hold to allow the polymer to build a uniform crystal structure through bushing length and cross-section. Eventually, thermal blanket insulation was removed to allow free convection cooling to room temperature. During the process, shell temperature profiles were uniform, smooth, and tracked input set-points throughout processing time, as presented in **Figure 6.1**(a). While oscillations, overshoot, and undershoot were observed in mandrel temperature data, see **Figure 6.1**(b). These differences can be attributed to controller types, locations, and heating zones of the system. In the shell, separate heating zones were used, as explained previously, that assisted in obtaining this uniform temperature profile through shell length. A single heater and controller were used to control heating through the mandrel and that made it difficult to acquire uniform temperature profile through mandrel length. The efforts to eliminate these differences failed because it was impossible to insert more than one cartridge heater in the mandrel zone. Moreover, the main goal of acquiring uniform temperature profile through shell and mandrel was to provide uniform temperature distributions for polymer during heating and holding temperature processes. Experimental data, presented in **Figure 6.1** and **Figure 6.2**, proved that oscillation, overshoot and undershoot throughout mandrel did not have big influence on polymer temperature profile because the polymer is an insulating material; therefore, no further action was required for improve mandrel temperature distributions.

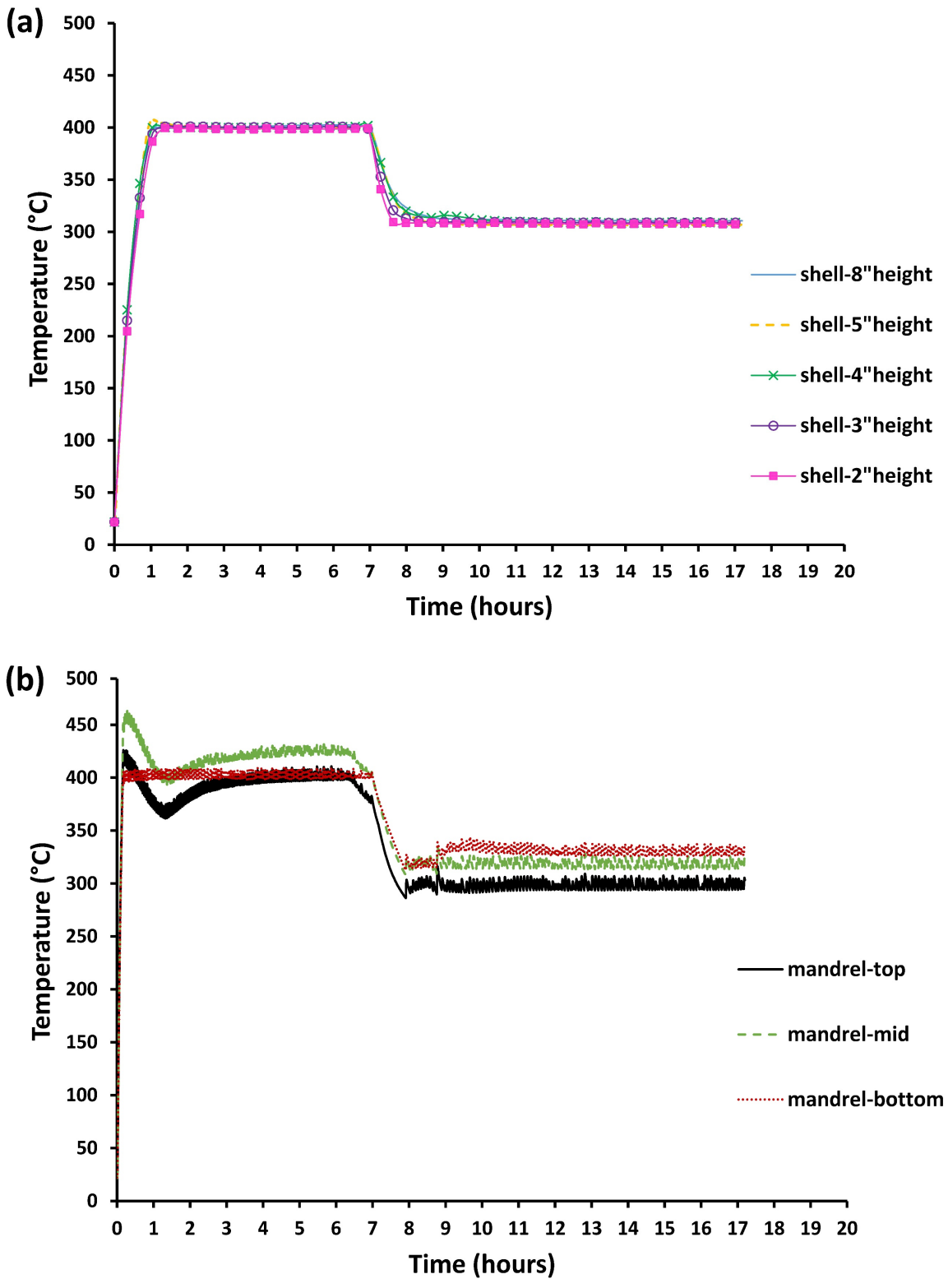

Figure 6.1. Temperature profiles of (a) shell and (b) mandrel during processing compression molded neat PEEK bushings.

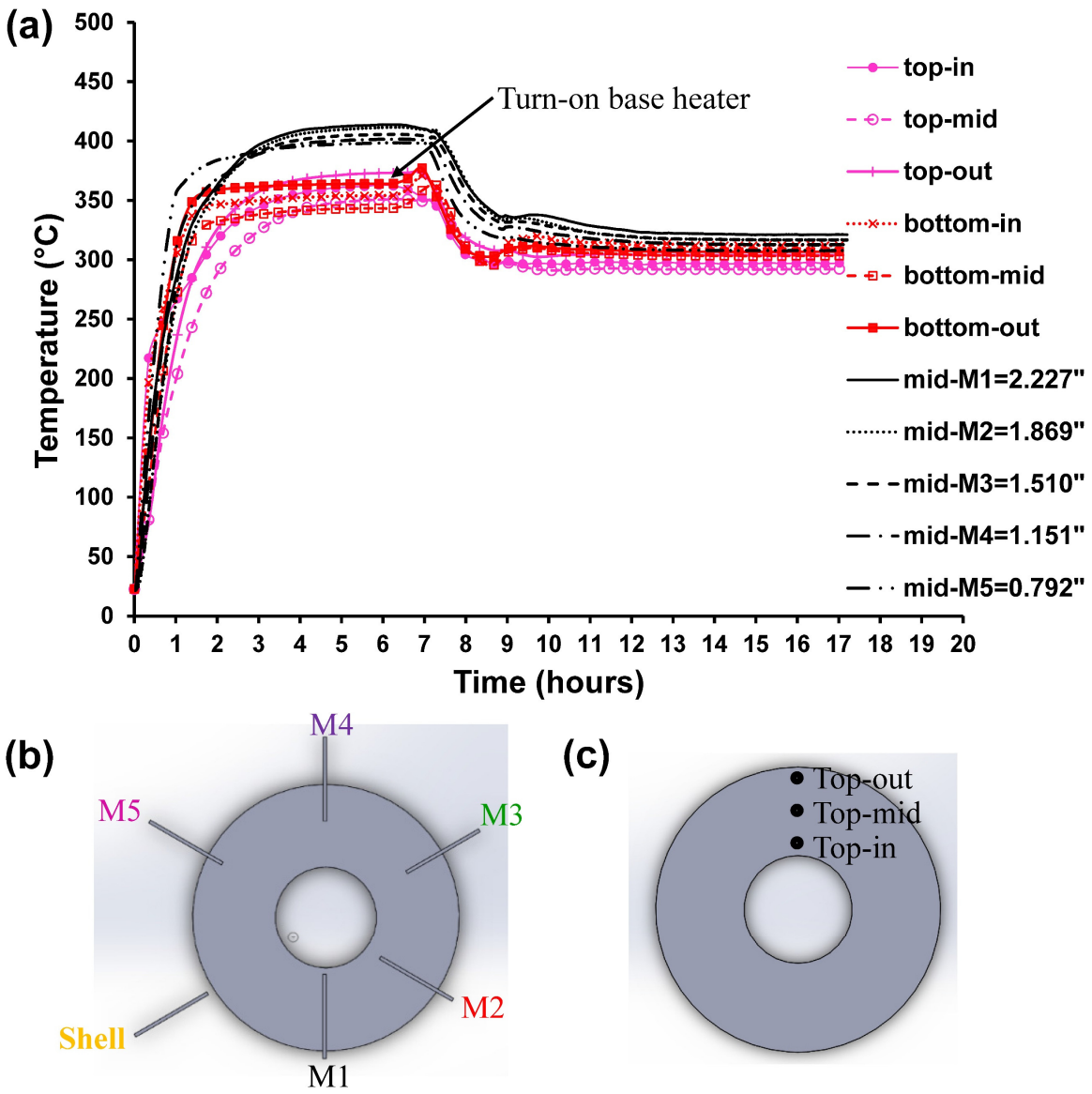

Figure 6.2. (a) Temperature profiles of neat PEEK polymer during compression molding process. Thermocouple positions along bushing cross-section at (b) mid-height and (c) top-height.

On the other hand, after reaching system steady state at set-points of 400 °C, polymer temperature at mid height reached 399 °C – 410 °C through its cross-section, see **Figure 6.2**(a). The highest polymer temperature was observed near mandrel because temperature was higher at

that position compared with mandrel top and bottom, see **Figure 6.1**(b). It was also noticed that maximum polymer temperature at top and bottom, **Figure 6.2**(a), never reached 400 °C because heat was lost through convection and conduction to environment. Temperature ranges at polymer top and bottom sections were 352 °C – 373 °C and 344 °C – 364 °C, respectively. Turning base heater on helped increasing temperature to a range of 365 °C – 378 °C through polymer bottom cross-section. After melting polymer, control set-points were reduced to crystallization temperature Tc of 309 °C. As system reached its second steady state point, it was noticed that temperature differences throughout polymer mold were ~ 25 °C. Lowest polymer temperature was observed in middle thickness of top mold section (top-mid) while highest polymer temperature was indicated in the mid height near mandrel, as illustrated in **Figure 6.2**(a).

CF/PEEK composites process followed same procedure as neat PEEK polymer compression molding process, except the holding temperature was 302 ºC for composites instead of 309 ºC for neat polymer; therefore, similar temperature profiles of shell and mandrel was detected. The resulting temperature profiles of CF/PEEK composite bushing during the process are presented in **Figure 6.3**. Thermocouples throughout bushing cross-section and height were placed in similar positions to the neat PEEK setting, see **Figure 6.2**(b) and (c).

The controllers set-points were initially programed on 400 ºC to melt the material. When system reached steady state, the control set points were reduced to CF/PEEK crystallization temperature (302 ºC) and hold to allow the material to build a uniform crystal structure throughout bushing length and cross-section. Ultimately, thermal blanket insulation was removed and the system was left to cool to room temperature. Following the behavior detected in the neat polymer process, shell temperature profiles during the composite processing were uniform, smooth, and tracked input set-points throughout processing time, as shown in **Figure 6.1**(a). While oscillations,

overshoot, and undershoot were observed in mandrel temperature data for the same reasons explained previously, see **Figure 6.1**(b). By comparing the temperature profiles after reaching system steady state for both processes of neat PEEK in **Figure 6.2**(a) and CF/PEEK composites in **Figure 6.3**, it was noticed that less temperature differences throughout the processed composite bushing compared with the neat polymer bushing. Thus, the presence of carbon fibers in the PEEK polymer enhanced temperature distribution throughout the processed bushing.

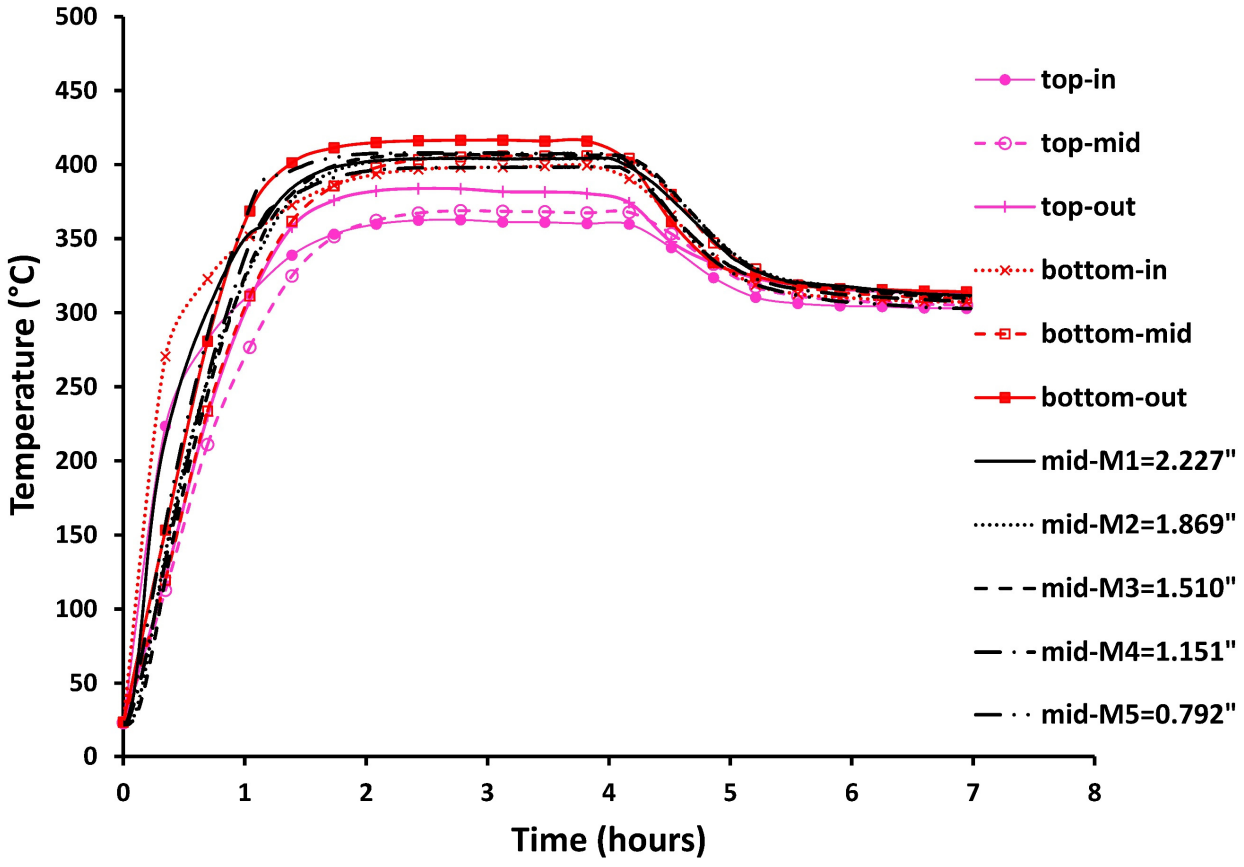

Figure 6.3. Temperature profiles of CF/PEEK polymer composites during compression molding process.

6.3 Process Melting Time and Holding Time at Crystallization Temperature

Temperature distributions through neat PEEK and CF/PEEK composite bushing cross-section at middle height were further studied to estimate time required for melting the materials as well as the holding time necessary for the system to reach its steady state at crystallization temperature. For that, temperature profiles through mold radius at middle height for different time of heating and cooling process were presented in **Figure 6.4**(a) and (b) for neat PEEK process and **Figure 6.5**(a) and (b) for CF/PEEK composite process.

For the case of neat polymer, it was observed that the system needed about 4 hours to reach its steady state during heating to 400 C, see **Figure 6.4**(a). Moreover, the system needed another 4 hours to reach its steady state after reducing control set-points to crystallization temperature as illustrated in **Figure 6.4**(b). For CF/PEEK polymer composite, the process reached its steady state after 2 hours during heating to 400 C as presented in **Figure 6.5**(a). Same time, i.e. 2 hours, was spent to cool the CF/PEEK from melting point to the crystallization temperature and reach its steady state, see **Figure 6.5**(b).

Eventually, the time required for reaching system steady state in the case of CF/PEEK process was almost half the time required for neat PEEK process because the carbon fibers improved polymer thermal conductivity. So, it can be concluded that adding carbon fibers to the PEEK polymer assisted in accelerating the compression molding process.

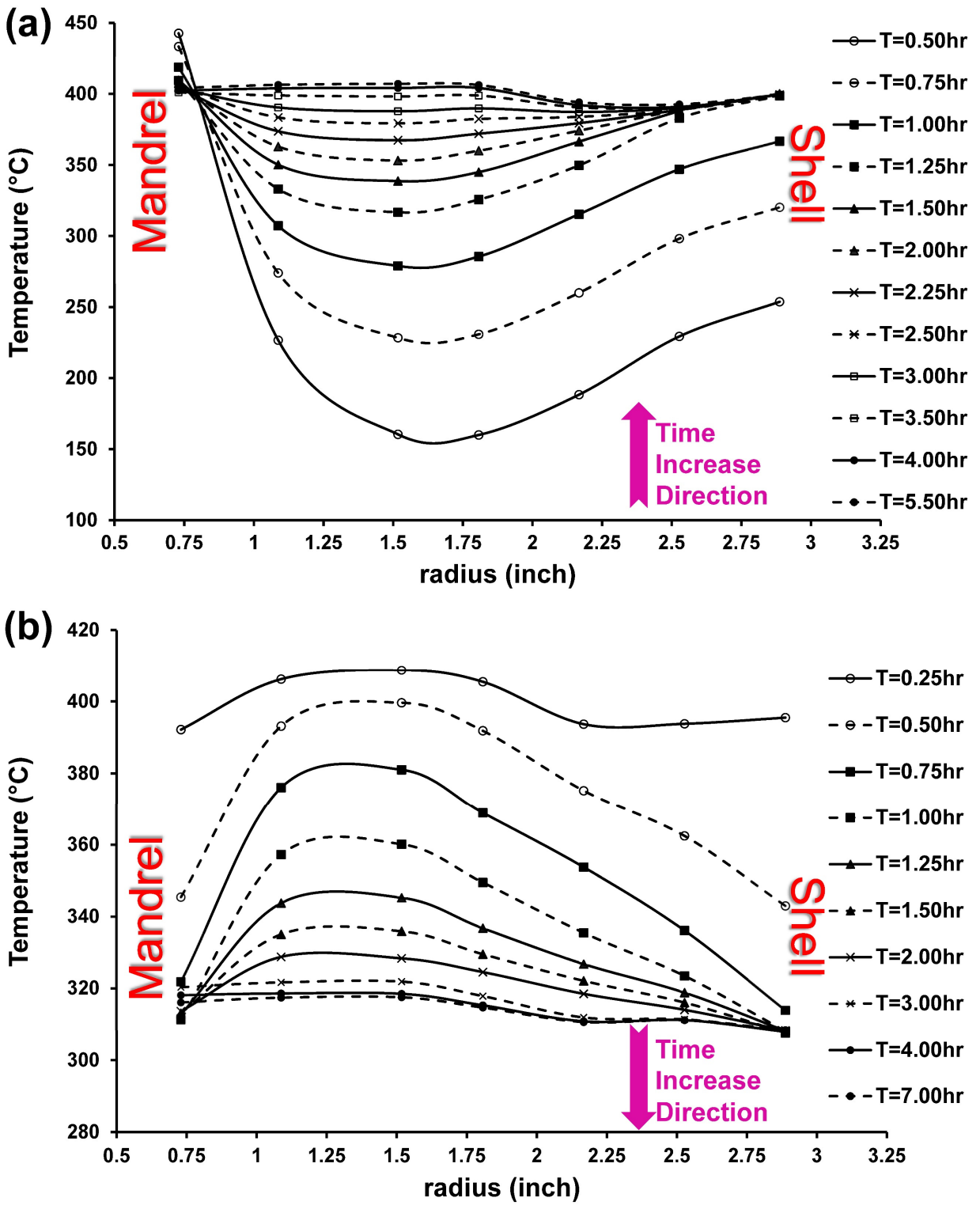

Figure 6.4. Temperature profiles of neat PEEK middle height bushing during (a) heating process and (b) cooling process of compression molding.

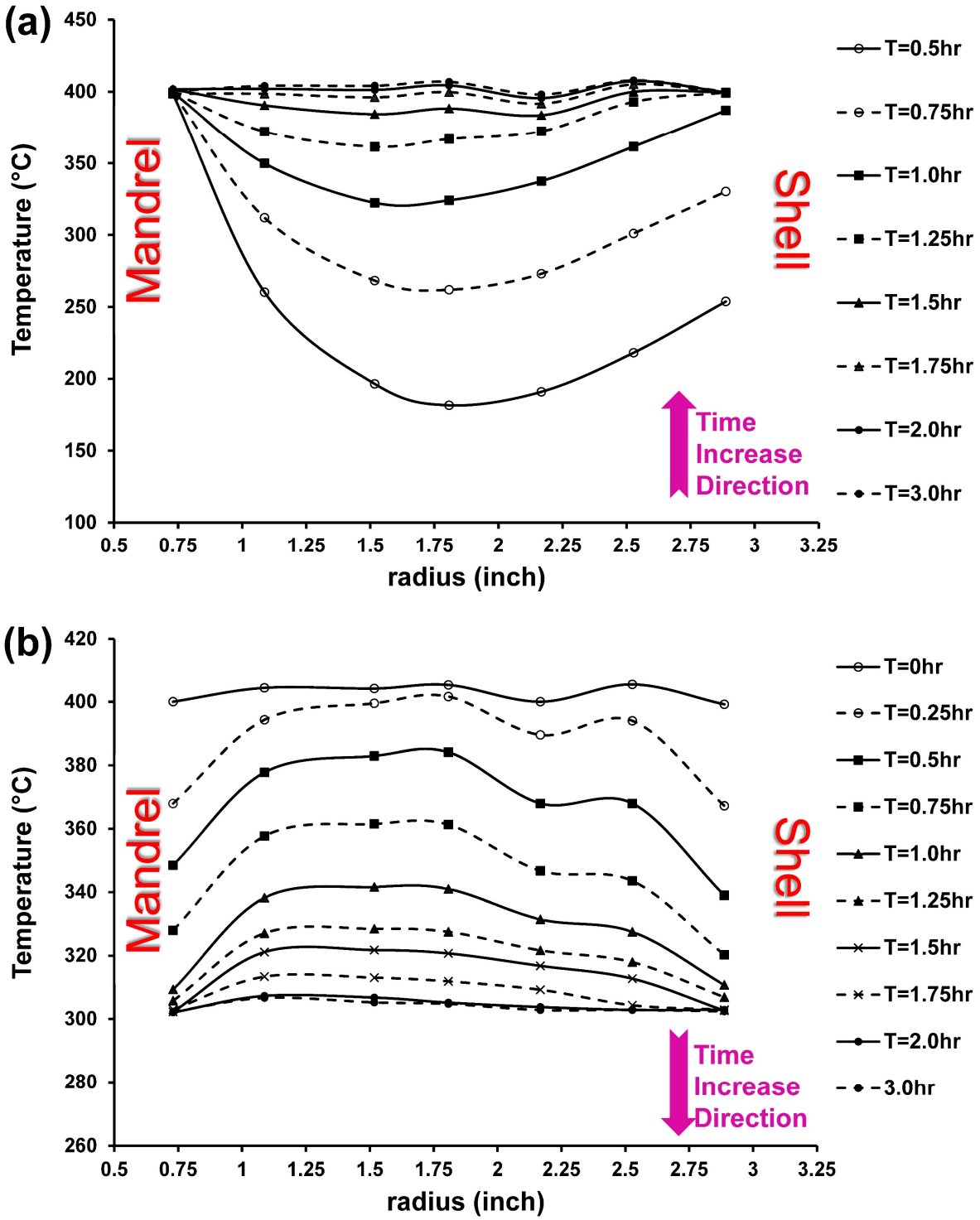

Figure 6.5. Temperature profiles of CF/PEEK middle height bushing during (a) heating process and (b) cooling process of compression molding.

6.4 Thermal Analysis

Total of 72 DSC specimens for neat PEEK and CF/PEEK composites were prepared from the bushings produced with four different strategies as explained in previous section. DSC - Q2000 was used to find enthalpy of fusion (ΔH_c) for each specimen by heating them to 400 C at a rate of 20 C/min. Then, crystallinity percentage was calculated from the ratio between enthalpy of fusion (ΔH_c) to enthalpy of fully crystallized PEEK (ΔH_f = 130 J/g [37]).

6.4.1 Neat PEEK

Crystallinity percentage for different processing strategies are presented in **Figure 6.6** and **Figure 6.7** throughout bushing radius and length, respectively. Based on DSC measurements, traditional compression molding process with free convection cooling, represented by strategy A, produced bushing with wide range of crystallinity (22.5-37.9) %. Holding temperature at crystallization until system reached its steady state, strategy B with holding temperature for 4 hours, produced bushing with consistent crystallinity (29.0-32.1) %. That is potentially caused by providing enough time for polymer to build its crystal structure. On the other hand, DSC results indicated that holding temperature for additional time of 10 hours and 15 hours, strategy C and D respectively, had small influence on increasing overall average crystallinity % and enhancing consistency throughout bushing; where crystallinity ranges of strategy C and D were (30.0-33.5) % and (30.3-33.2).

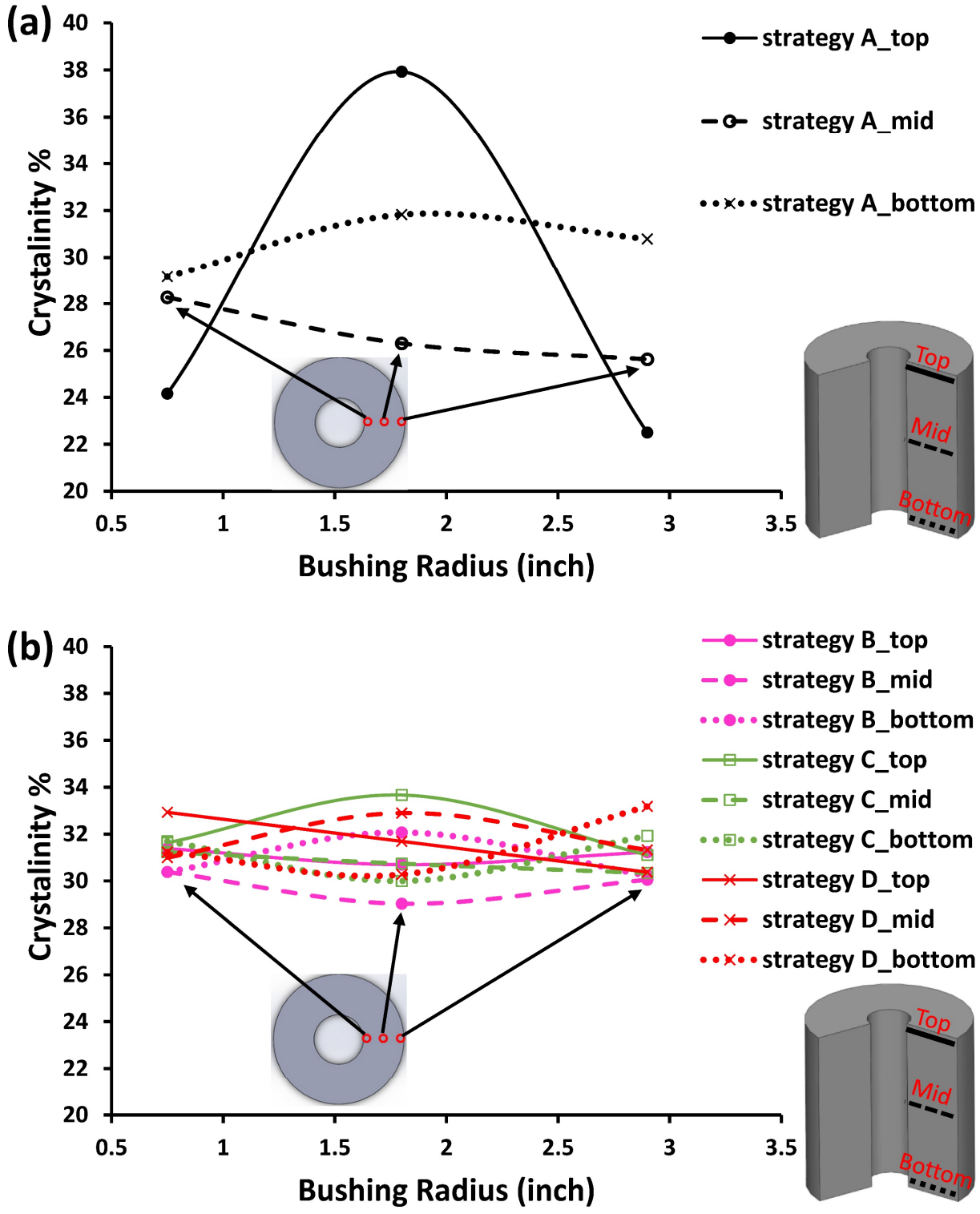

Figure 6.6. Crystallinity distributions of neat PEEK bushings along bushing radius for different processing strategies. (a) strategy A and (b) strategies B, C, and D.

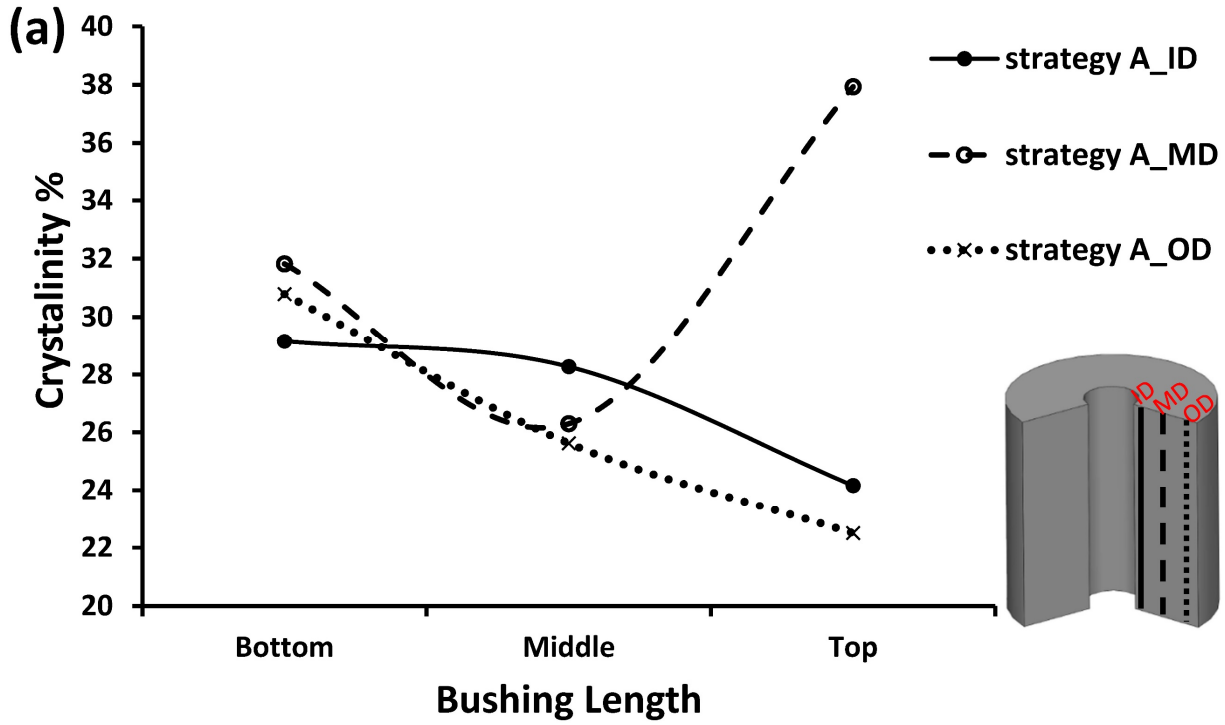

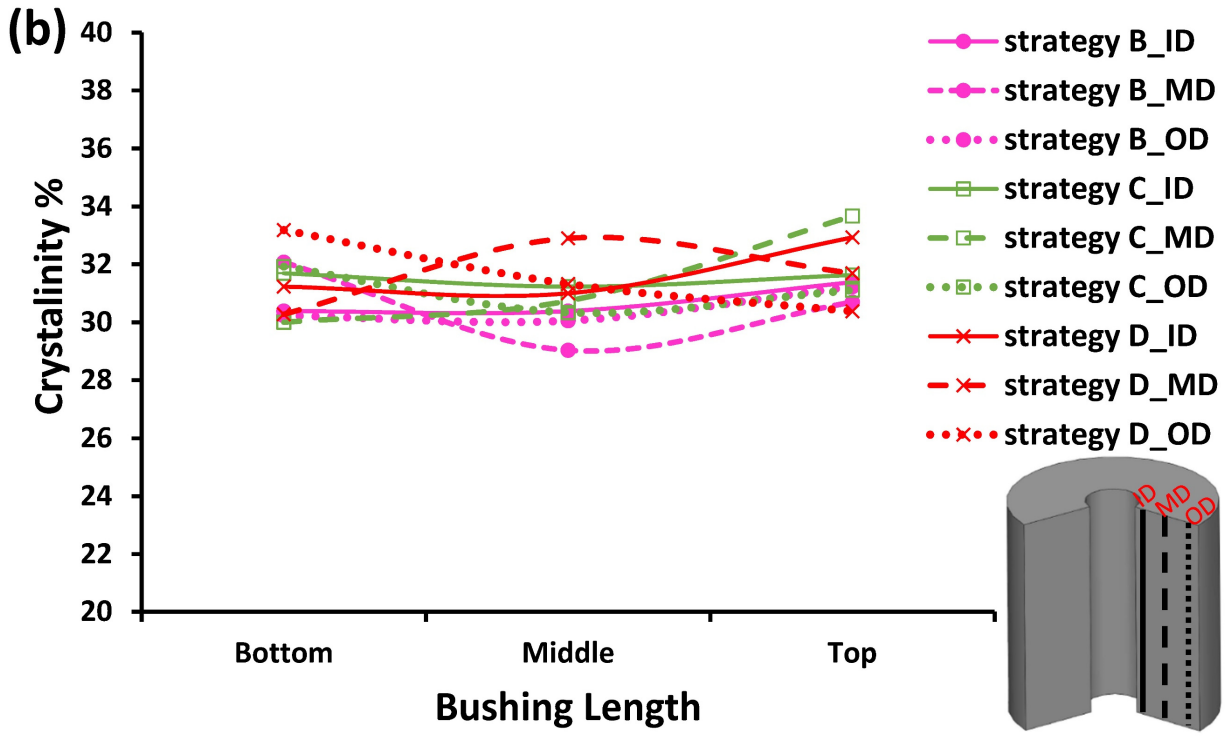

Figure 6.7. Neat PEEK bushings crystallinity distributions throughout bushing length for different processing strategies. (a) strategy A and (b) strategies B, C, and D.

Moreover, the effects of changing time of holding temperature at crystallization during compression molding process on average crystallinity and variability of thick wall neat PEEK bushings are presented in **Figure 6.8**. It was noticed that holding temperature for 4 hours had huge influence on shifting the crystallinity to a higher level and reducing the variability of the polymer to the minimum values. Holding temperature for further time kept similar variability and barely increased the average crystallinity of the thick wall bushing. That could be attributed to the highly aromatic structure of PEEK backbone that produced relatively stiff chains. Thus, polymer chains mobility was restricted after reaching a certain crystallinity percentage that prevented the polymer from building further crystal structure. Similar behavior was observed by Arzak et.al [62] during annealing process of small samples, where crystallinity % didn't change after increasing annealing time from 1hr to 24hrs. To this end, holding temperature at crystallization assisted in reducing crystallinity variability throughout bushing from 33% to 6%, which resulted in producing more consistent thick compression molded parts.

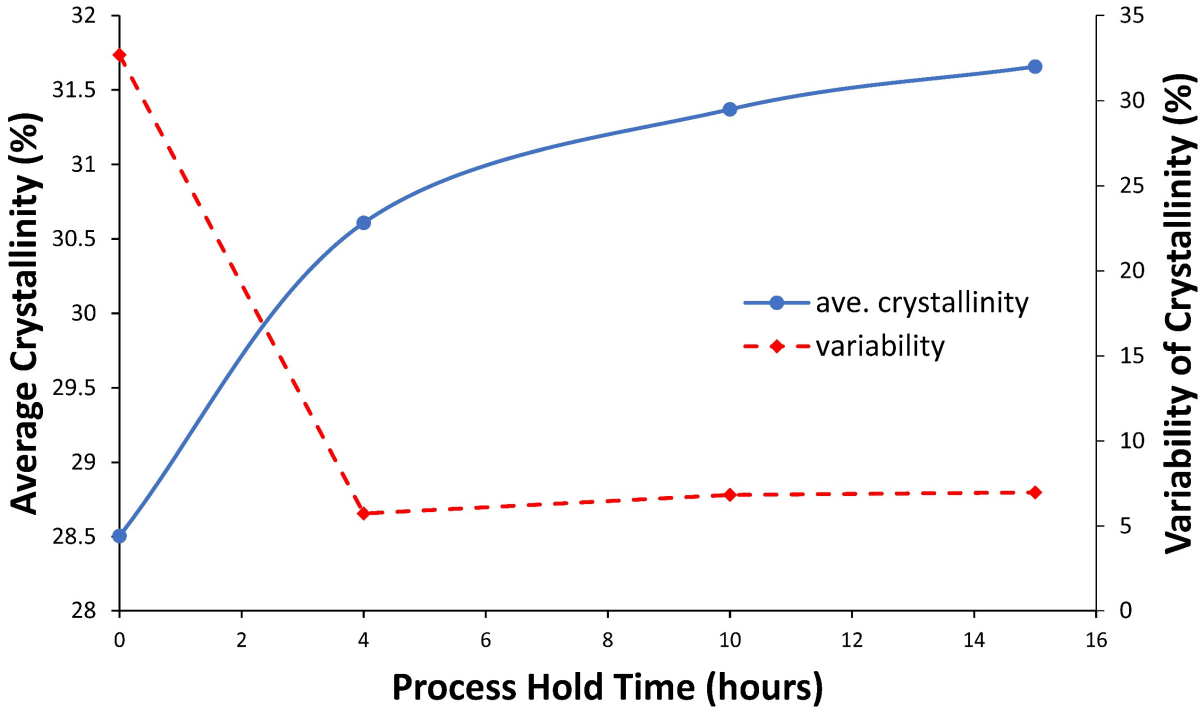

Figure 6.8. The influence of changing time of holding temperature at crystallization during compression molding process on average crystallinity and variability of thick wall neat PEEK bushings.

Differential Scanning Calorimetry (DSC) curves of bushing top section processed using traditional free convection cooling method vs. holding temperature at crystallization method are illustrated in **Figure 6.9**(a) and (b), respectively. Double melting point was observed in DSC curve at top middle thickness of bushing processed in strategy A, **Figure 6.9**(a), which indicates building different crystal structures within the polymer in that particular section. PEEK stiff backbone nature usually enhances chains' tendency to produce constrained rigid amorphous and disordered small crystals if the process of crystallization from melt was not given sufficient time to finalize the structure. As a consequence, double melting behavior originates because holding the

temperature for small time is not enough to fully develop the secondary crystal structure between the primary lamellar and reorganize the less-ordered structure [50]. Double melting point appears during DSC trace because melting the secondary structure with less-ordered and thinner lamellar thickness is followed by melting the primary structure with higher-ordered and thicker lamellae at a higher temperature [82].

In strategy A, there was no external temperature holding using control system, i.e. free convection cooling. However, losing heat throughout the part was not fast enough, i.e. heat was automatically held in some positions especially mid thickness, because of having thick insulated material. In addition, the holding time wasn't enough to fully build the secondary crystal structure that resulted on appearing the double melting point in bushing mid thickness of strategy A. On the other hand, fast cooling rate can result on building small crystal structure compared with slow cooling rate that allows increasing spherulite crystal radius [47, 49]. In strategy A, cooling rate near inner and outer diameters of thick part was fast which resulted in building small crystal structure compared with mid thickness that exposed to lower cooling rate. Subsequently, thick high performance polymer processed in strategy A had different crystal structure at inner and outer diameter compared with middle thickness structure in addition to having dual crystal structure, primary and secondary structures, in the same position of bushing middle thickness. The double melting points phenomenon was disappeared and the peak became narrower after holding temperature at crystallization, **Figure 6.9**(b), because providing enough time built the same crystal structure throughout part cross-section and length.

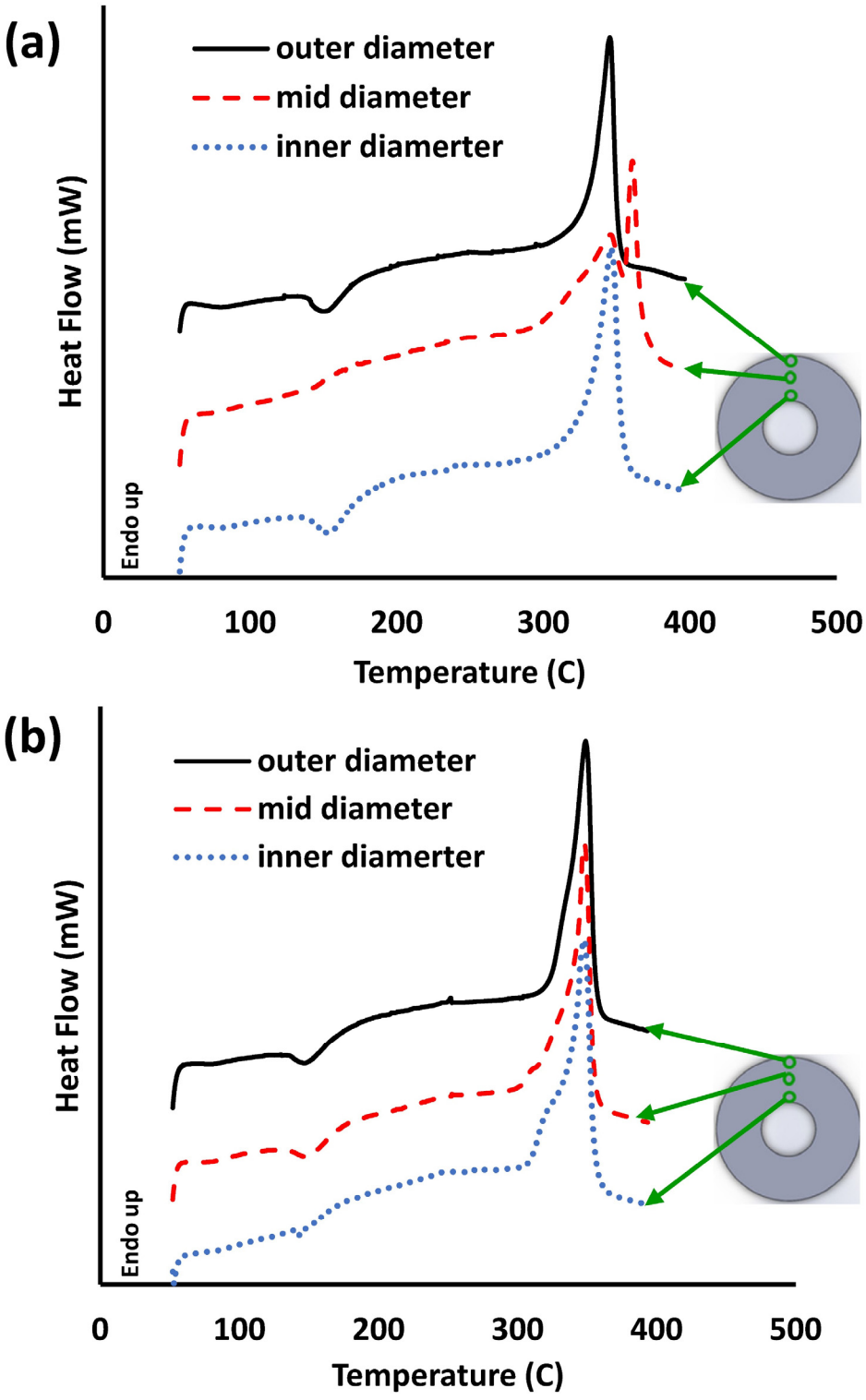

Figure 6.9. DSC curves of neat PEEK bushing top section processed using (a) traditional free convection cooling method vs. (b) holding temperature at crystallization for 15 hours.

6.4.2 PEEK Filled Carbon Fiber Composite (CF/PEEK)

DSC results of CF/PEEK composite showed that free convection cooling process produced bushing with crystallinity range of (23.1 – 29.8) %. While holding temperature at crystallization for 15 hours produced bushing with crystallinity range of (27.6 -31.7) %. Crystallinity percentages of CF/PEEK composite throughout bushings processed using different strategies are demonstrated in **Figure 6.10**(a) and (b). It was observed that top height of bushing processed using free convection cooling had lowest crystallinity because cooling process was accelerated at that section more than the other bushing sections. Holding temperature for sufficient time assisted in acquiring more consistent crystallinity throughout the bushing. However, it did not highly increase the overall crystallinity of the bushing because it already was approaching ultimate material crystallization capabilities.

The crystallinity of neat PEEK vs. CF/PEEK composites for traditional free convection cooling and holding temperature for 15 hours are introduced in **Figure 6.11**(a) and (b), respectively. The crystallinity curves of CF/PEEK bushing processed using traditional free convection cooling had similar trend to the neat PEEK bushing processed using same strategy. In both cases, the top bushing section had the lowest crystallinity. However, the composite bushing top section did not show high crystallinity at the middle thickness because it did not experience a double melting phenomenon that appeared in neat polymer bushing. In general, top bushing location suffered from accelerating cooling by convection; this was accompanied with reheating from the hotter material within the bushing. These combined processes introduced complicated heat transfer environment with fluctuating thermal gradient that had a huge impact on building various microstructure and producing double melting point in neat polymer, as explained previously. While, CF presence eliminated this scenario by enhancing polymer thermal

conductivity that forced shaping and reducing thermal gradient behavior throughout the material. Thus, Double melting peaks disappeared at the top section of the composite part because normalizing heat distributions along the bushing with the CF involvement prevented heat lock inside the material, and consequently hindered variance in crystal formation.

Moreover, unlike neat bushing, CF/PEEK bushing reflected a low crystallinity at the bottom near the outer diameter; this could be attributed to enhancing the cooling rate with the CF presence. However, the bushing middle height outer diameter experienced a higher crystallinity compared with the bushing outer diameters at the top and bottom heights. As it is known, the material tends to lose the heat through the path with the highest thermal gradient. Thus, the heat lost direction at the bushing top and bottom sections was radially and longitudinally, i.e. through bushing radius and length. While bushing middle height section was losing most of the heat radially. Thus, middle section was losing the heat in a relatively slower rate compared with the top and bottom section. This allowed the material in this section to build more crystalline structure, and subsequently maintain higher crystallinity. Excluding the differences that addressed above, the overall crystallinity profiles of CF/PEEK and neat PEEK bushings for both traditional convections cooling process and holding temperature process were similar.

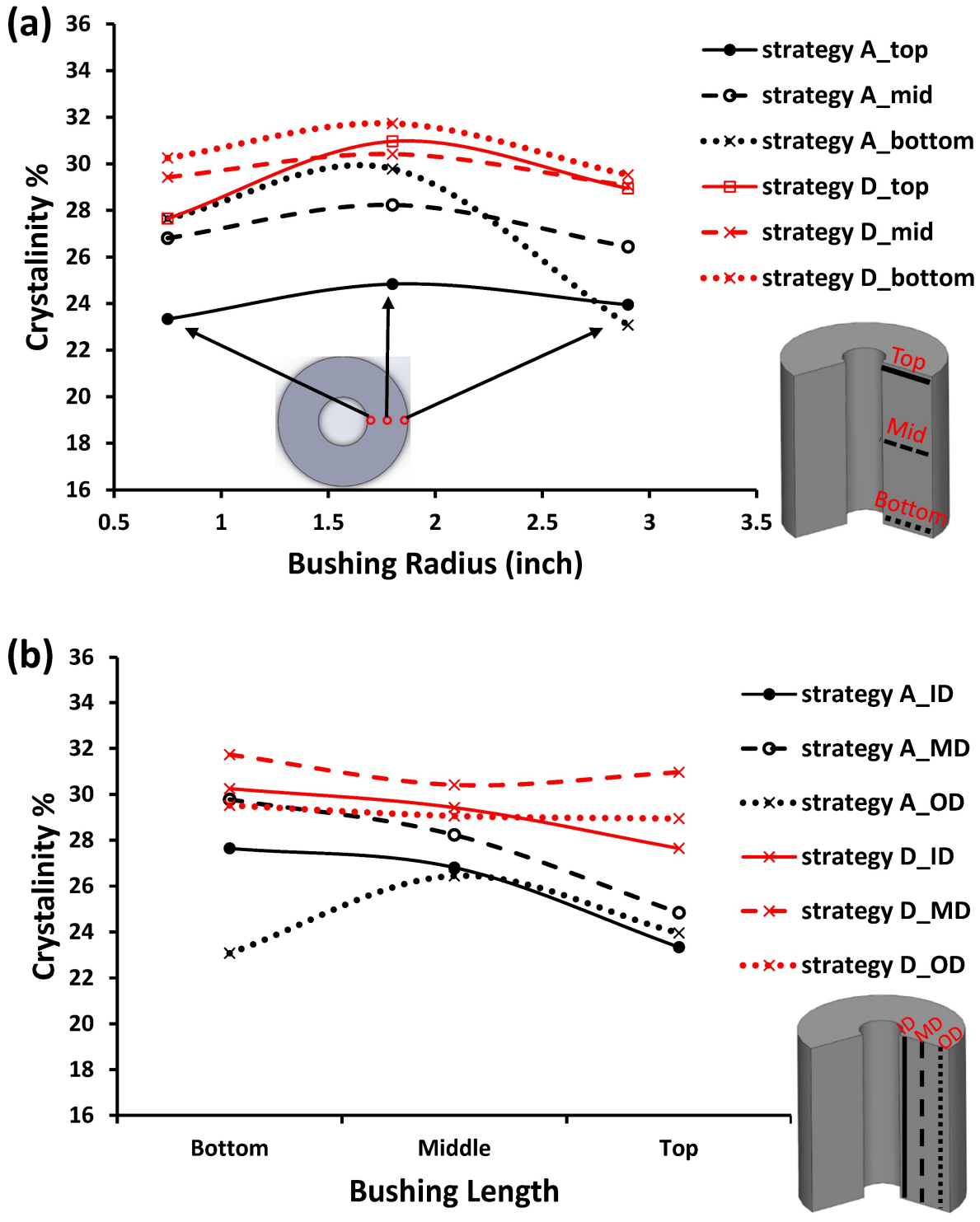

Figure 6.10. Crystallinity distributions of CF/PEEK composite bushings along (a) bushing radius and (b) bushing height for different processing strategies. ID: bushing inner diameter, MD: bushing middle diameter, OD: bushing outer diameter.

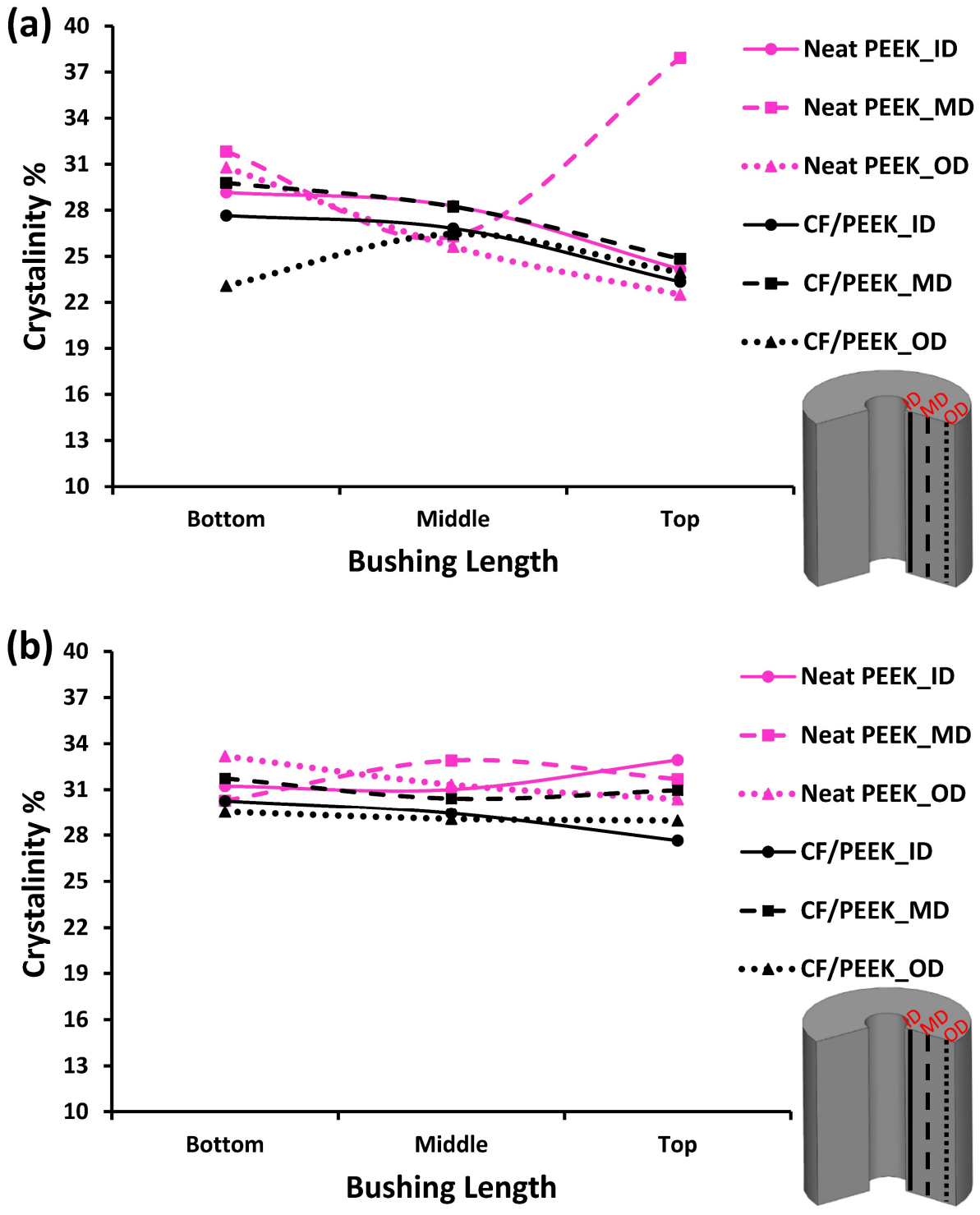

Figure 6.11. Crystallinity distributions of neat PEEK vs. CF/PEEK composite bushings for (a) free convection cooling process and (b) holding temperature at crystallization for 15 hours. ID: bushing inner diameter, MD: bushing middle diameter, OD: bushing outer diameter.

Although similar crystallinity profiles were produced throughout both neat and composite bushings regardless their processing strategies, it is important to mention that the variability in crystallinity throughout CF/PEEK bushing processed using traditional free convection cooling, in **Figure 6.11**(a), was lower than neat PEEK bushing produced using same strategy. Introducing CF filler to polymer made crystallinity varies by 18% throughout free convection cooling bushing compared with 33% variability in the neat polymer bushing. In this case, CF reduced variability in crystallinity along traditional free convection cooling bushing by enhancing the material thermal conductivity and reducing thermal gradient throughout thick long bushing. In general, enhancing material thermal conductivity accelerates the cooling process, and subsequently prevents polymer from building its crystal structure. However, CF overcome this issue by playing significant role in accelerating crystallization process through increasing surface area and enhancing crystal structure initiation. These CF actions had huge favor on both processing time as well as crystallization amount and variability throughout bushing. The processing time was reduced by half, from 4 hours in case of neat PEEK to 2 hours for composites as it was observed previously. While similar overall crystallinity percentages with lower variabilities were produced throughout CF/PEEK bushing compared with neat bushing processed using traditional free convection cooling.

Holding temperature for sufficient time helped neat and composite bushings to enhance crystallinity uniformity as presented in **Figure 6.11**(b). The resultant variabilities from this processing strategy were 6% and 8% for neat PEEK and CF/PEEK bushings, respectively. However, it is important to mention that holding temperature at crystallization had more influence on neat polymer bushing compared with composite bushing. The variability was reduced from 33% to 6% for the neat PEEK bushing while CF/PEEK bushing crystallinity variation was reduced from 18% to 8% only. In both scenarios, holding temperature at crystallization enabled the material

to build additional crystal structure until it reached the ultimate polymer capacity. However, the variation along free convection cooling neat PEEK bushing was much higher than CF/PEEK bushing produced using same strategy (33% vs. 18%). Thus, manipulating the process by holding temperature at Tc had more influence on neat polymer over composites.

To this end, adding carbon fiber to polymer matrix assisted in reducing processing time and enhancing crystallinity distribution throughout the bushing processed using traditional free convection cooling by maximizing surface area and enhancing crystal structure formation. Holding temperature for sufficient time benefits thick parts produced from neat polymer more than thick composite products.

6.5 Polymer Morphology Distribution

Wide angle X-ray scattering WAXS was performed to further investigate the effect of changing processing strategies of thick polymer bushing and confirm whether there were significant changes in material structure. WAXS patterns along bushing processed using traditional free convection cooling are presented in **Figure 6.12**(a). While manipulated bushing processed by holding temperature at crystallization for 15 hours are shown in **Figure 6.12**(b). It was noticed that the peaks of middle height convection cooling bushing, in **Figure 6.12**(a), were sharper and longer, this is a sign of forming more crystal structure in that area. Much smaller peaks were shown at top and bottom height of same bushing, in **Figure 6.12**(a), which indicated having less crystallization. This could be attributed to the fast heat lost at the bushing ends compared with the middle bushing height, as explained in **section 6.4.2**, and subsequently not having enough time to build crystal structure in those sections. However, WAXS patterns were similar along bushing after holding temperature for 15 hours; this demonstrated forming identical structure along the

bushing, see **Figure 6.12**(b). Thus, the patterns differences along the traditional convection cooled bushing increased crystallinity variation along the bushing because cooling rate along the bushing was uncontrolled.

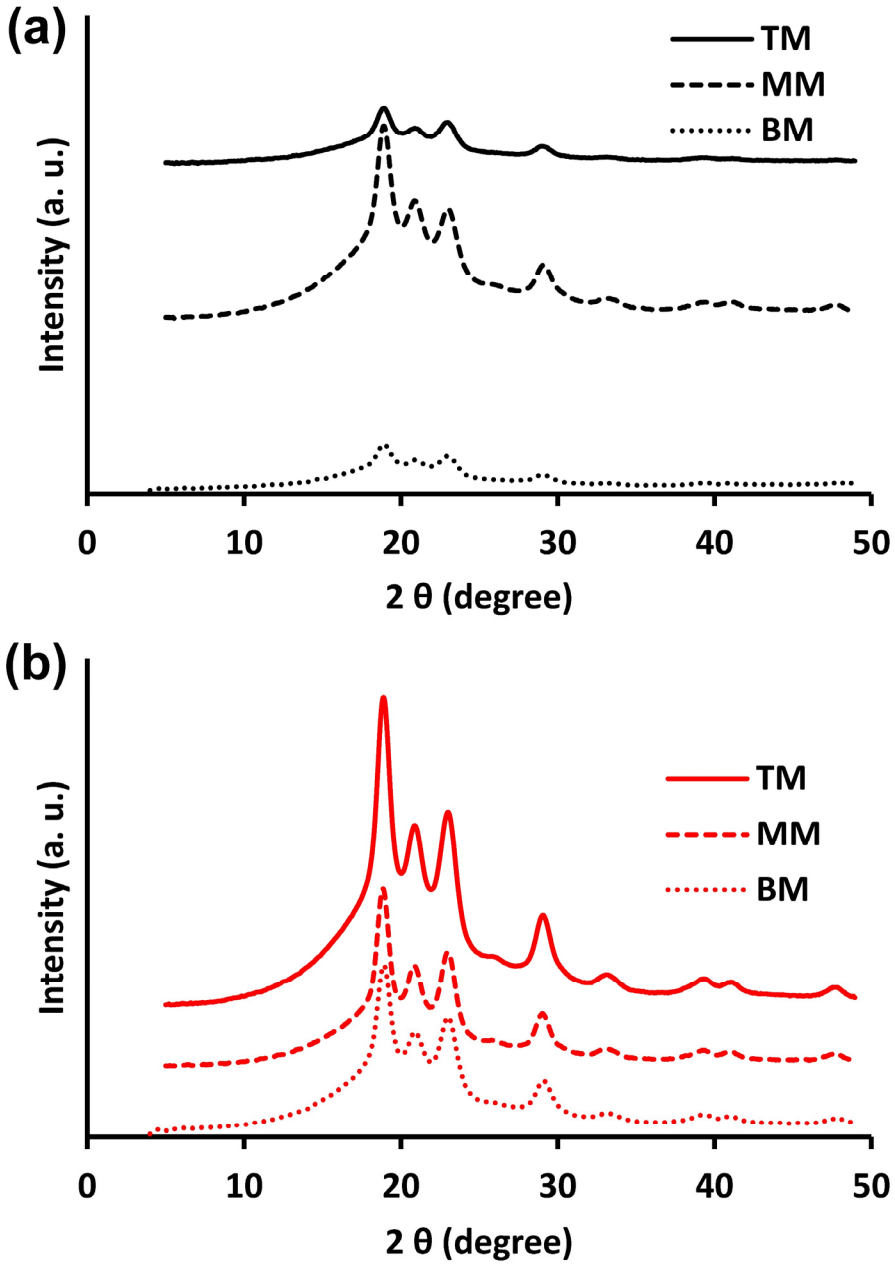

Figure 6.12. WAXS patterns throughout neat PEEK bushing length for (a) traditional free convection cooling method (b) holding temperature at crystallization for 15 hours. TM: Top height and Middle diameter of bushing, MM: Middle height and Middle diameter of bushing, BM: Bottom height and Middle diameter of bushing.

Moreover, comparisons of the two different processes (free convection cooling vs holding for 15 hours) at top, middle, and bottom bushing heights are presented in **Figure 6.13**(a), (b), and (c), respectively. WAXS patterns suggested forming similar crystal structure at the middle bushing regardless the processing method, see **Figure 6.13**(b), because the thick middle height section of convection cooled bushings slowly lose heat and that resulted in similar response as holding temperature at crystallization. While comparing the top bushing height of the two processes, in **Figure 6.13**(a), provided a clear indication of having less crystal structures in the case of free convection cooling compared with the same section of manipulated bushing. Similar behavior was observed for bottom bushing heights of both processes, as shown in **Figure 6.13** (c). The lower crystal structure content at top and bottom bushing height came from convection cooling effect at those sections that accelerated the cooling rate; while locking the heat by holding the temperature during the process produced uniform high crystal structure throughout the bushing.

To this end, WAXS patterns disclosed forming various morphologies along traditional free convection cooling bushing, while a uniform crystal structure was built throughout bushing processed by holding temperature for sufficient time. Although DSC revealed enhancing crystallinity uniformity throughout thick parts by manipulating the manufacturing processes, it didn't distinguish an obvious increase in crystal structure formation after holding temperature at crystallization. While WAXS measurements were able to highlight the crystalline structure increase as well as evaluate their uniformity by comparing the patterns along bushing for different processes.

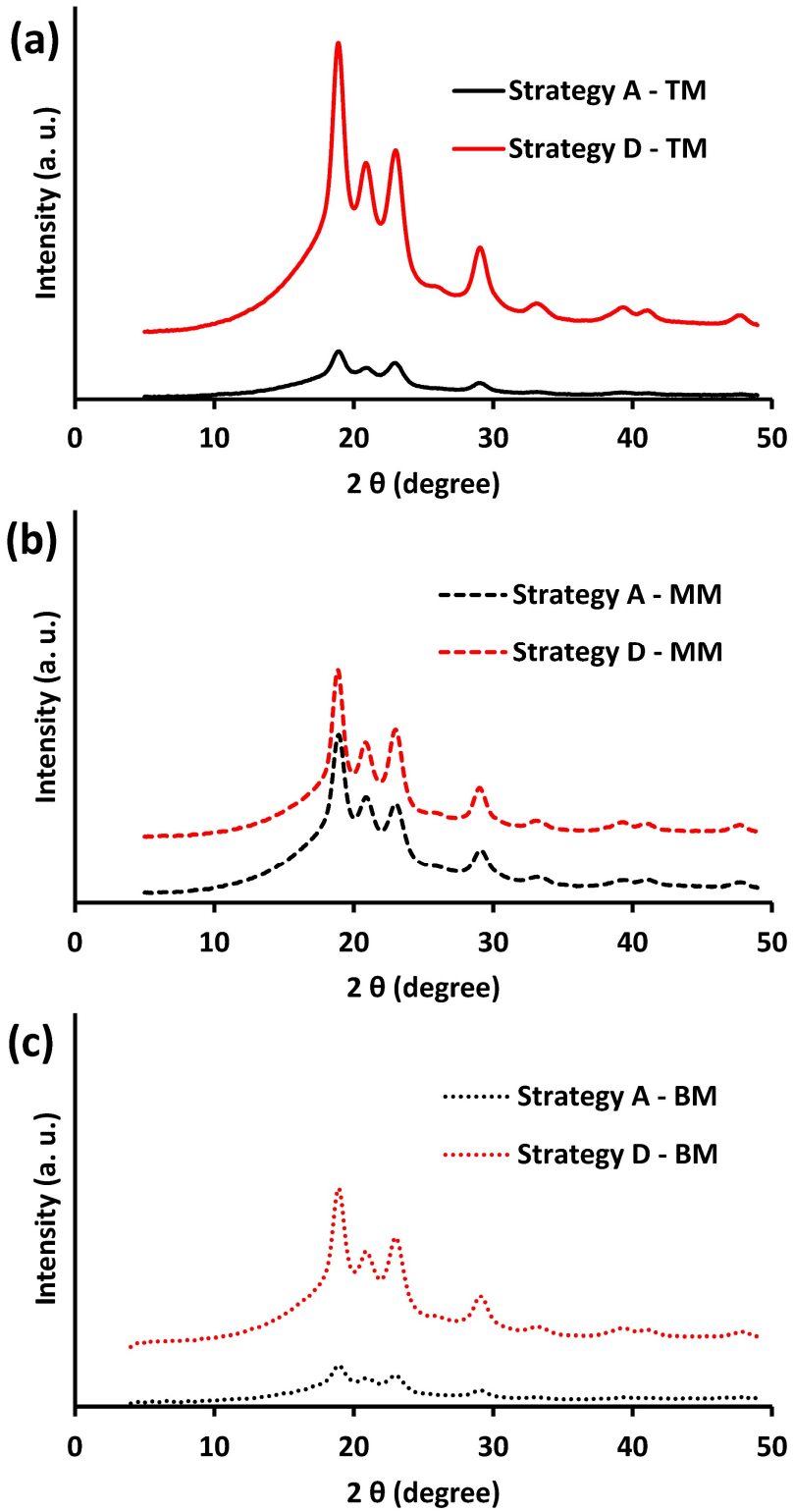

Figure 6.13. Neat PEEK WAXD patterns at bushing (a) top height, (b) middle height, (c) bottom height of different processing strategies.

6.6 Crystal Microstructure

Crystal microstructure of neat PEEK bushings processed using traditional free convection cooling method vs. holding temperature at crystallization for 15 hours are observed using polarized optical microscopy (POM). The crystalline structure distributions throughout the bushings processed using those strategies are shown in **Figure 6.14** and **Figure 6.15**. Different crystalline morphologies were observed along the bushing processed using free convection cooling (strategy A), as presented in **Figure 6.14**. The cooling process of strategy A was not uniform along the bushing where top bushing section lost the heat faster than other sections whereas middle bushing section was the slowest to lose the heat. Because slow cooling provide enough time for spherulites to grow large, while fast cooling prevent spherulite from growing to large structure [47, 49], various spherulite sizes were formed throughout the bushing processed using strategy A. large spherulites were produced at the middle bushing height, whereas small crystal structure were formed at the bushing top and bottom, as presented in **Figure 6.14**. However, it was found that involving additional processing step of holding temperature at crystallization for sufficient time assisted in forming similar size spherulite structures throughout the processed bushing, see **Figure 6.15**.

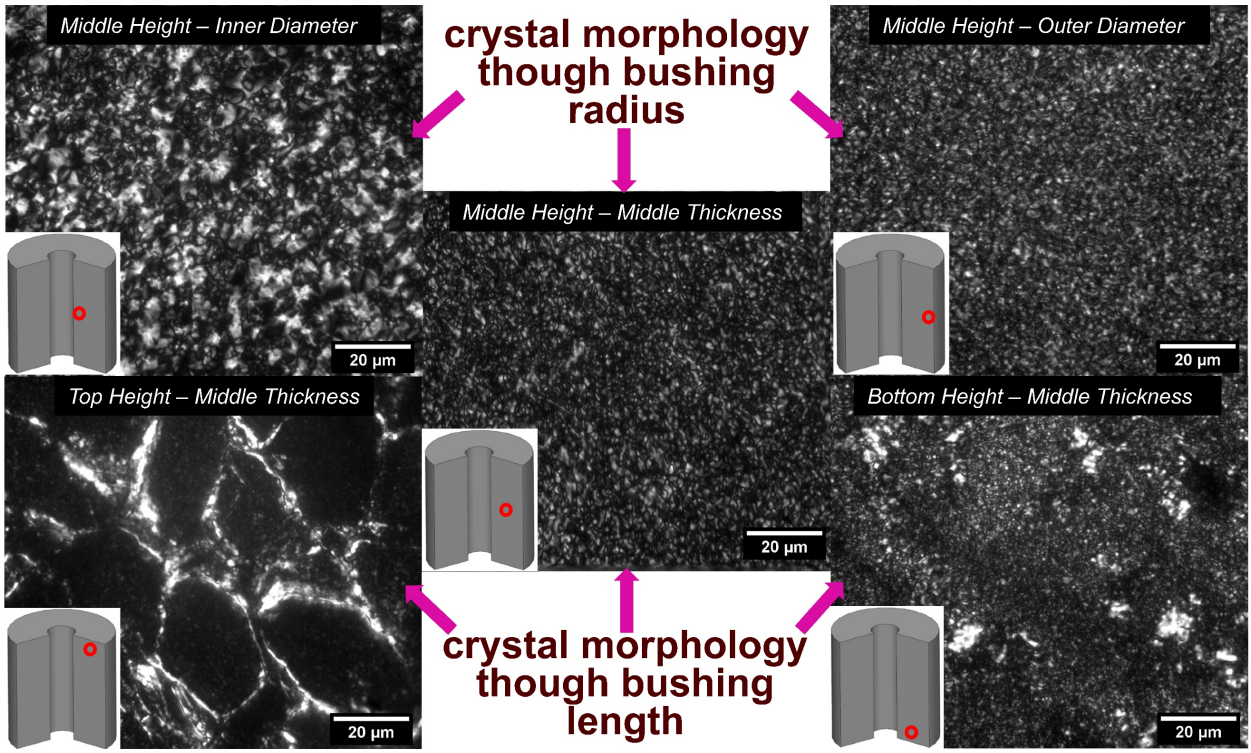

Figure 6.14. Crystal morphology distributions throughout neat PEEK bushings processed using traditional free convection cooling method without holding temperature at crystallization.

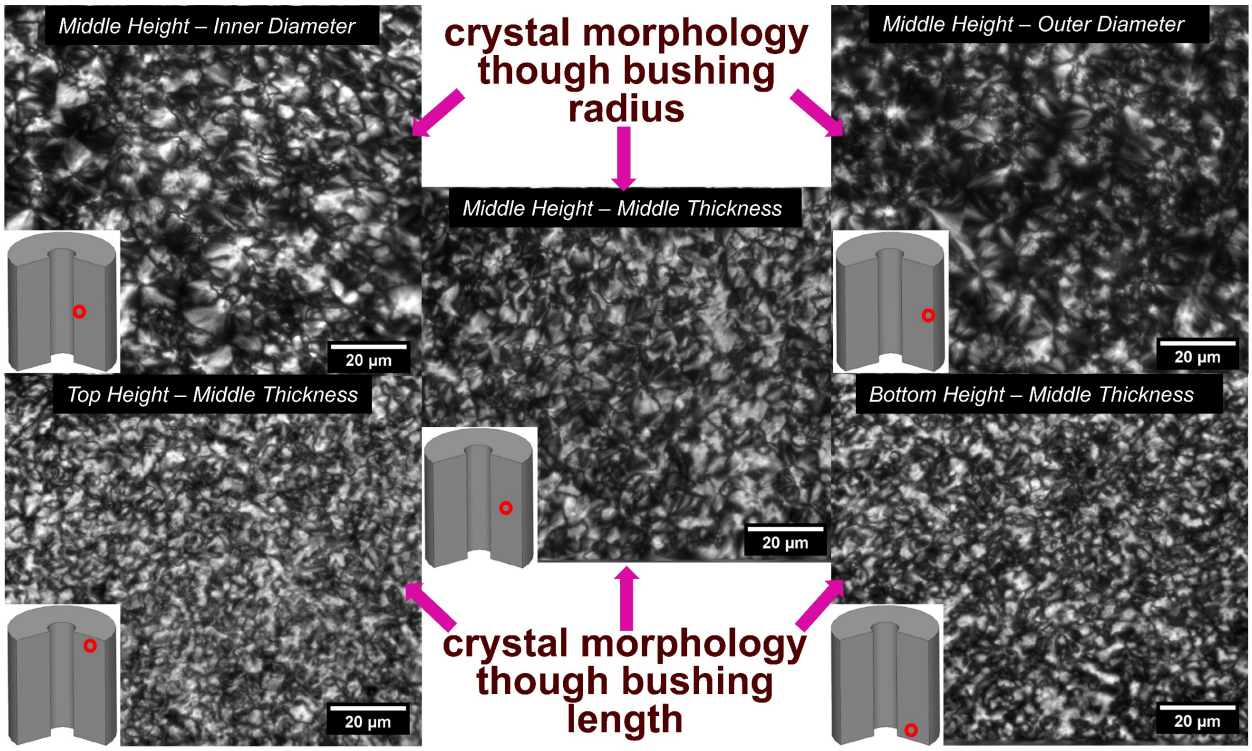

Figure 6.15. Crystal morphology distributions throughout neat PEEK bushings processed with holding temperature at crystallization for 15 hours.

Dispersion and average diameters measurements of carbon fibers in CF/PEEK composites were investigated using SEM characterization technique. SEM images of PEEK filled carbon fibers composites before compression molding process is presented in **Figure 6.16**. Those images indicated good distributions of carbon fibers in the polymer matrix. The average carbon fibers diameters and the standard deviations were 5.2 ±0.94 µm.

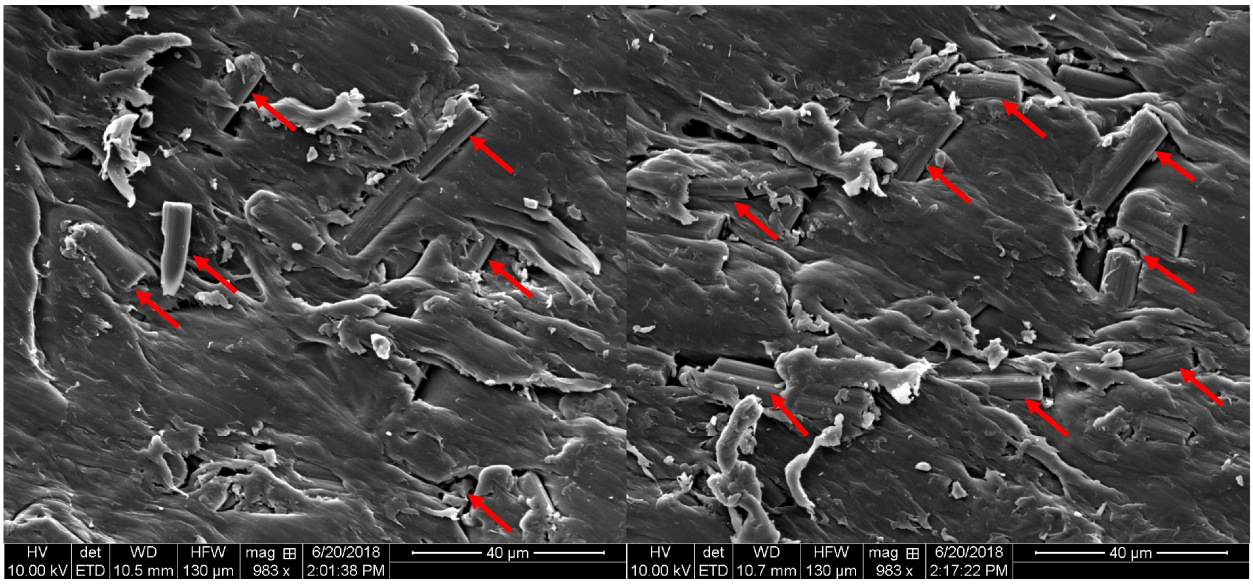

Figure 6.16. SEM images of CF/PEEK composites before compression molding process.

The compression molded CF/PEEK composites were observed under polarized optical microscopy (POM) to investigate whether the carbon fibers distributions in the PEEK composites were affected by the compression molding process. The POM images of the post-processed CF/PEEK composites using compression molding method are presented in **Figure 6.17**. The images indicated maintaining a good dispersion of carbon fibers, i.e. no CF clustering in the polymer matrix.

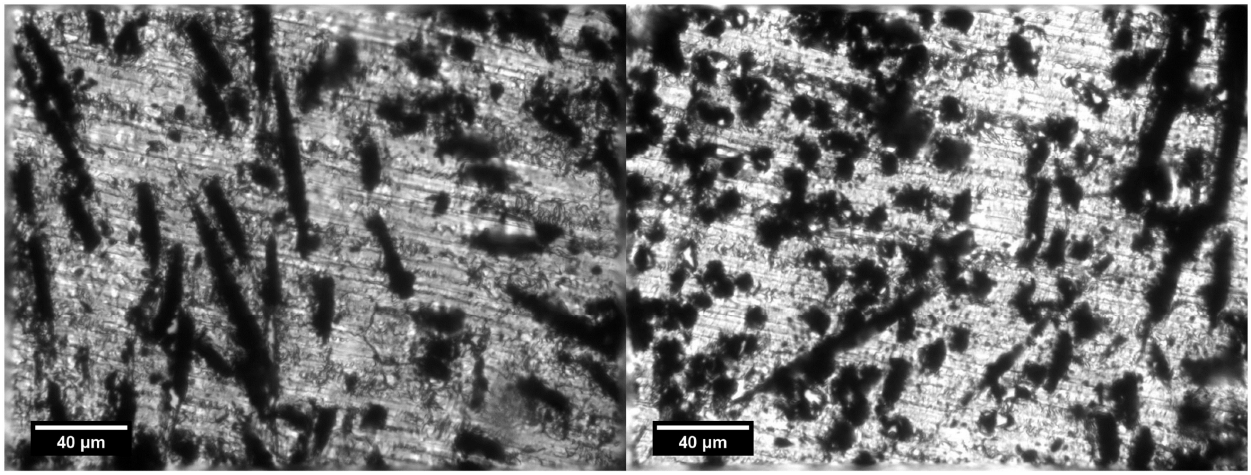

Figure 6.17. Polarized Optical Microscopy (POM) images of CF/PEEK composites after compression molding process.

Further POM characterizations were performed on post-processed CF/PEEK composites to investigate the effect of changing the compression processing strategies on the composite microstructure modifications. Crystal morphology distributions throughout CF/PEEK composite bushings processed using traditional free convection cooling method vs. processing strategy of holding temperature at crystallization for 15 hours are presented in **Figure 6.18** and **Figure 6.19**, respectively.

Similar morphologies were observed along bushing processed using free convection cooling procedure. No signs of spherulite structures were detected at the top, middle, and bottom height of the processed bushing, see **Figure 6.18**(a)-(c). Unlike CF/PEEK composite, neat PEEK produced non-uniform spherulite structures after using free convection cooling process as explained previously as seen in **Figure 6.14**. Thus, carbon fiber fillers assisted in obtaining more uniform microstructure along the bushing processed using traditional free convection cooling by enhancing the heat distribution uniformity throughout the bushing.

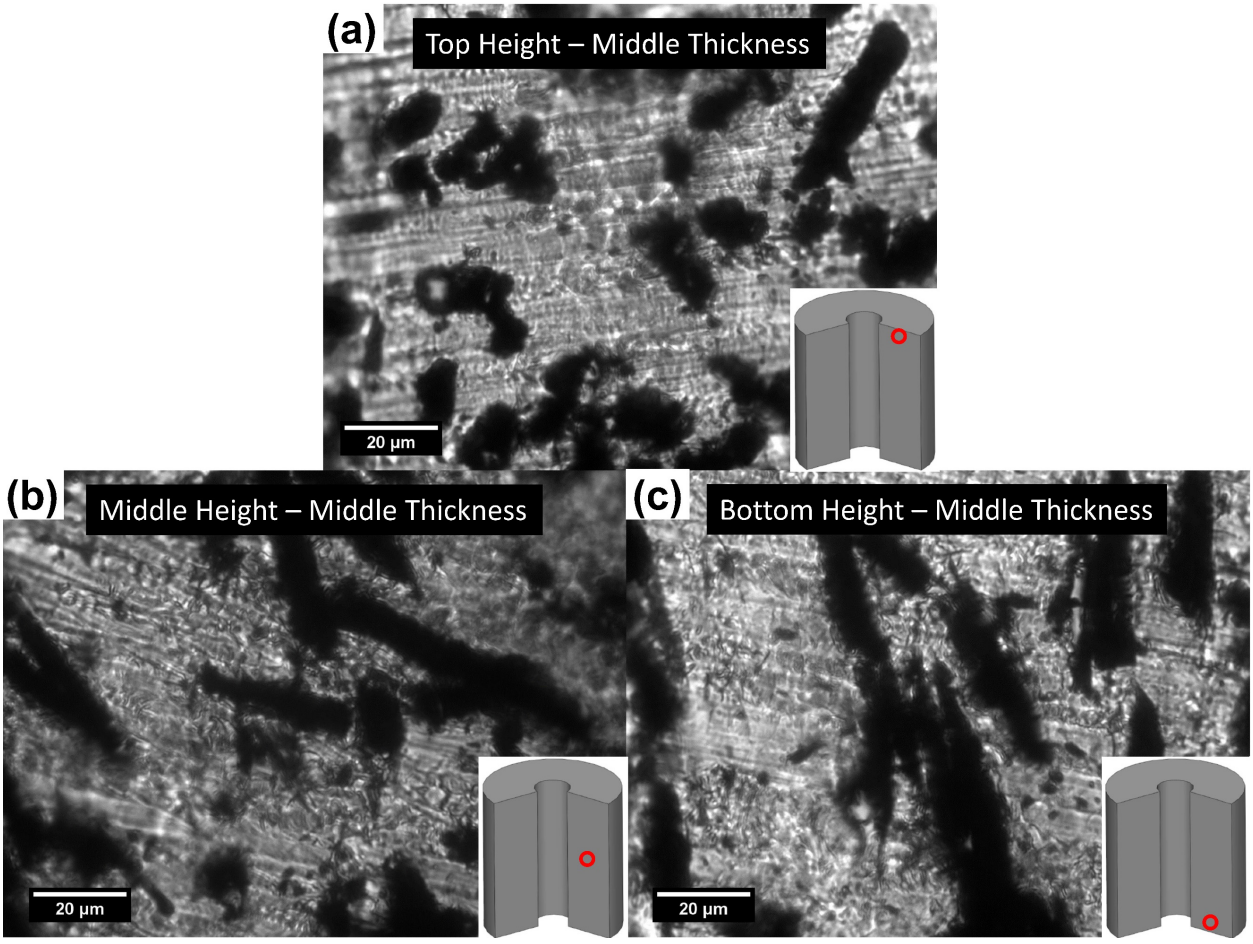

Figure 6.18. CF/PEEK composite microstructure distributions throughout bushings processed using traditional free convection cooling method without holding temperature at crystallization. (a) Top bushing height. (b) Middle bushing height. (c) Bottom Bushing height.

In contrast, distinct crystal structures accompanied with similar morphology distributions were identified along bushing top, middle, and bottom bushing after holding temperature at crystallization for sufficient time, as presented in **Figure 6.19**(a)-(c). Those spherulites indicated having higher crystallinity in polymer composite after adding the step of holding temperature to the molding process. This additional step provided the time needed for polymer to grow the spherulite structures throughout the matrix.

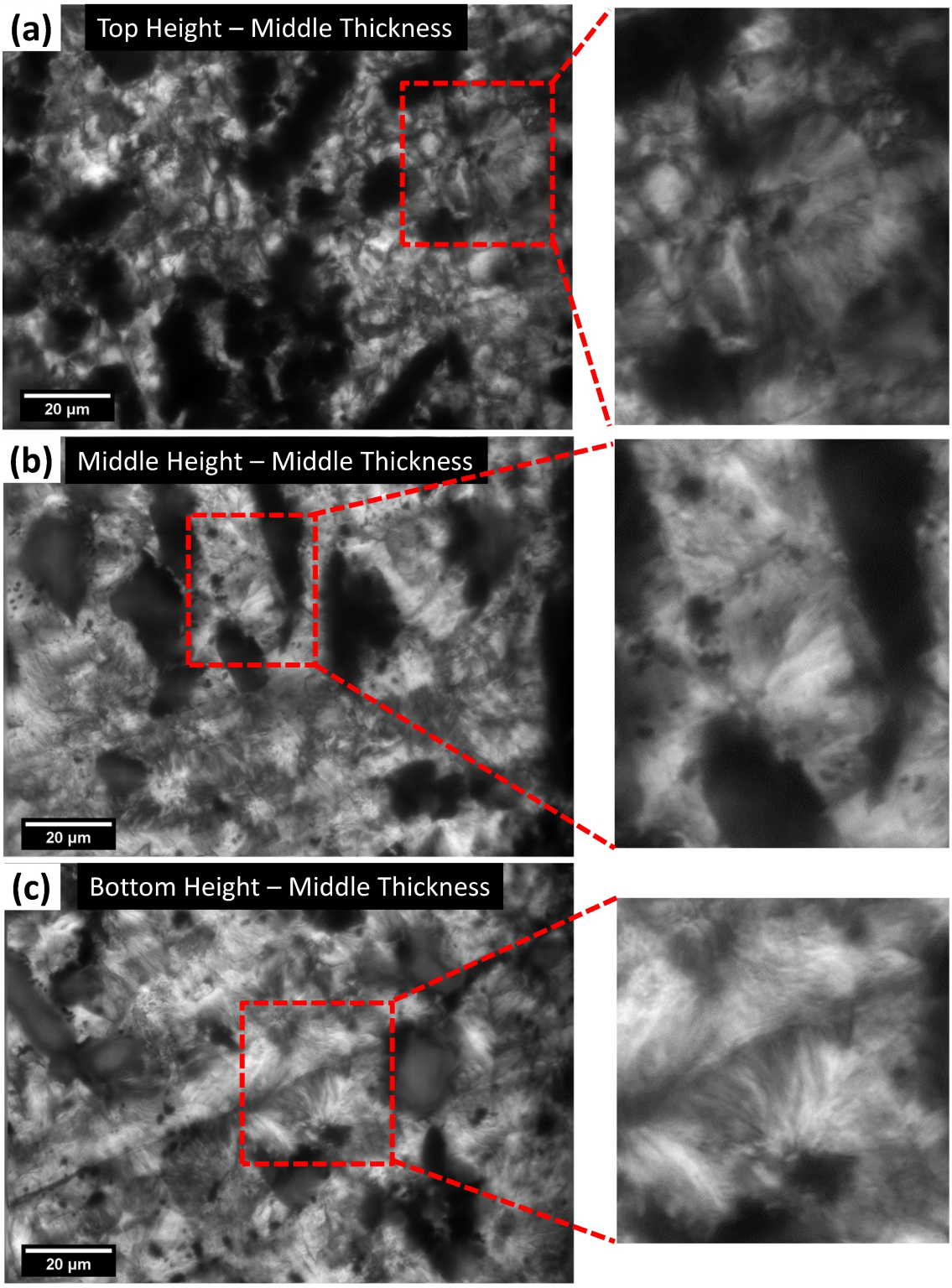

Figure 6.19. CF/PEEK composite microstructure distributions throughout bushings processed with holding temperature at crystallization for 15 hours. (a) Top bushing height. (b) Middle bushing height. (c) Bottom Bushing height.

The microstructure images of both neat PEEK and CF/PEEK bushing processed using the step of holding temperature for sufficient time ensure the formation of uniform crystal structure throughout the bushing. The images outcomes agreed with the DSC results presented in the previous section that showed that neat polymer and its composites formed same crystallinity and morphology throughout the bushing.

Although POM images of CF/PEEK showed the spherulite structure absence along bushing with free convection cooling process, DSC results exhibited some crystallinity percentages in the composite processed using this traditional method. It is known that one of the main CF roles in composites is maximizing the surface area that assists in forming more crystal structure. However, it is important to consider the fact that CF minimized time required for cooling process because it enhances thermal conductivity and accelerates heat loss that could limit crystallization process. Thus, different factors were involved in shaping the composite microstructure during traditional convection cooling process of thick wall parts. The outcomes of balancing those factors influenced the composite morphology behavior through initiating uniform crystal structures that were too small to be seen under POM. However, holding temperature at crystallization for sufficient time assisted in growing those crystal structure to become visible under microscope.

Eventually, POM observations of neat PEEK and CF/PEEK composites crystal structures supported DSC and WAXS results. Higher and more consistent crystallinity were predicted for the case of holding temperature process. These estimations agreed with the spherulite crystal structure distribution observed by POM for the same processed material.

6.10 Dynamic Mechanical Behavior

The influence of manipulating the compression molding process on the mechanical response of polymer bushing along wide range of temperature (30 – 300) °C was investigated using DMA. This technique is a powerful tool that provides sensitive measurements for damping and modulus variations as functions of temperature. Information regarding those behaviors can demonstrate substantial understanding of polymer chain interactions at molecular levels, and subsequently reflect the polymer crystal structure distribution and content.

The temperature dependence of storage modulus and tan δ for PEEK along bushing processed using traditional free convection cooling are presented in **Figure 6.20**(a) and (b), respectively. While manipulated bushings processed by holding temperature at crystallization for 4 hours and 15 hours are shown in **Figure 6.21** and **Figure 6.22**, respectively. The general trends indicated a minor decrease of storage modulus associated with temperature increase up to glass transition onset temperature that then fell drastically to reach plateau region. In this region, the storage modulus dropped slowly until it reached the crystal melting zone. The damping response, represented by tan δ curves, started with minor increase accompanied by raising temperature up to glass transition onset temperature. After this temperature, the material damping behavior rapidly increased to reach its highest value at the polymer glass transition temperature and then decreased dramatically. The damping lowest dropping point was higher than its value at the onset.

The storage modulus and tan δ patterns along wide temperature range between (30 °C – 300 °C), presented in **Figure 6.20**(a) and (b), highlighted the properties variation along the top, middle, and bottom heights of traditional free convection cooling bushing. Lowest storage modulus values were observed at the top bushing section for all temperatures.

Holding temperature at crystallization for 4 hours and 15 hours produced more uniform modulus distribution throughout each bushing as shown in **Figure 6.21**(a) and **Figure 6.22**(a). Tan δ traces of those two processing methods had close peaks height throughout each bushing, as presented in **Figure 6.21**(b) and **Figure 6.22**(b), although the 15 hours hold reflected better similarities in their peaks' intensities. These behaviors indicated having similar molecular damping, and thus similar amorphous content along each bushing. However, the breadths of 4 hours temperature hold process varied along the bushing, which indicated the possibility of introducing more than one structure in some locations. This could be caused by the lack of holding time, i.e. the holding time was not enough to fully develop the secondary structure between the primary lamellae. Therefore, providing additional holding time (15 hours), in **Figure 6.22**(b), assisted in fully developing the secondary structure introduced in the previous strategy (4 hours hold), and thus producing similar breadths and structures throughout the bushing.

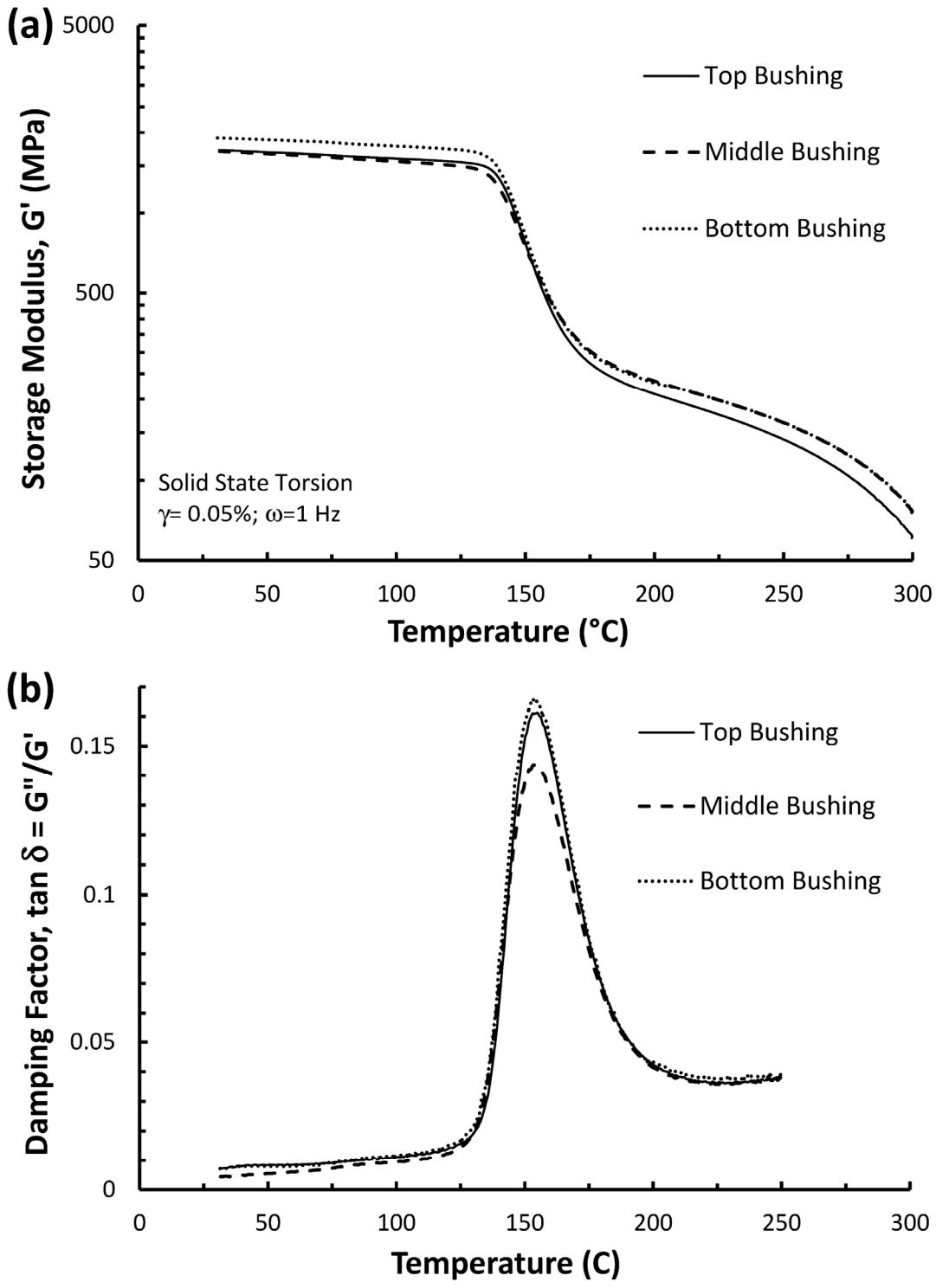

Figure 6.20. Temperature dependence of (a) storage moduli and (b) tan δ throughout PEEK bushing processed using traditional free convection cooling without holding temperature at crystallization.

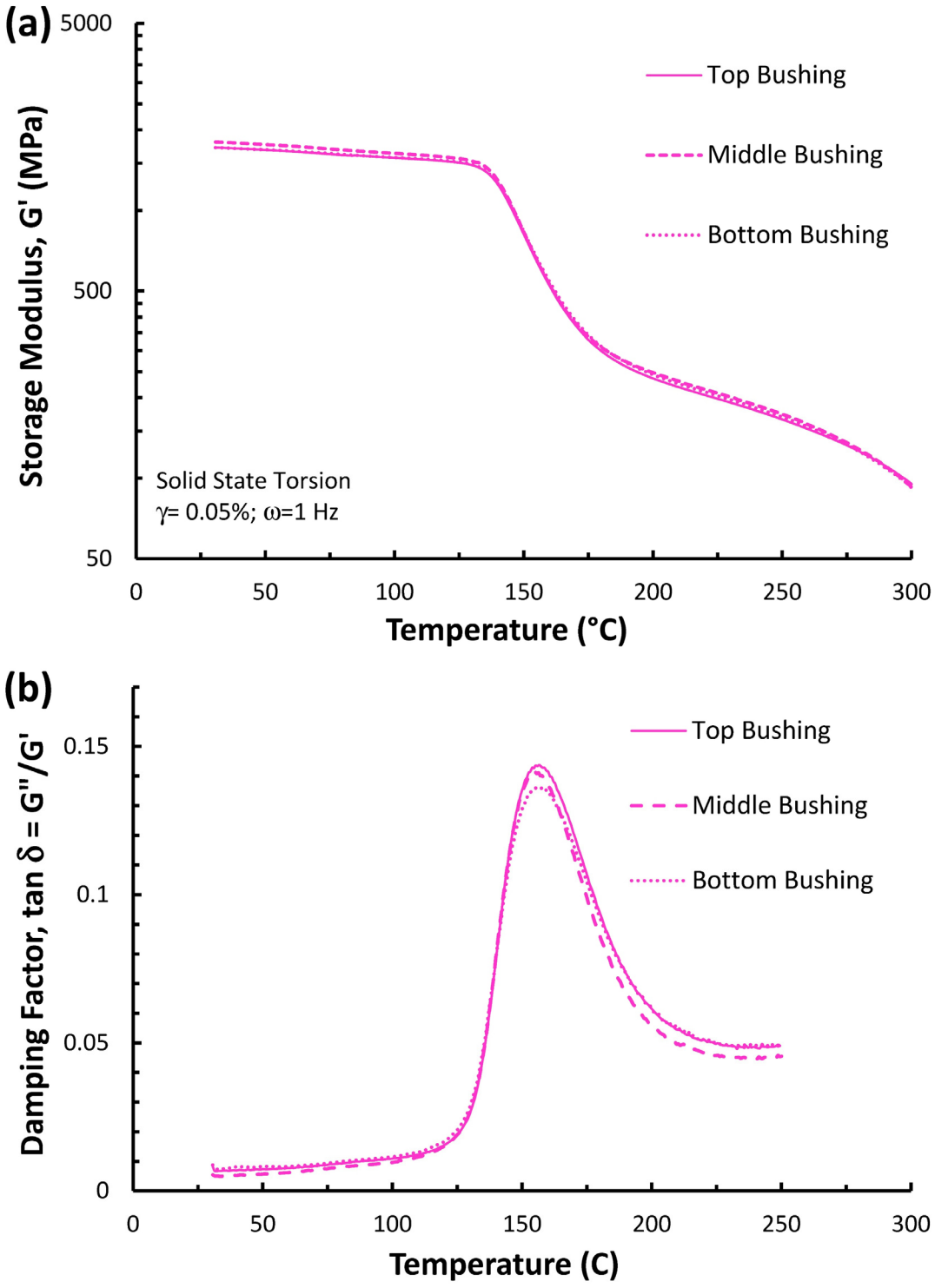

Figure 6.21. Temperature dependence of (a) storage moduli and (b) tan δ throughout PEEK bushing processed holding temperature at crystallization (309 °C) for 4 hours.

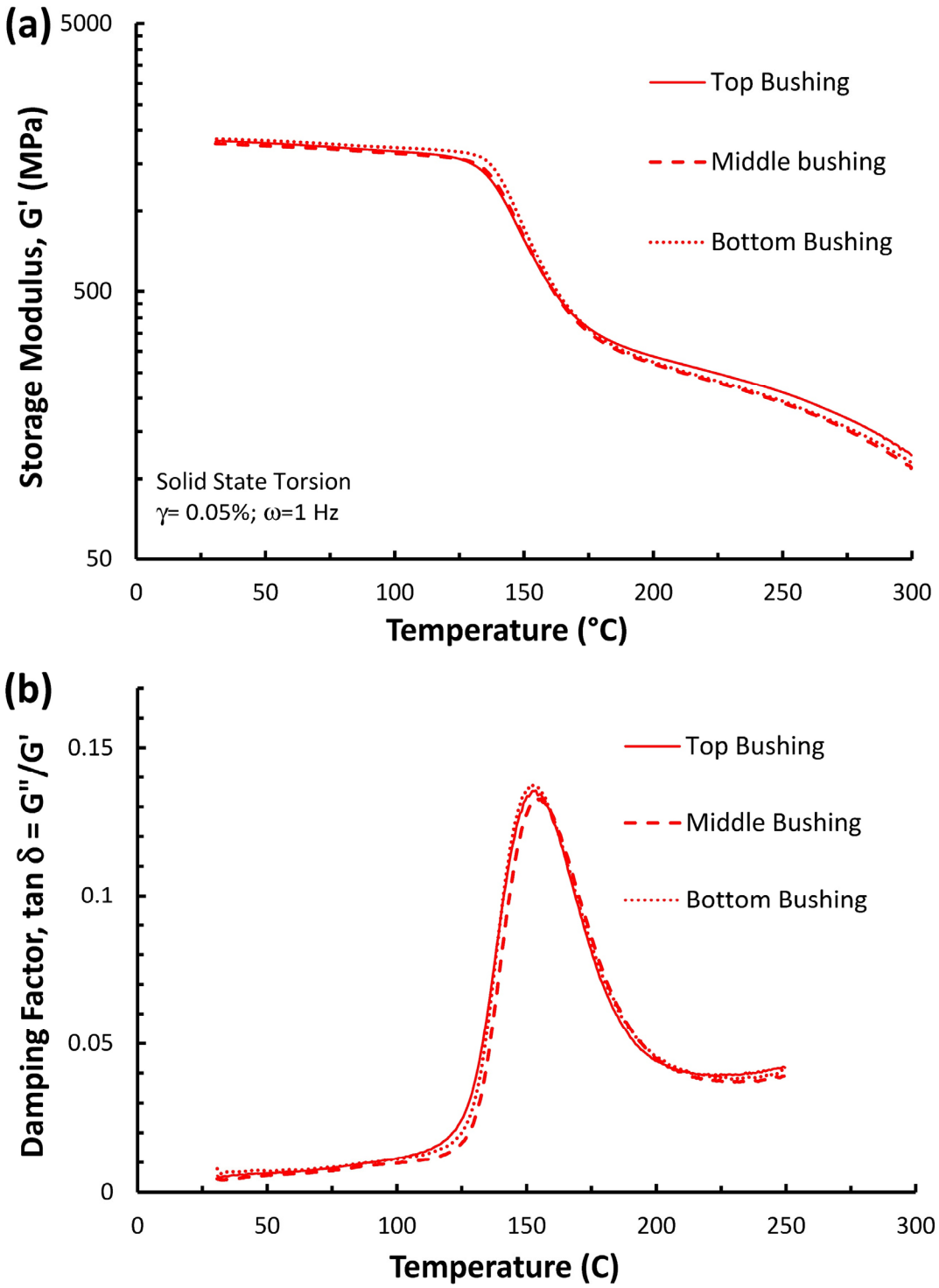

Figure 6.22. Temperature dependence of (a) storage moduli and (b) tan δ throughout PEEK bushing processed holding temperature at crystallization (309 °C) for 15 hours.

To better shed the light on the mechanical responses of bushings processed using different strategies, comparisons of all processing strategies have been made at each bushing section. Storage modulus and tan δ comparisons of the different processes (free convection cooling vs holding temperature for 4 hours and 15 hours) at top bushing heights are presented in **Figure 6.23**(a) and (b), respectively. While storage modulus and tan δ comparisons of PEEK bushing at middle and bottom heights are presented in **Figure 6.24**(a) and (b) and **Figure 6.25**(a) and (b), respectively.

In the temperature range between 30 °C and 300 °C, PEEK specimens at top bushings processed using all strategies, in **Figure 6.23**(b), displayed glass transition temperatures between 153.6 °C – 156.7 °C. While middle and bottom bushings for those processing strategies, in **Figure 6.24**(b) and **Figure 6.25**(b), exhibited glass transition temperatures ~ 154 °C – 155 °C and 152.5 °C – 156.5 °C, respectively. It can be noticed that changing the holding time had the lowest influence on Tg at the middle bushing sections. In addition, holding temperature for 15 hours during the process had more influence on top and bottom bushing compared with the middle sections. Moreover, the glass transition temperatures along the traditional free convection cooling were reported as 153 °C – 155 °C. Whereas the Tg range values along the bushing processed by holding temperature at crystallization for 4 hours and 15 hours were 155 °C – 156.7 °C and 152 °C – 154 °C, respectively. It was observed that the 15 hours holding time produced bushing with lowest glass transition temperatures. While the 4 hours hold produced bushing with highest Tg values.

The storage modulus for top, middle, and bottom bushings height of different processing strategies in **Figure 6.23**(a), **Figure 6.24**(a), and **Figure 6.25**(a) displayed a minor temperature dependence below glass transition temperature. Holding temperature at crystallization for 15 hours

caused an increase in the modulus (below Tg) by 100 MPa at the top, middle, and bottom bushing compared with other strategies. Experiencing small changes in storage modulus below Tg could be attributed to hindering chain mobility along this region.

In glass transition and rubber plateau regions, the influence of crystallinity and rigid-amorphous polymer fraction changes can be clearly distinguished. Although glass transition is mainly associated with polymer amorphous domain, crystalline region influence on this transition is well recognized [83]. The decrease in modulus along glass–rubber regions is caused by the rigid-amorphous progressive relaxation [84] where the amorphous phase between the lamellae start to flow, i.e. the amorphous polymer chains exhibit higher mobility and become less constrained. The intensity of this behavior dependents on morphology and thermal history of the polymer. Higher crystal contents strengthen polymer structure, and consequently performs higher modulus. It is worth mentioning that the modulus curve of traditional free convection cooling process exhibited a significant drop above Tg compared with other strategies, as presented in **Figure 6.23**(a), **Figure 6.24**(a), and **Figure 6.25**(a) for the top, middle, and bottom bushings sections, respectively. This behavior indicated having highest amorphous content in the bushing processed using the traditional method. Holding temperature at crystallization and increasing the holding time reduced the fall off in modulus because the crystal structure is enhanced. Holding temperature for 15 hours performed the highest modulus curve in the plateau region followed by the processes of 10 hours hold and 4 hours hold curves, respectively. Thus, the process of 15 hours holding time had highest crystal structure content which enhanced the mechanical damping characteristics at plateau region.

Unlike crystal structure, amorphous influences material damping response. In general, tan δ intensity at Tg is inversely proportional to crystallinity [84]. Thus, the area underneath tan δ peak provides good insights regarding the participated molecular segments in the relaxation process.

The intensity and the breadth of the area under tan δ peak, in **Figure 6.23**(b), **Figure 6.24**(b), and **Figure 6.25**(b), provided an indication about the crystal content and variability of structure distributed along the material. It was noticed that traditional free convection cooling had the highest tan δ peak, i.e. highest damping, throughout the entire bushing sections compared with the other processing strategies. While holding temperature for 15 hours had the lowest molecular damping. The damping peak of the material processed by holding temperature until reaching system steady state (4 hours hold) laid between the other processing strategies, i.e. free convection cooling and the 15 hours hold. The peak intensity was decreasing by increasing time of holding temperature at crystallization which was another proof of increasing the crystal content by holding temperature and increasing the holding time.

Moreover, increasing tan δ peak breadth is a sign of increasing variability of crystal structure content within same spot. It was interesting to see a broader peak for the 4 hours holding time process compared with the cases of free convection cooling and 15 hours hold. Same response was detected along top, middle and bottom bushings sections, see **Figure 6.23**(b), **Figure 6.24**(b), and **Figure 6.25**(b), respectively. This behavior was an indication of producing different crystal structures within same location in the bushing processed using the strategy of 4 hours temperature hold. During this process, secondary structures were introduced between the primary crystal structures because there was not enough time to fully develop the secondary structure to become similar to the primary lamellae. Thus, the additional holding time for 15 hours reduced the peak breadth to its original value, i.e. became similar to the free convection cooling, because sufficient time passed to fully develop the secondary structure and produce a similar structure throughout the polymer.

Samples along bushing processed using 15 hours holding time exhibited higher storage modulus than all other strategies across the entire temperature spectrum, which were attributed to acquiring higher and more consistent crystallinity of the bushing processed using this strategy. It can be clearly seen that, compared to holding temperature at crystallization, α-transition derived from free convection cooling obtained highest peak intensity accompanied with more amorphous contents. It is worth mentioning that holding temperature beyond the time required for system to approach its steady state status had a marginal effect on PEEK damping behavior near Tg regime.

The DSC and POM outcomes, obtained in pervious section, support the current DMA findings. All techniques reflected the structures diversity along the bushing experienced free convection cooling, while similar crystal structures were developed in the bushing processed by holding temperature at crystallization for sufficient time.

Given the results obtained up to the current stage, a definitive interpretation on significant improvement of mechanical properties and crystal structure distributions along thick high performance polymer can be achieved by manipulating the compression molding manufacturing process.

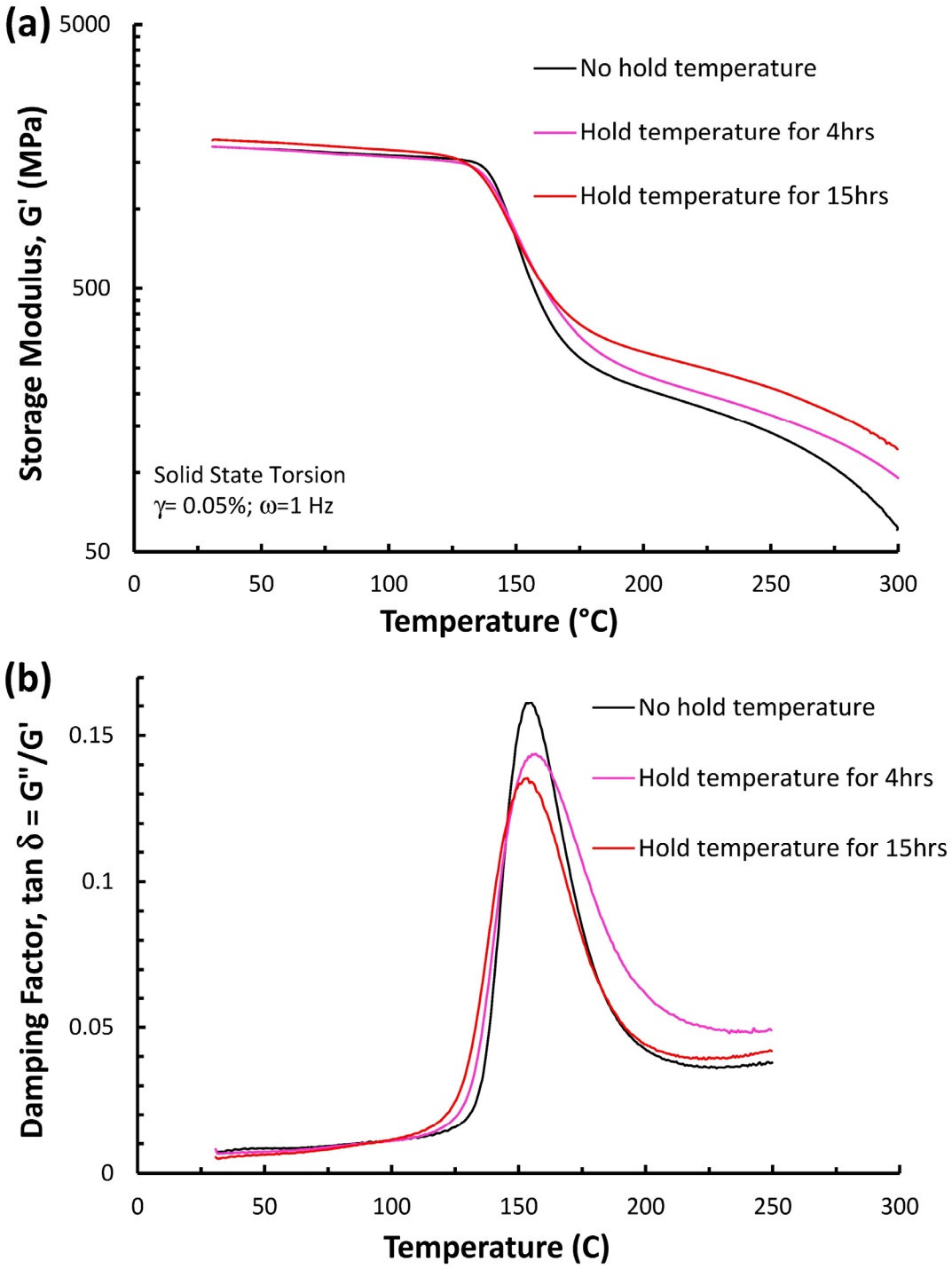

Figure 6.23. Temperature dependence of (a) storage moduli and (b) tan δ for top height PEEK bushing processed using various strategies.

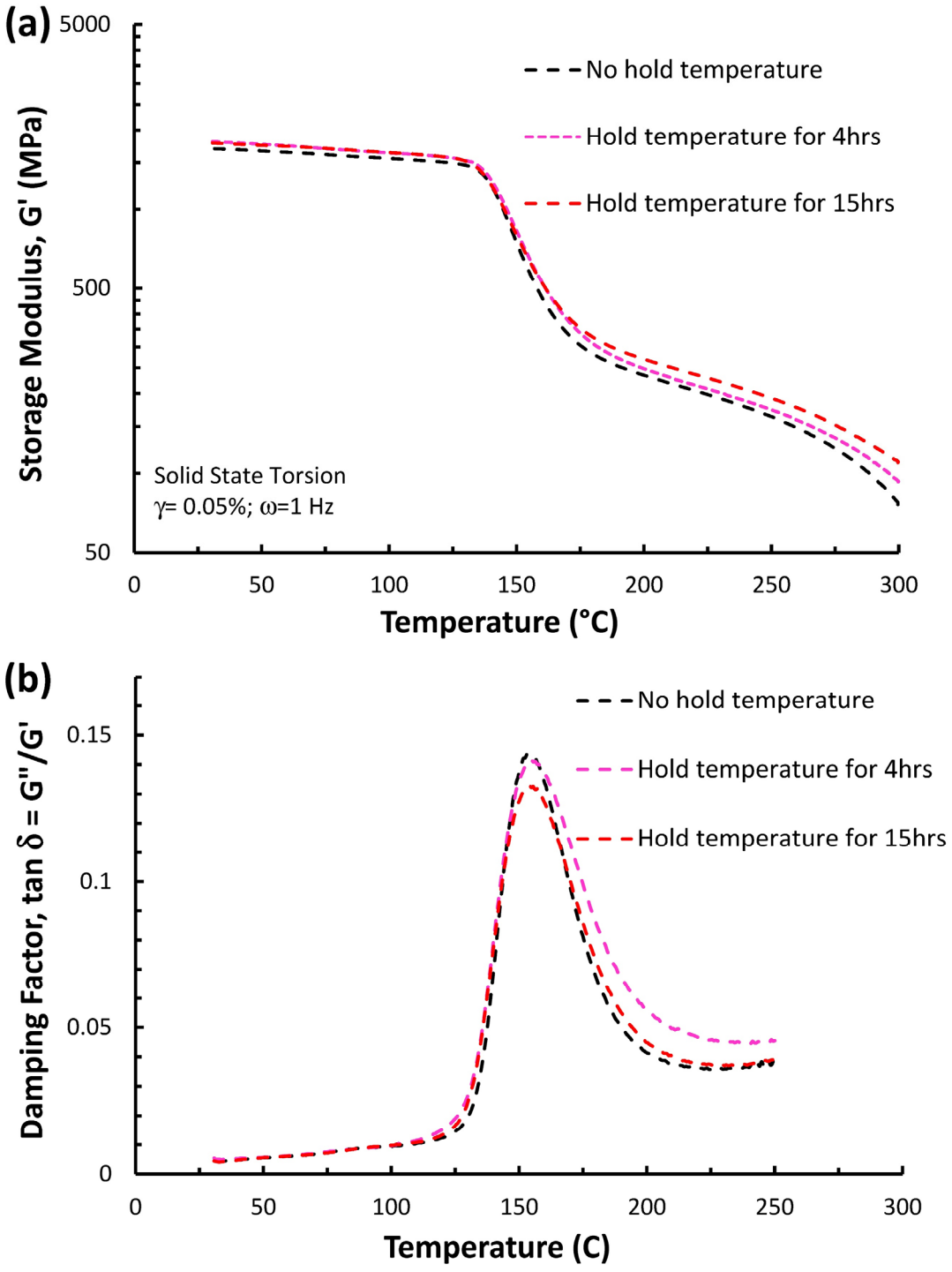

Figure 6.24. Temperature dependence of (a) storage moduli and (b) tan δ for middle height PEEK bushing processed using various strategies.

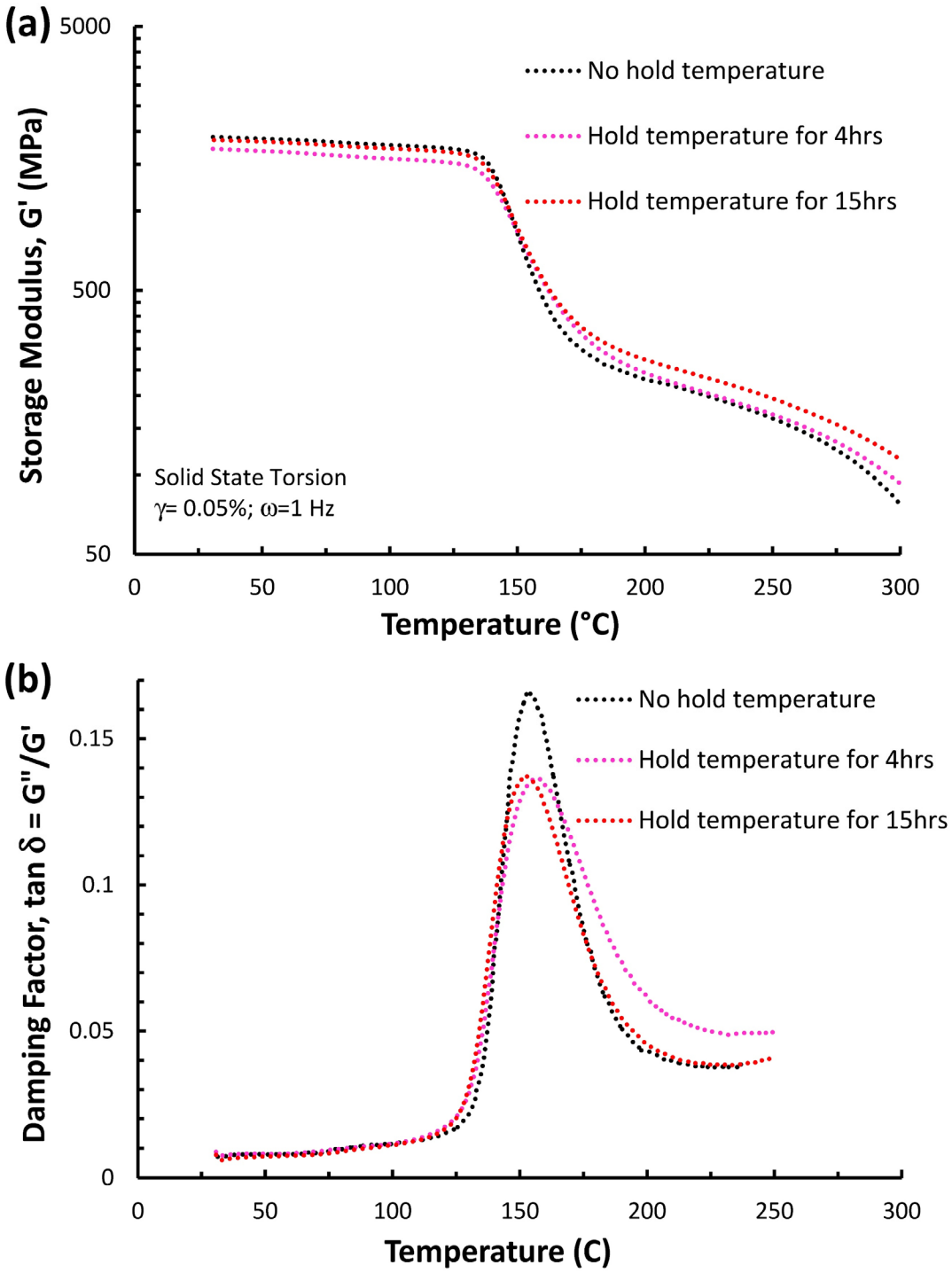

Figure 6.25. Temperature dependence of (a) storage moduli and (b) tan δ for bottom height PEEK bushing processed using various strategies.

6.7 Compression Behavior

6.7.1 Neat PEEK Behavior at Room Temperature and Elevated Temperature

Compression tests were performed at room temperature throughout bushing length and cross-section for all processing strategies to investigate the influence of manipulating the compression molding process on the mechanical properties of the produced product. Stress – strain curves were calculated from force – displacement data collected during the tests. Modulus of elasticity was found from the slope of initial straight-line portion of stress-strain curves. Modulus of elasticity at room temperature along bushing thickness and length for different strategies are presented in **Figure 6.26** and **Figure 6.27**, respectively.

It was noticed that the top section of the bushing processed using strategy A had lowest average modulus and highest deviation compared with middle and bottom bushing, see **Figure 6.26**(a) and **Figure 6.27**(a). Holding temperature for 4 hours enhanced modulus uniformity throughout the bushing, as demonstrated in **Figure 6.26**(b) and **Figure 6.27**(b). The modulus uniformity was acquired by preventing the top section from rapid convection cooling which allowed the polymer in that area to build its crystal structure, and subsequently boost the modulus at the top section. It was interesting to observe the average modulus increase at the top bushing section without increasing the average modulus in the other sections. Perhaps the reason could be correlated with the amount of holding time which was enough to build the primary structure; however, it was not enough to perform secondary structure between the primary lamellas. Acquiring resembled average modulus in strategy C and strategy B throughout both bushings regardless adding extra six hours to the holding time was supporting the above claim. Moreover, the process of holding temperature at crystallization for up to 15 hours, strategy D, resulted in higher and more consistent modulus of elasticity throughout the bushing radius and length as

shown in **Figure 6.26**(b) and **Figure 6.27**(b), respectively. The 15 hours holding time was sufficient to allow the polymer to build secondary crystal structures between the primary structure and reduce the structure imperfection [48, 62].

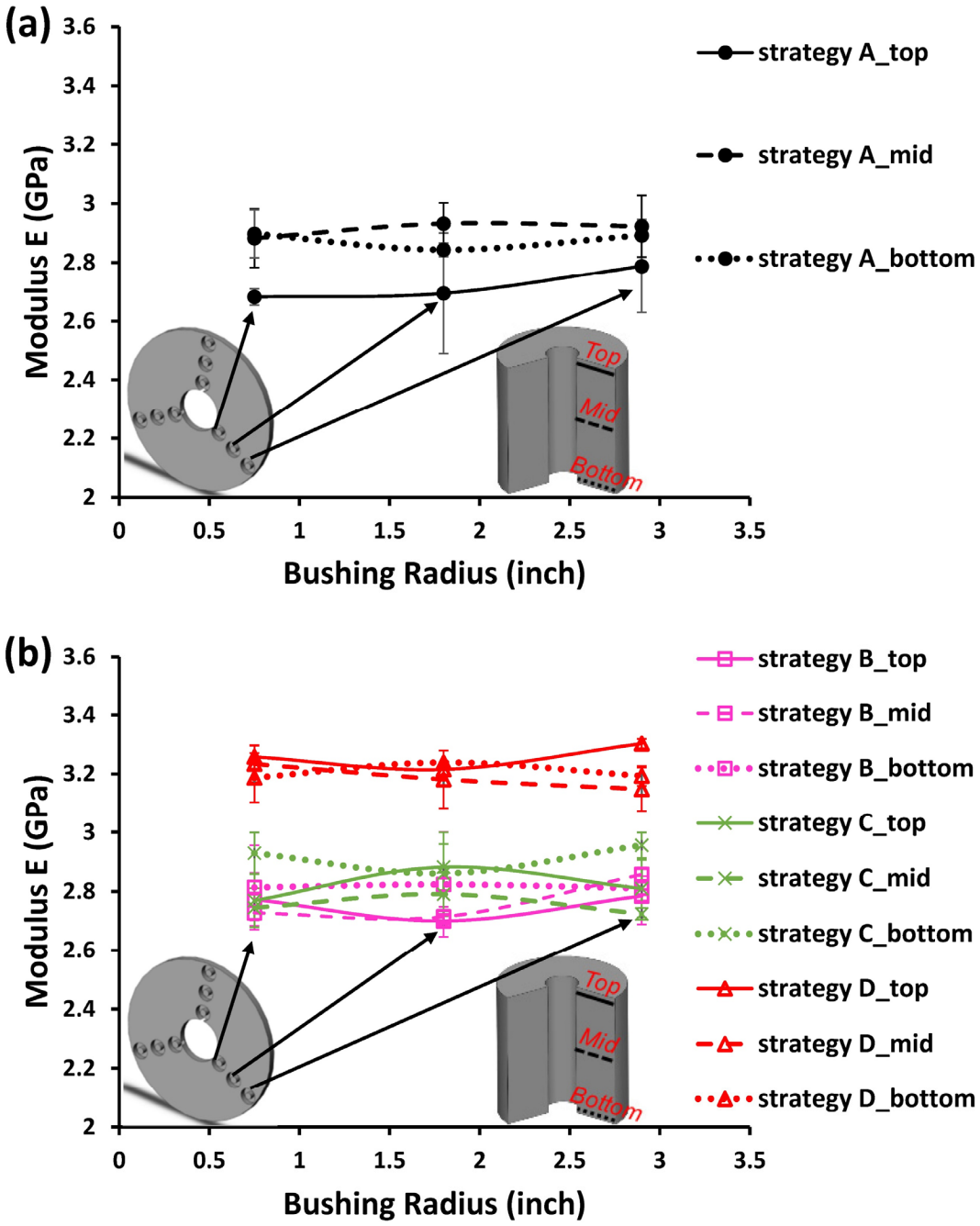

Figure 6.26. Compression Modulus of Elasticity at room temperature of neat PEEK bushings for different processing strategies. (a) strategy A and (b) strategies B, C, and D throughout bushing radius.

From the system temperature profiles results in previous section, it was found that four hours was the minimum time required for the system to reach its steady state. As a result, four hours was the minimum time required for reaching system steady state and for getting a uniform compression modulus at room temperature throughout the bushing without further increasing the entire modulus values. While 15 hours holding was the optimum time to rise the average modulus throughout the bushing.

The effects of changing time of holding temperature at crystallization during compression molding process on average compression modulus and variability of thick wall neat PEEK bushings at room temperature is presented in **Figure 6.28**. It was observed that free convection cooling, strategy A, produced bushing with modulus varied by 4.2%. Controlling the polymer process by cooling to crystallization temperature and holding for 4 hours, strategy B, resulted in reducing modulus variability to 3.5% which could be associated with enhancing the modulus at the top bushing section. Whereas, increasing holding time to 10 hours indicated minimal effects on modulus ranges compared with previous strategy. Further increase in time of holding temperature at crystallization to 15 hours reduced modulus variation to 2% and increased modulus average values by 13% as illustrated in **Figure 6.28**. This increase in modulus and decrease in variability happened because the amorphous phase is denser and polymer crystallinity is improved [62] by providing adequate time for polymer to fully build its secondary structure between lamellar primary structure [48]. As a result, stronger structure with higher and consistent modulus can to be acquired. To this end, room temperature compression tests demonstrated that controlling cooling process can reduce modulus variation from 4.2% to 2% and increase modulus by more than 13%. Average modulus and variability at room temperature of bushings processed using four different strategies are summarized in **Table 6.2**.

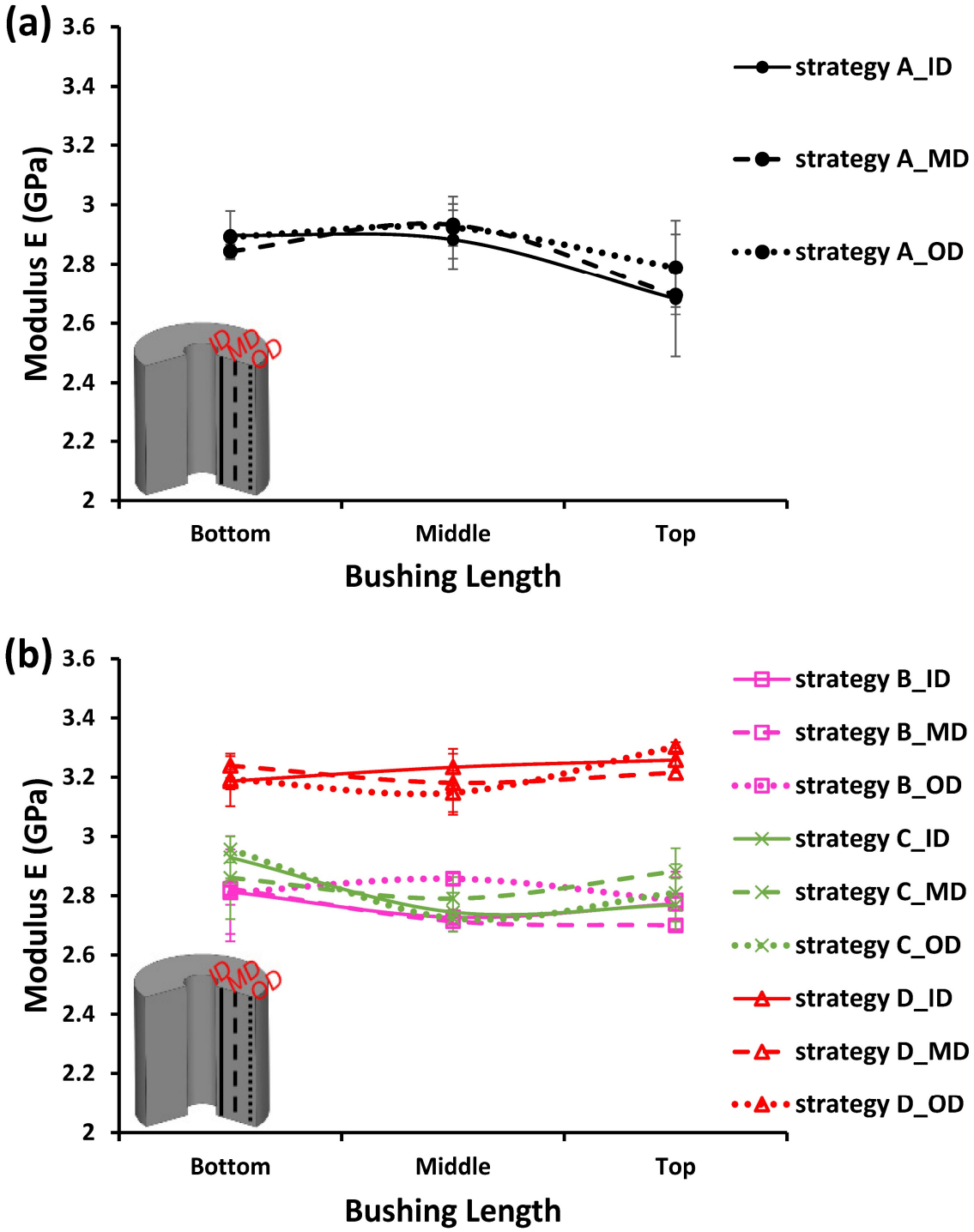

Figure 6.27. Neat PEEK compression Modulus of Elasticity at room temperature throughout bushing length for different processing strategies. (a) strategy A and (b) strategies B, C, and D.

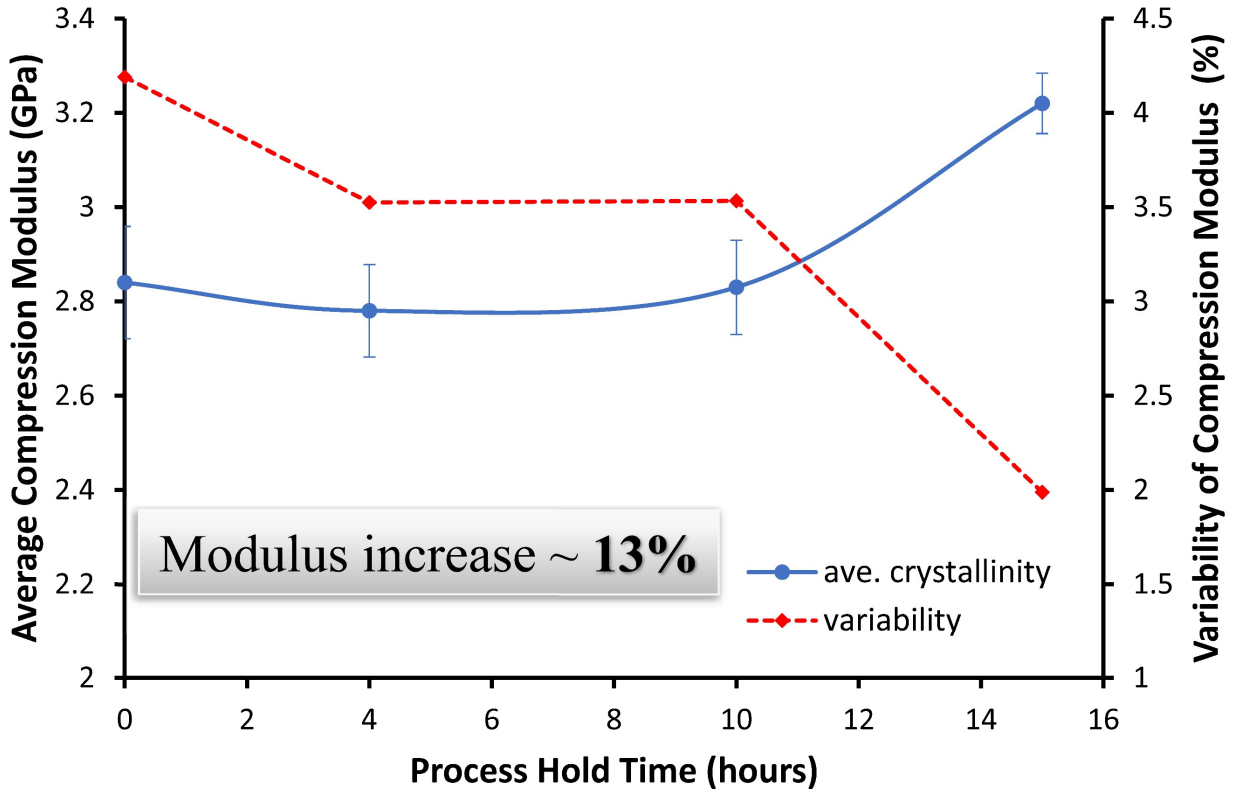

Figure 6.28. The influence of changing time of the hold temperature at crystallization during compression molding process on average bending modulus and variability of thick wall bushings at room temperature.

Compression Modulus of Elasticity of bushings produced using all four strategies was investigated at elevated temperature conditions. Those tests were essential to confirm whether the manipulated polymer produced in in this research can still perform higher and uniform modulus values throughout the bushing when this material is used in elevated temperature environments. Compression testing procedures at high temperature followed similar procedures to room temperature compression tests. A convection oven with PID controlled assisted in acquiring the required testing conditions.

Stress – strain curves were extracted from force – displacement data collected during the tests. Modulus of elasticity at elevated temperature along bushing thickness and length for different strategies were found from stress-strain curves and presented in **Figure 6.29**(a) and (b).

Modulus of elasticity of strategy A and strategy B at elevated temperature demonstrated similar behavior to Modulus of elasticity predicted at room temperature. However, a gradual increase in average modulus values of the entire bushing was observed by increasing holding time to 10 hours, strategy C, unlike the room temperature tests which could not detect a distinct increase in the modulus. The modulus at elevated temperature was more sensitive to the crystal structure changes because the amorphous part was softened because the polymer was above Tg, and consequently the load was mainly handled by the crystal structure content. Thus, elevated temperature tests reflect the real influence of enhancing the crystal structure on the modulus values. Moreover, Strategy D with holding temperature at crystallization for 15 hours indicated highest and most consistent modulus throughout the bushing comparing with other processing strategies.

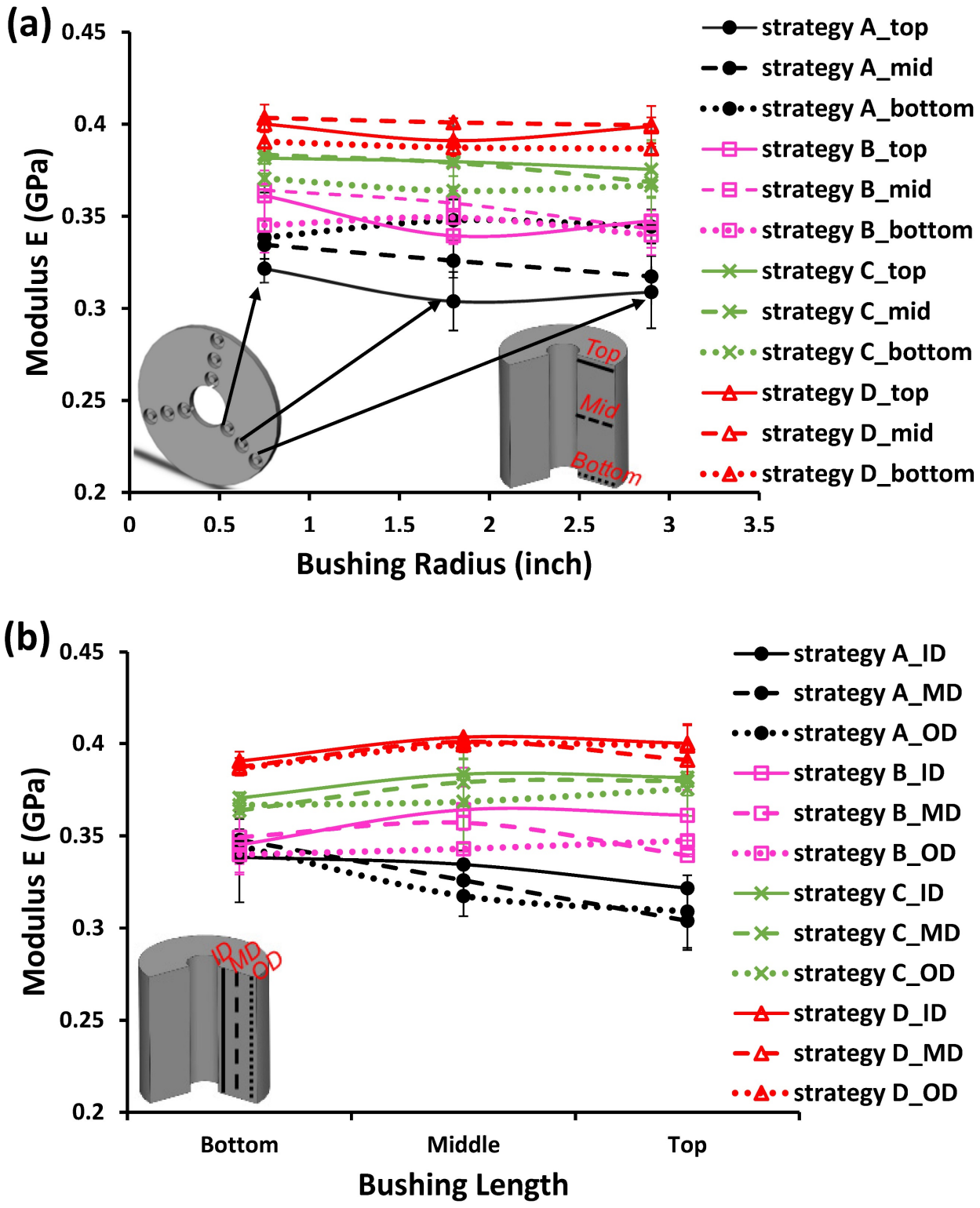

Figure 6.29. Neat PEEK compression Modulus of Elasticity at 225 ºC elevated temperature throughout (a) bushing radius and (b) bushing length for different processing strategies.

The effects of changing time of holding temperature at crystallization during compression molding process on average compression modulus and variability of thick wall neat PEEK bushings at elevated temperature are presented in **Figure 6.30**. This figure indicated that overall modulus variability would be 5.5% when bushing produced using traditional free convection cooling strategy. Adding the step of holding temperature at crystallization and increasing the holding time assisted in enhancing the overall modulus values and reduced the variability. Holding temperature for 15 hours reduced modulus variability by more than a half, from 5.5% to 2.0% and increase modulus by more than 21%. The values of average modulus and variability at elevated temperature of all strategies are summarized in **Table 6.2**. Eventually, controlling polymer process by holding at crystallization temperature for sufficient time can influence thick semi-crystalline polymer morphology which subsequently alter the product mechanical properties.

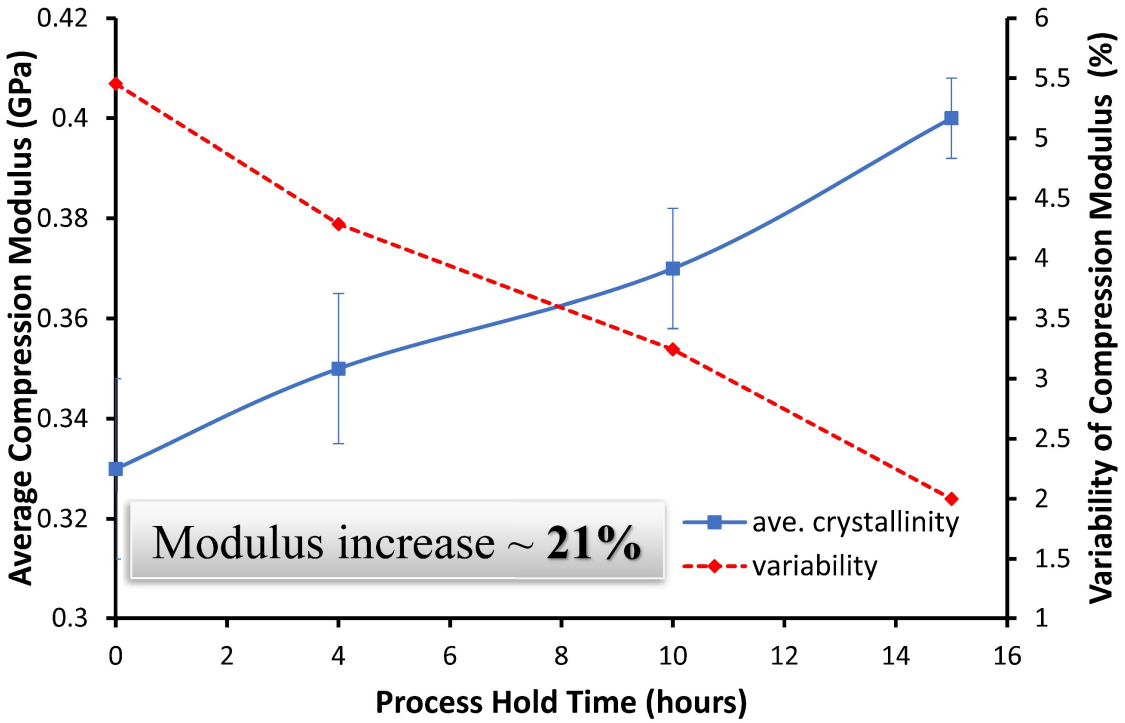

Figure 6.30. The influence of changing time of the hold temperature at crystallization during compression molding process on average bending modulus and variability of thick wall bushings at 225°C elevated temperature.

Table 6.2. Average and variability of PEEK compression Modulus of Elasticity at room temperature and 225 ºC elevated temperature for bushings processed using different strategies.

Strategy Type	Room Temperature		225ºC Elevated Temperature	
	Average Modulus (GPa)	Variability (%)	Average Modulus (GPa)	Variability (%)
A (free convection)	2.84 ± 0.12	4.2	0.33 ± 0.02	5.5
B (hold temperature 4hrs)	2.78 ± 0.10	3.5	0.35 ± 0.02	4.3
C (hold temperature 10hrs)	2.83 ± 0.10	3.5	0.37 ± 0.01	3.2
D (hold temperature 15hrs)	3.22 ± 0.06	2.0	0.40 ± 0.01	2.0

6.7.2 Crystallinity and Morphology Influences on Modulus

The crystal structure effects are more noticeable at elevated temperature. This could be attributed to softening the polymer amorphous part after passing its Tg which hinders its ability to handle the load and introduces most of the applied load to the crystal structure part of the polymer. Thus, modulus sensitivity to crystal structure changes becomes more detectable at elevated temperature. Accordingly, this section focused on the elevated temperature results to investigate PEEK crystallinity and morphology influence on modulus values.

PEEK morphology images at the locations of compression Modulus specimens along thickness and height of bushing processes using traditional free convection cooling strategy is presented in **Figure 6.31**(a) and (b), respectively. While the microstructure images associated with the compression modulus locations along thickness and height of bushing processes by holding

temperature at 309 °C for 15 hours is shown in **Figure 6.32**(a) and (b). Strong relations between PEEK crystal morphology and compression modulus values were observed. Various structures were detected along the traditional free convection cooling bushing, as explained in previous section. The structure variations highly influenced the modulus throughout the bushing. For instance, the microstructure image at the inner diameter of the middle bushing height, in **Figure 6.31**(a), reflected a high crystal structure content in this location compared with the other two images for the middle and outer diameters. At the same time, it can be seen that the compression modulus in that location (inner diameter) had the highest values. Moreover, material structure image at top section of free convection cooling bushing, in **Figure 6.31**(b), had lowest crystal content and subsequently lowest modulus compared with other sections along bushing height in the graph. On the other hand, manipulating the manufacturing process by holding temperature at crystallization for sufficient time produced similar spherulite structures throughout the bushing, as observed in **Figure 6.32**(a) and (b), and thus all compression modulus values were comparable.

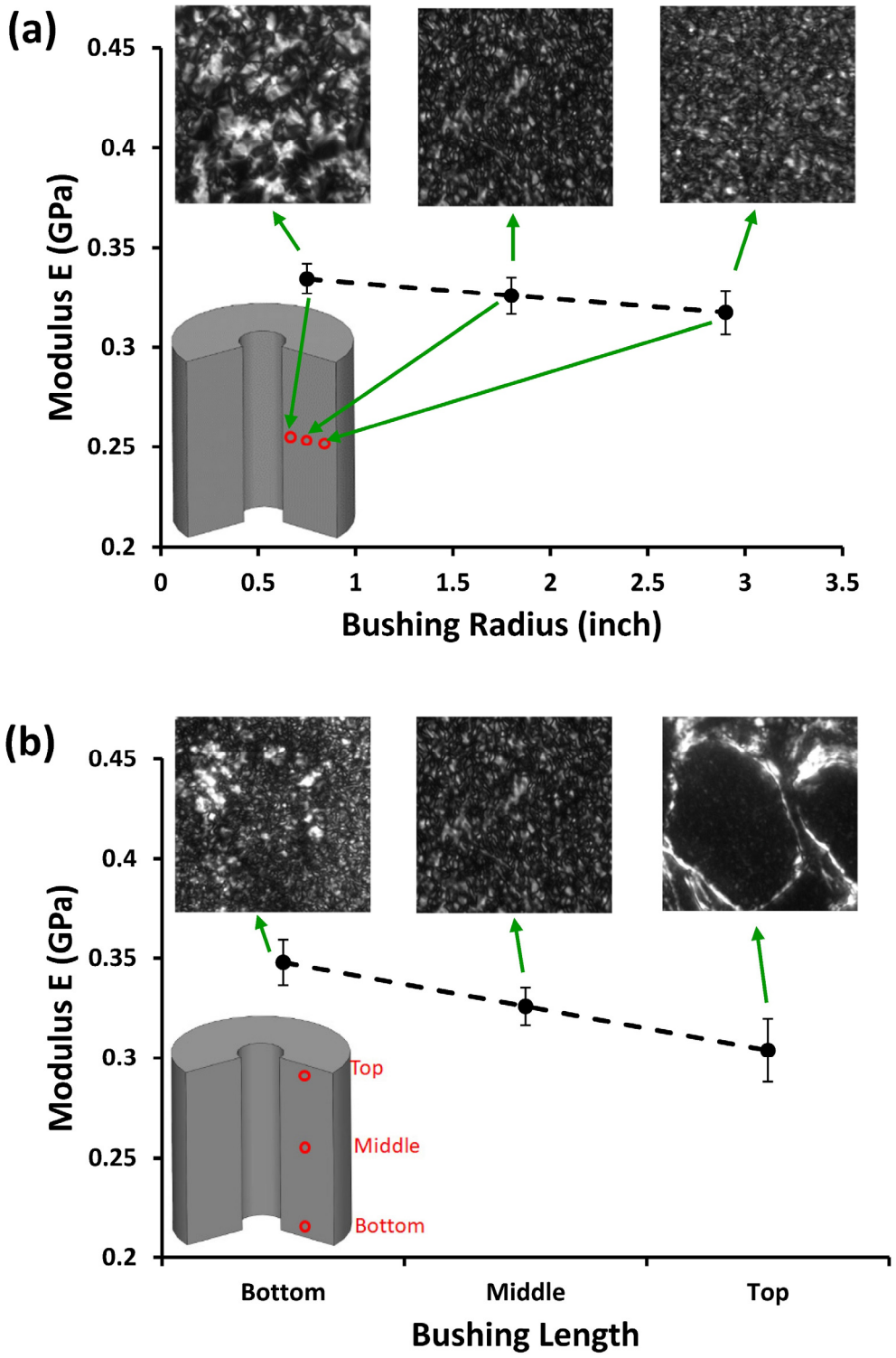

Figure 6.31. PEEK morphology images at the location of compression Modulus of Elasticity at 225 ºC elevated temperature along (a) bushing thickness and (b) bushing height for traditional free convection cooling process.

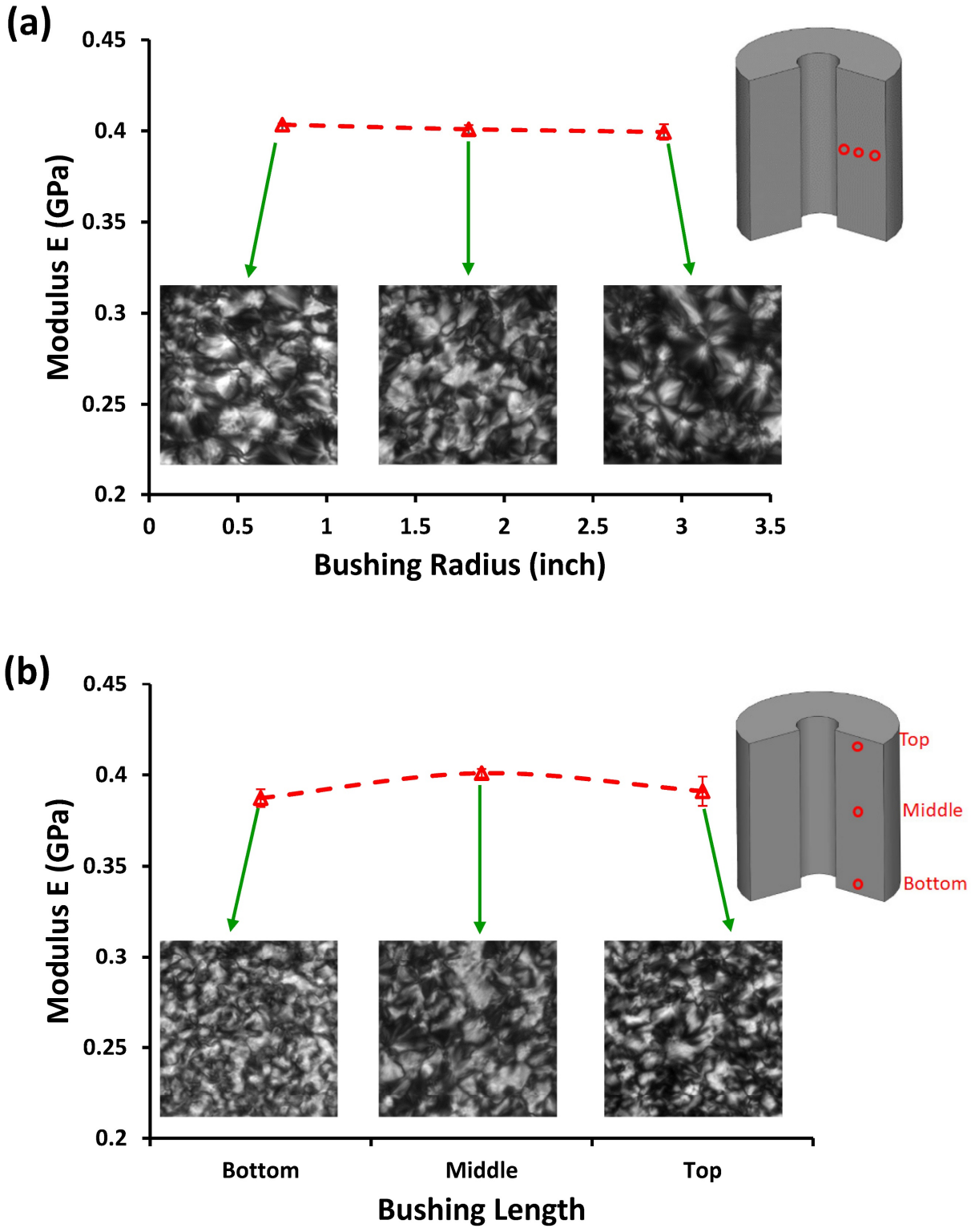

Figure 6.32. PEEK morphology images at the location of compression Modulus of Elasticity at 225 ºC elevated temperature along (a) bushing thickness and (b) bushing height for the process of hold temperature at crystallization (309 °C) for 15 hours.

Moreover, the influence of manipulating the polymer manufacturing process on the correlation of crystallinity verses storage modulus and compression Modulus of Elasticity is presented in **Figure 6.33**. It was observed that both storage modulus and compression modulus are strongly correlated with crystallinity. This plot reflected linear increase in the PEEK compression modulus and storage modulus associated with the crystallinity increase as a result of temperature hold and increasing the holding time. To this end, manipulating the polymer manufacturing process by holding temperature at crystallization beyond the time required for the system to reach its steady state has significant influence on producing thick products with uniform and enhanced mechanical properties and structural integrity.

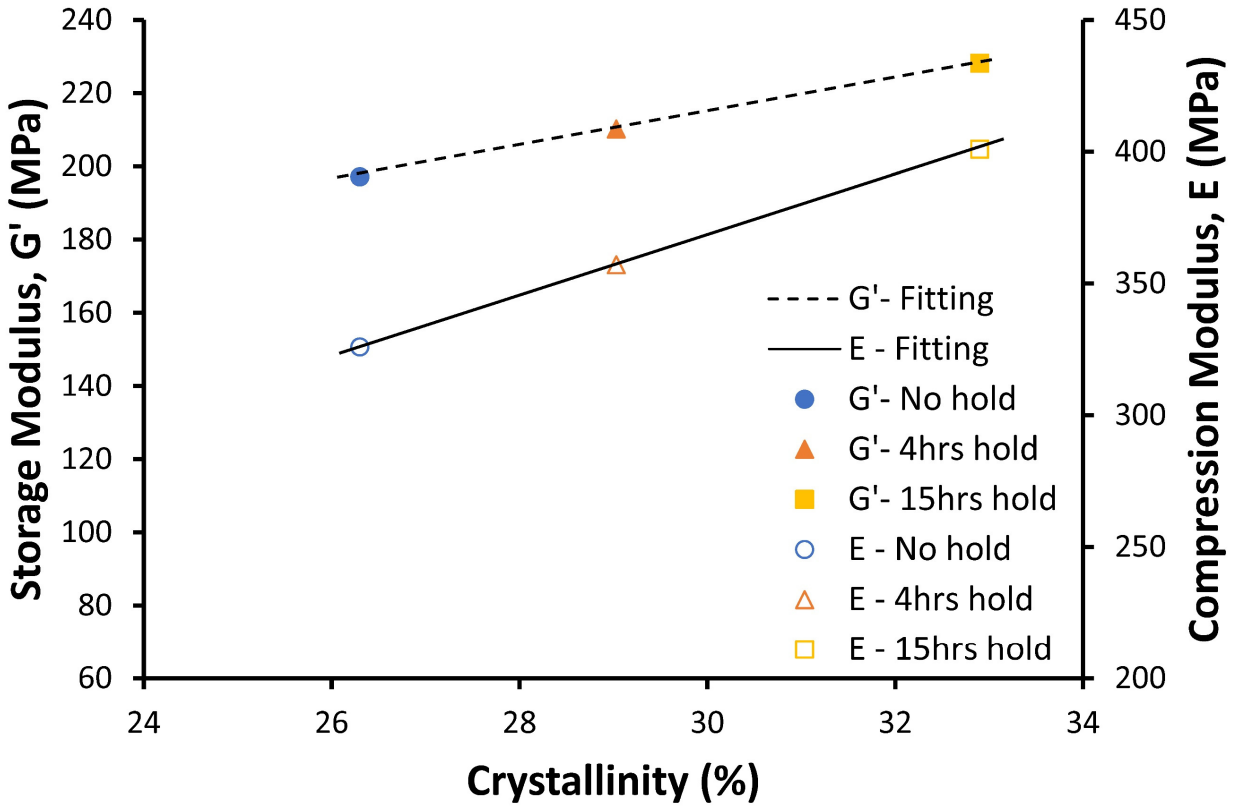

Figure 6.33. Neat PEEK storage modulus and compression Modulus of Elasticity vs. crystallinity at middle bushing height for various processing strategies.

6.7.3 CF/PEEK Behavior at Room Temperature and Elevated Temperature

Compression Modulus of Elasticity of CF/PEEK composite bushings were investigated at room temperature and 225 ºC elevated temperature conditions. The tests performed throughout length and cross-section of bushings produced using different strategies. Force vs. displacement data collected during the tests was utilized to find stress – strain curves. The latter was used to obtain compression modulus of elasticity at different testing conditions.

Modulus of elasticity along CF/PEEK bushing processed using traditional free convection cooling strategy vs. holding temperature at crystallization for 15 hours are presented in **Figure 6.34**(a) and (b) for room temperature and elevated temperature testing conditions, respectively. In all testing results, CF/PEEK exhibited higher modulus values compared with neat PEEK regardless testing conditions and processing strategies. This is a common behavior when rigid particles' influence the matrix [85]. The modulus differences between PEEK polymer and its composite were more distinguished at the 225 °C because CF maintains its structure at this temperature, i.e. CF does not melt or decompose, and subsequently retain its modulus at elevated temperature. Although CF inclusion disrupted the traditional crystal formation within PEEK matrix (as explained in **section 6.6**) and did not show further increase in the overall crystallinity compared with neat PEEK in **Figure 6.11**, it enhanced the overall matrix structure and resulted on higher modulus response, especially at elevated temperature where polymer became softer.

On the other hand, it was observed that modulus values of bushing processed using free convection cooling method and bushing processed using 15 hours holding strategy were similar, i.e. the results were consistent within experimental error. These observations were applied for the tests held at room temperature, in **Figure 6.34**(a), as well as elevated temperature conditions, in

Figure 6.34(b). Thus, holding temperature had no influence on modulus values for all testing conditions.

It was interesting to see no changes in modulus after holding temperature for sufficient time despite the composite morphology changes and spherulite crystal structures formation within the manipulated material, which were observed in previous section in **Figure 6.19**. The mechanical properties of composite materials are usually influenced by the interfacial area between CF and matrix. This interfacial area can play significant role in restricting the composite's ability to hold and transfer the load, and subsequently drops the mechanical properties of the composite. Thus, strengthen the matrix cannot enhance the overall mechanical behavior of the composite in most cases because interfacial strength dominates the composite's performance. Carbon fibers never melt during the composite fabrication process. Interactions between PEEK and CF phases to produce the composite are established between molten PEEK and solid CF. Therefore, several factors can impact the composite's interfacial strength such as filler size and volume fraction as well as the applied shear rate during the process. In the current situation of CF/PEEK composite, CF volume fraction was relatively high which amplified the interfacial area effects on the compression behavior of the composite. Thus, the influence of interfacial area presents by the CF dominated the polymer structure morphology manipulation effect. These observations showed that the CF/PEEK compression behavior was controlled by CF influence rather than PEEK structure morphology. Because there was no effect of changing the processing strategies on the CF/PEEK behavior and properties, no further investigations were performed for CF/PEEK composites.

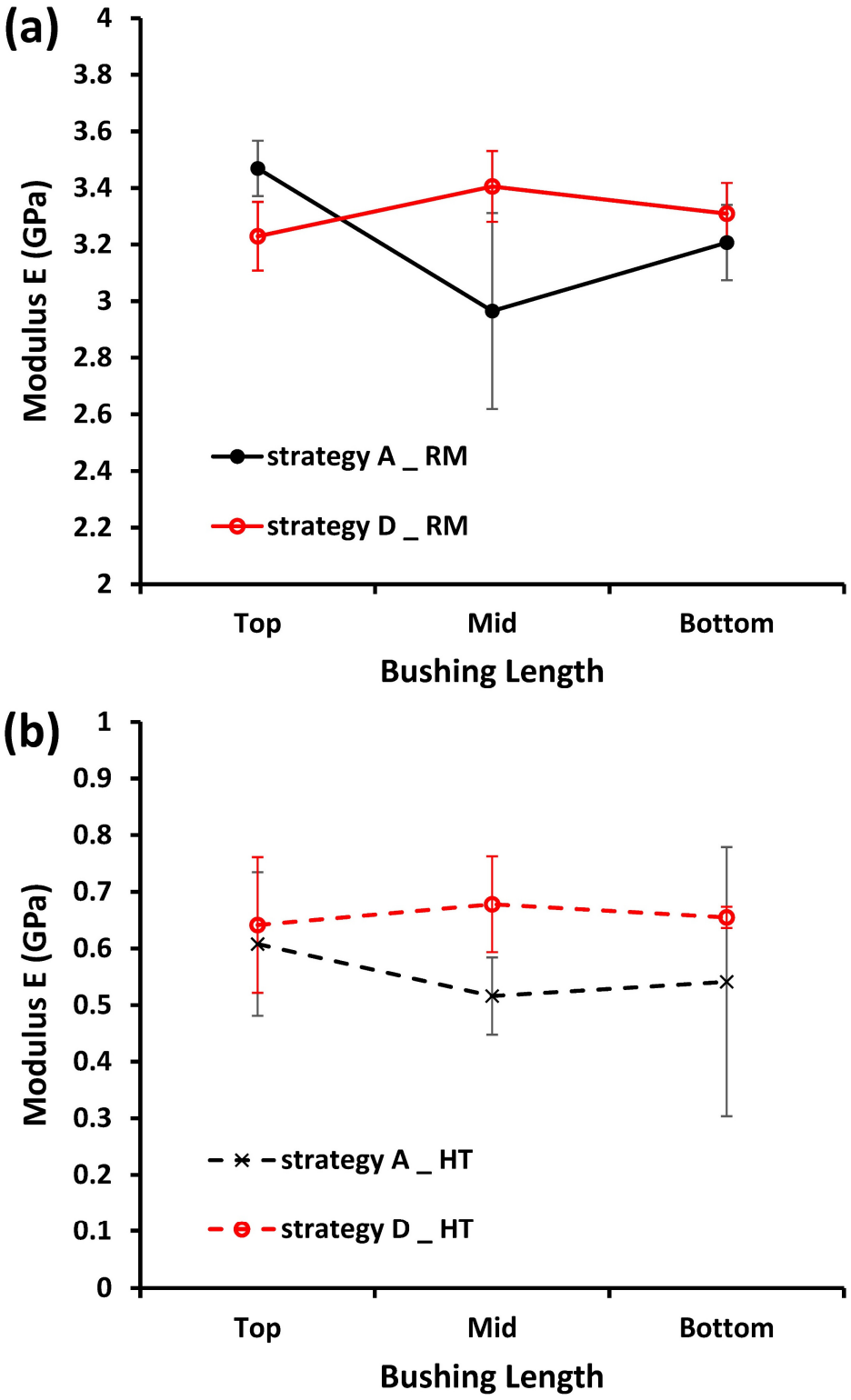

Figure 6.34. CF/PEEK compression Modulus of Elasticity found at (a) room temperature and (b) 225ºC elevated temperature throughout bushing length for different processing strategies.

6.8 Flexural Behavior

Three-point bending tests at room temperature and 225 ºC elevated temperature were carried out throughout bushing length for all processing strategies. Flexural stress – strain curves were established from those tests and used to find modulus of elasticity in bending E_b, as demonstrated in **Figure 6.35** and **Figure 6.36**, respectively.

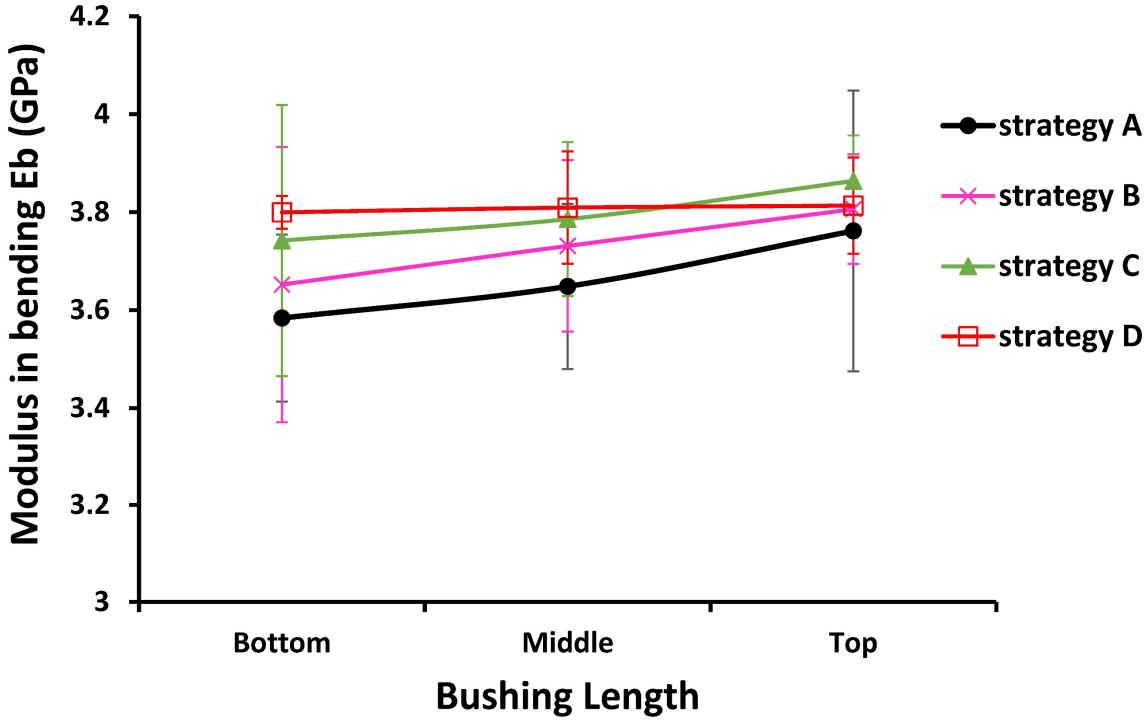

Figure 6.35. Modulus of Elasticity in bending found at room temperature throughout PEEK bushing length for different processing strategies.

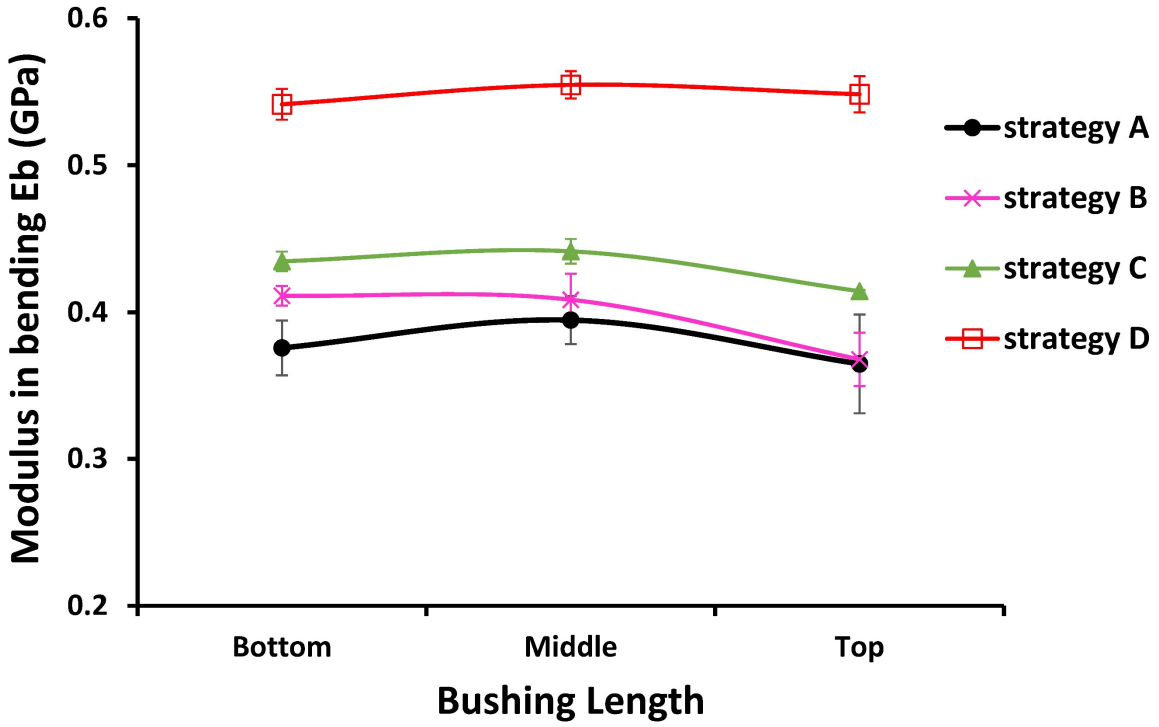

Figure 6.36. Modulus of Elasticity in bending found at 225ºC elevated temperature throughout PEEK bushing length for different processing strategies.

The processing strategies have minimal effects on bending modulus at room temperature, while those strategies show significant influence on the bending modulus when the material is tested at 225 ºC. The effects of changing time of holding temperature at crystallization during compression molding process on average bending modulus and variability of thick wall neat PEEK bushings at 225°C are presented in **Figure 6.37**. It was noticed that holding temperature for 4 hours had some influence on shifting the bending modulus to a higher level and reducing the variability throughout the bushing. Although holding temperature for 10 hours showed small influence on enhancing the modulus, it had a significant impact on reducing variability along the bushing. The highest modulus and lowest variability were achieved by holding the process at crystallization temperature for 15 hours.

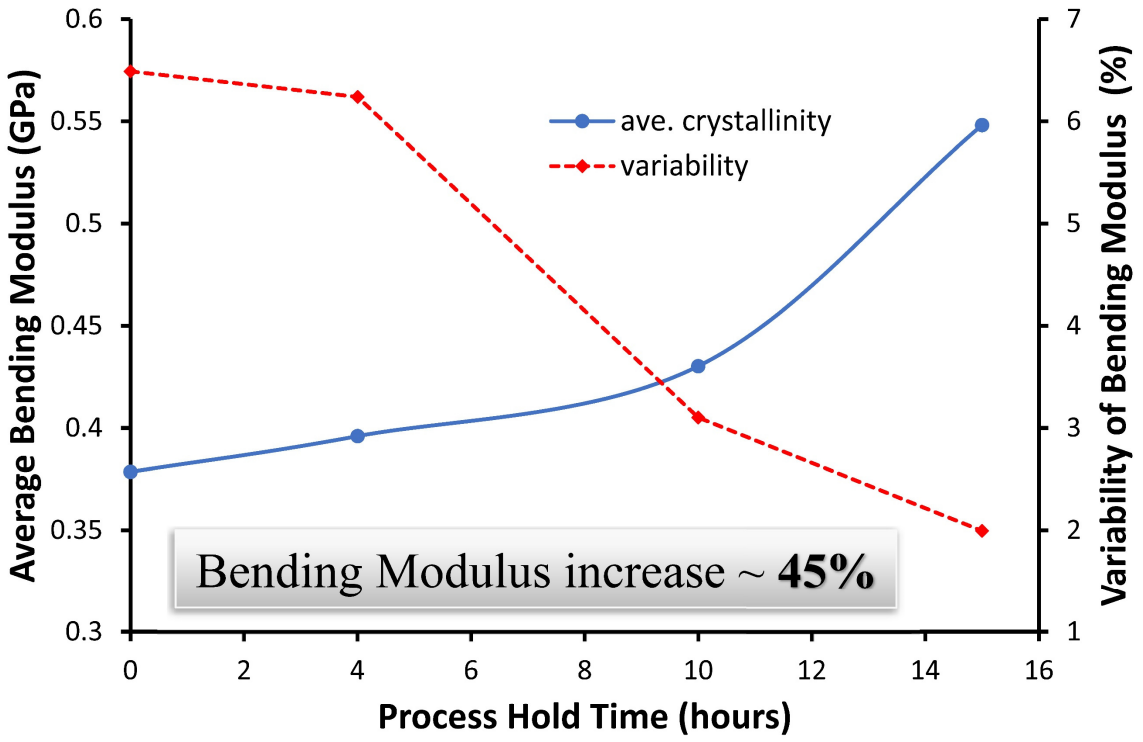

Figure 6.37. The influence of changing time of hold temperature at crystallization during compression molding process on average bending modulus and variability of thick wall and tall bushings.

The average bending modulus values of each strategy at elevated temperature and the variability along the bushings are presented in **Table 6.3**. It was noticed that free convection cooling makes the bending modulus measurements among different bushing locations to vary by 6.5% along the bushing, while cooling to 309 ºC and holding for 15 hours reduces the variation to 1.9% throughout the bushing. To this end, the flexure test at elevated temperature shows that holding the temperature for 15 hours increases the bending modulus of elasticity by approximately 45%.

Table 6.3. Average and variability of Modulus of Elasticity in bending found from 3-point-bend tests at 225 ºC elevated temperature for bushings processed using different strategies.

Strategy Type	Bending Modulus (MPa)	Variability (%)
A (Free convection)	378.5 ± 24.6	6.5
B (Hold temperature 4hrs)	395.9 ± 24.7	6.2
C (Hold temperature 10hrs)	430.2 ± 13.3	3.1
D (Hold temperature 15hrs)	548.1 ± 10.9	1.9

6.9 Mann-Whitney analysis

Mann-Whitney is a non-parametric statistical analysis method [86]. This technique was applied to investigate whether the introduced manufacturing processing strategies had significant influence on the mechanical properties throughout the large PEEK bushings. Thus, a decision can be made to validate the observed mechanical properties of the manipulated compression molding processes.

Mann-Whitney outcomes of bending and compression modulus tested at room temperature and elevated temperature are indicated in **Table 6.4**. The analysis showed that holding temperature during the process had no effect on flexure modulus at room temperature, as mentioned previously. However, there were significant changes in the modulus obtained from compression tests at room temperature and elevated temperature as well as flexural tests at elevated temperature. For all those tests, Mann- Whitney outcomes indicated significant modulus changes for top vs bottom bushing processed using free convection cooling, strategy A. Moreover, the analysis revealed a significant increase in modulus by holding temperature at Tc for 15 hours, strategy D, comparing with free convection cooling process performed in strategy A. While holding temperature for 15 hours

introduced null changes for top vs bottom bushing which indicated forming uniform modulus throughout the bushing processed using strategy D. To this end, Mann-Whitney analysis supported the mechanical properties observations in previous sections. These outcomes represented a firm validation for the influence of manipulating compression molding process on the mechanical properties of thick products.

Table 6.4. Mann-Whitney outcomes of Modulus of Elasticity at room temperature (RM) and 225 ºC elevated temperature found from flexural tests and compression tests for bushings processed using strategy A and strategy D. "NO" means Mann-Whitney indicates no changes in modulus, "YES" means Mann-Whitney shows significant changes in modulus.

	Strategy A Top vs Bottom	Strategy D Top vs Bottom	Strategy A vs Strategy D Top Section	Strategy A vs Strategy D Bottom Section
Compression Modulus @ RM	YES	NO	YES	YES
Compression Modulus @ 225 ºC	YES	NO	YES	YES
Bending Modulus @ RM	NO	NO	NO	NO
Bending Modulus @ 225 ºC	YES	NO	YES	YES

7 COMPUTATIONAL ANALYSIS METHODS

In this chapter, experimentally validated Finite Element models for thick compression molding bushing are presented. Those numerical models were developed to simulate the compression molding system and predict the time required for the heating process. Multiple external parameters were manipulated to evaluate the effects of manufacturing imperfection and changing the processing procedures on thermal profile of compression molding system. Thus, highlight the parameters that raise major concern on the compression molding process as well as reveal the optimum processing conditions to produce better products and enhance the production line.

7.1 Developing Finite Element thermal models

Inspired by manufacturing processing of thick bushing, a numerical model was developed to predict the processing time required for heating the polymer to its melting temperature. The proposed model, presented in **Figure 7.1**, consisted of shell on the outside and mandrel on the inside of the mold. The polymer was held between the top and the bottom rings. The gaskets were added between the rings and the polymer which were used to prevent the leak in the actual process.

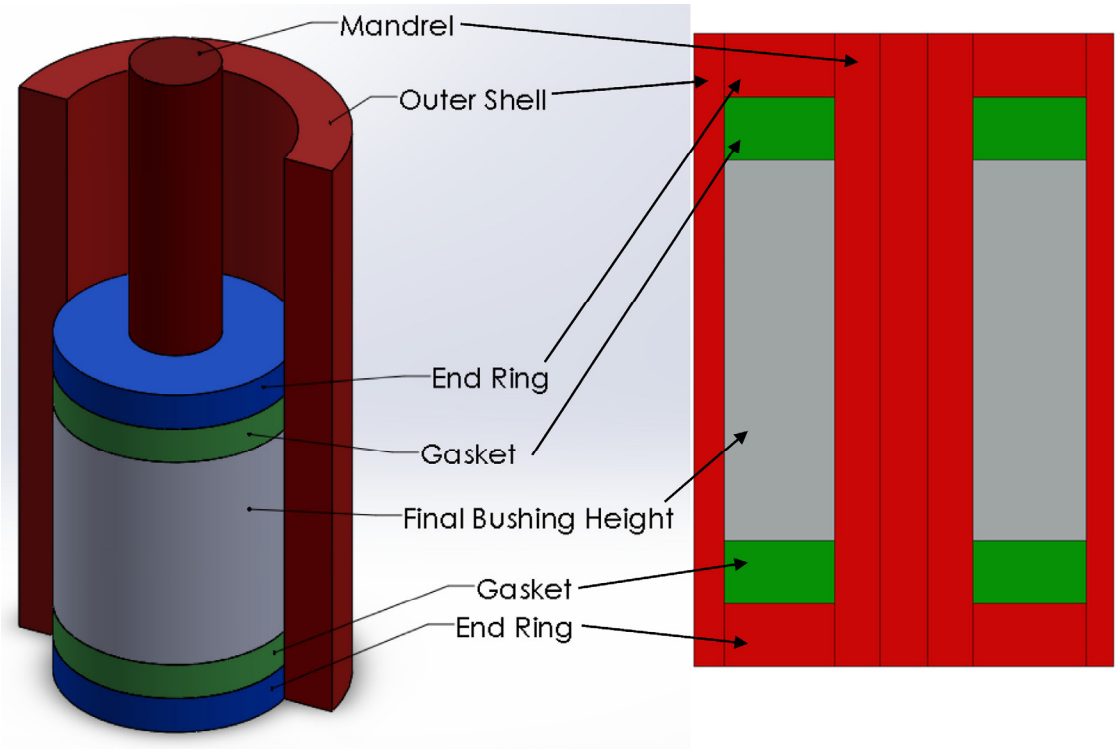

Figure 7.1. Finite Element Analysis model for bushing compression molding system.

The Finite Element Analysis model simulated the actual experimental molding dimensions with 6" polymer final height. The shell dimensions were (OD = 6.625", ID = 5.761", and L=10") while the mandrel dimensions were (OD = 1.5", ID = 0.75", and L=10"). Rings, gaskets and polymer diameters were (OD = 5.761" and ID = 1.5") while their heights were (1", 1", 6") respectively. Shell and mandrel materials used in the system were 304 stainless steel and PTFE respectively. The material properties of the model components are presented in **Table 7.1**.

Table 7.1. Finite Element Analysis model for bushing compression molding system.

	Property	Unit	Shell/Mandrel	Bushing	Gasket
1	Thermal Conductivity (k)	W/m-K	16.2	0.25	0.25
2	Specific heat at constant pressure (cp)	J/kg-K	500	2160	1500
3	Density (ρ)	kg/m3	7999.5	1260	2200

Temperature variation with time and position were the main interest in this model. FEA solution for the transient heat conduction equation [87], presented below, was adopted in this study to provide a spatial distribution over time which can be used to determine the time required for the system to reach steady state at the desired temperatures.

$$\rho C_p \frac{\partial t}{\partial \tau} = \nabla . (k \nabla t)$$

Where

k = Thermal Conductivity (W/m-K).

ρ = Density (kg/m^3).

cp = Specific heat (J/kg-K).

Different boundary conditions were applied on shell outer surface, mandrel inner surface, and end-rings, depending on each model case. The model was run with these boundary conditions:

1- Constant surface temperature: $T|_{x=0,L} = T_c$

2- Perfectly insulated surface (adiabatic surface): $\left.\frac{\partial T}{\partial X}\right|_{x=0,L} = 0$

3- Convective boundary condition: $\left[k\frac{\partial T}{\partial X} + hT\right]_{x=0} = 0$

Heat Transfer coefficient (h) for natural convection heat transfer boundary conditions was calculated based on equation below for laminar flow (Ra < 10^9).

H=Nu*k/L

Where

k = Thermal Conductivity (W/m-K).

L = Surface Length.

For laminar flow Ra $\leq 10^9$,

$$\text{Nu} = \text{Nusselt Number} = 0.68 + \frac{0.670\ \text{Ra}^{1/4}}{[1 + (0.492/\text{Pr})^{9/16}]^{4/9}}$$

Ra = Reynold Number = Pr * Gr

$$\text{Pr} = \text{Prandtl Number} = \frac{\mu\ \text{C}_\text{p}}{\text{k}}$$

μ = Air Viscosity = $1.87*10^5$ N-s/m^2

cp = Specific Heat (J/kg-K).

$$\text{Gr} = \text{Grashof Number} = \frac{\text{L}^3\ \rho^2\ \text{g}\ \Delta\text{T}\ \beta}{\mu^2}$$

ρ = Density (kg/m^3).

g = Acceleration of Gravity = 9.81 (m/s^2)

$\Delta T = T_{surface}-T_{air}$ (C)

β = Expansion Coefficient = 1/ T_f (1/K)

T_f = Film Temperature = $(T_{air} + T_{surface})/2$

7.2 Parametric Study of Numerical Simulation

A numerical heat transfer model was established using ABAQUS 6.12 software. Different boundary conditions were developed to simulate multiple compression molding scenarios. Some boundary conditions were kept same in all cases such as the outer shell surface temperature, Tc = 400 ºC. Insulated boundary at the bottom end-ring outer surface was applied to all models as well because compression molding was resting on an insulated base. The system was initially started at a uniform room temperature (25 ºC).

The main outcomes from simulating this process were to predict the time required for heating the mold to 400 ºC as well as to study the effect of changing the boundary conditions, such as applying heat at mandrel internal surface and having a gap between the ring and the shell caused by manufacturing errors, on final system thermal response. The numerical model results highlighted the parameters that had major effects on the process. Adjusting those boundaries and reducing, or eliminating, the undesired parameters would assist in improving the compression molding thermal behavior. The numerical simulation undertook these parametric studies:

- Heating outer shell to 400 ºC and assigning convection boundary conditions (BC) to the top surface. In this case, mandrel inner surface and mold bottom surface were assumed to be insulated.
- Heating outer shell and inner mandrel surfaces to 400 ºC and applying insulated BC at the bottom mold. Additional BCs were considered to simulate the external effects and the manufacturing errors within the system, which introduced different system behaviors:
  - Convection BC at the top surface.
  - Insulation BC at the top surface.
  - Gap, 0.05” clearance, between end-rings and shell.

- Extended gasket (or pot gasket). Gaskets with thickness 0.05” were added between the end-rings and the shell.

- Heating outer shell and top mold surfaces (simulate convection oven BCs). The mandrel treated as a solid bar in this case, while insulated BC was assigned to the bottom mold.

The boundary conditions of different compression molding system scenarios are summarized in **Table 7.2**.

Table 7.2. The conditions of different Finite Element Analysis case studies of compression molding system.

Case Study	Mold Top Surface	Mandrel Inner Surface
Heating outer shell surface	Convection	Insulation
Heating outer shell surface and inner mandrel surface	Convection	400
Adding insulation at top mold surface	Insulation	400
Convection oven heating conditions	400	Insulation
0.05” clearance gap between end-rings and shell	Convection	400
Extruded gasket in gap between end-rings and shell	Convection	400

8 COMPUTATIONAL ANALYSIS RESULTS AND DISCUSSION

8.1 Time Required for Compression Molding Heating Process

Time required for heating the compression molding system was one of the major concerns that needed to be predicted by numerical simulation models. The main focus was on developing experimentally validated Finite Element Analysis model to estimate the thermal profiles and the time required for heating process which can substitute the expensive experiments. To achieve this target, the lab experimental system conditions, i.e. applying heat on the inside mandrel and the outside shell, were used in the simulation to predict the time required for the system to reach its steady state and compare the numerical and experimental thermal profiles. To this end, top, middle, and bottom heights of bushing inside the compression molding system were considered to cover the thermal profiles of the entire product during the process, as presented in **Figure 8.1**.

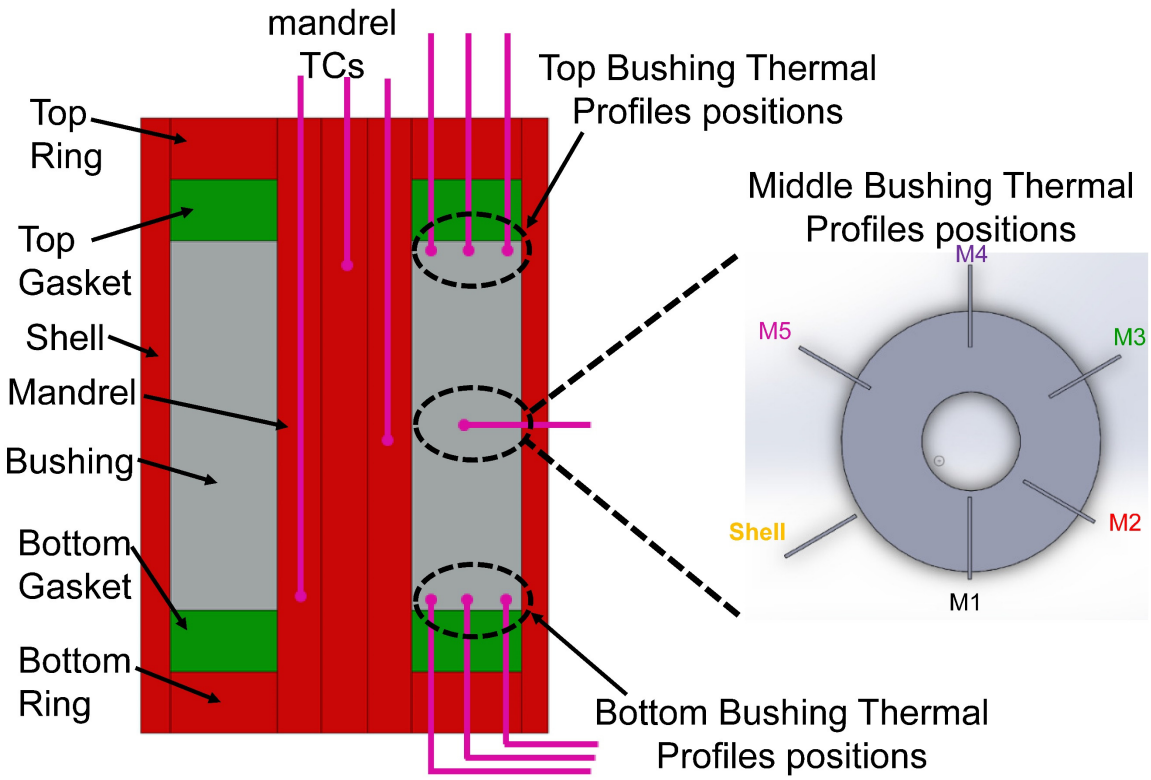

Figure 8.1. Temperature profile locations on numerical model of compression molding system.

The numerical temperature profiles versus the experimental profiles during the molding process were presented in **Figure 8.2**(a)-(c) for top, middle, and bottom bushing heights, respectively. It was noticed that FEA predictions had a good match with the experimental thermal profiles. It is also important to mention that the time required for reaching system steady state for both numerical model and experimental setting was 4 hours. The similarities in thermal profiles and processing time for both FEA and experiments ensure the validation of the numerical model productivity and accuracy.

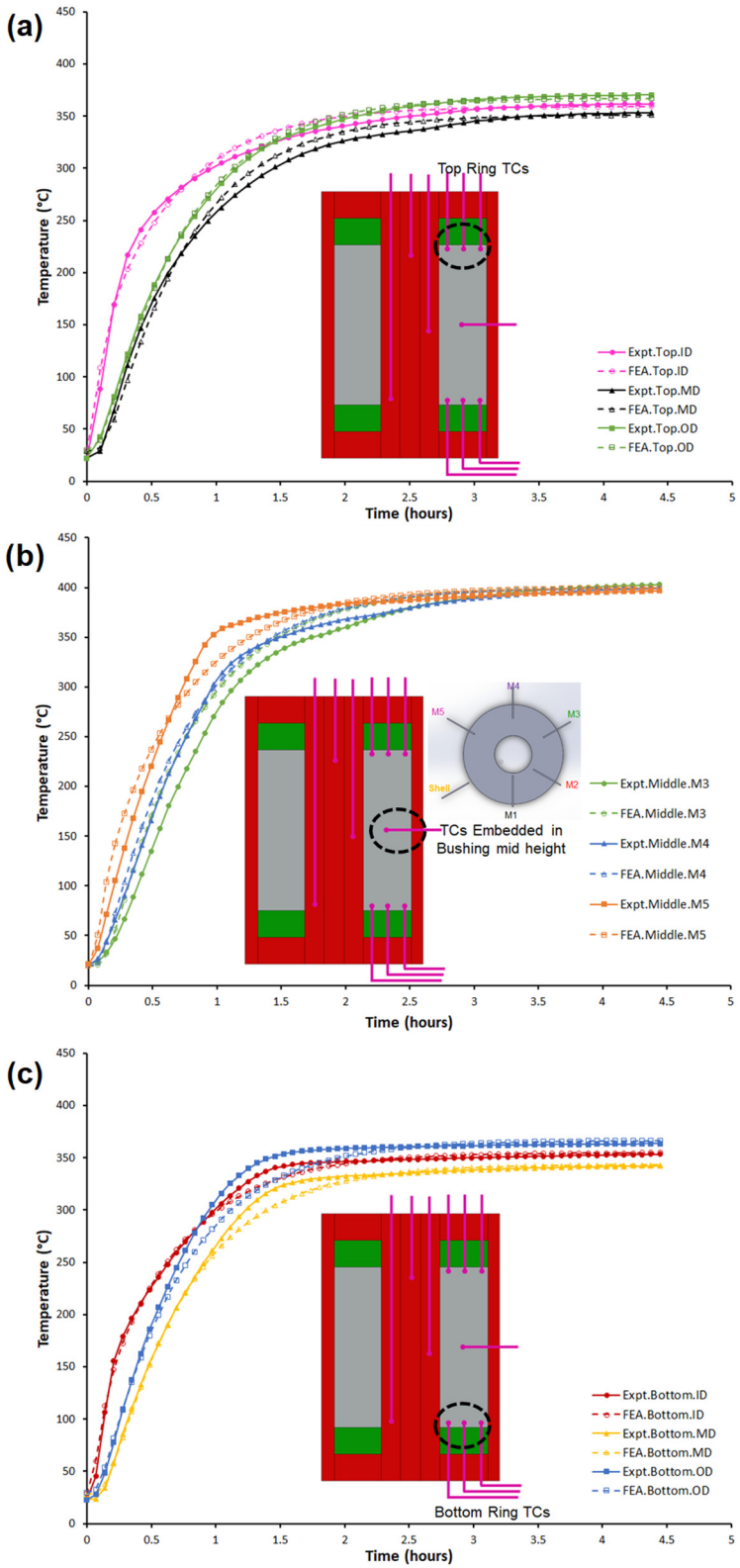

Figure 8.2. Comparing experimental temperature profiles with numerical FEA model profiles throughout (a) top, (b) middle, and (c) bottom bushing heights during compression molding process.

8.2 Influence of Processing and Mold Manufacturing Imperfections (Tooling Quality)

The FEA numerical models were implemented to unravel the external parameters that had significant influence on thermal profile of compression molding. Six scenarios were considered to investigate the effect of changing processing procedure as well as the influence of mold manufacturing imperfection. The boundary conditions of these six cases were presented in details in the previous chapter. Temperature distributions after 5 hours for all different cases of numerical compression molding models are presented in **Figure 8.3**. It was noticed that heating outside shell only, **Figure 8.3**(a), was the slowest case to reach the temperature steady state among other cases because heat was applied on one side only. Considering heating the inner mandrel surface in addition to the outside shell surface, **Figure 8.3**(b-e), helped reaching final steady state faster. It was observed that the polymer mid thickness is the last point to reach steady state in all settings regardless the type of the boundary conditions on the system because the polymer is an insulator. However, the boundary conditions effects appear clearly as we compare the overall time required for reaching steady state at set points of 400 ºC. The case of heating outer shell only reached system steady state after ~ 7 hours, while the case of applying heat at inner and outer system surfaces tended to reach its steady state within ~ 4hours.

Adding insulation at the top mold can reduce the convection effect to the environment as presented in **Figure 8.3**(c); this case showed the fastest system setting to approach its steady state compared with all other settings. Other parameters were introduced to the system in order to investigate their influence on the system thermal behavior such as the gap between the ring and the shell caused by manufacturing errors, see **Figure 8.3**(d). In addition, the effect of having extended gasket between ring and shell, which could happen if the gasket extrudes while pressing the powder, was considered in **Figure 8.3**(e). Gap and extended gasket clearances were assumed

to be 0.05", as explained previously. It was noticed that indicating gap or gasket between the ring and the shell would affect the polymer temperature distributions at the end bushing section. In addition, gap appearance had a higher influence on temperature profile than extended gasket because the gasket's thermal conductivity is higher than air. All previous compression molding cases were based on existing scenarios that could happen during the compression molding process. For instance, it was possible to control the boundary conditions of the compression molding system by using heater bands to apply heat on the outer shell, using cartridge to apply heat on the inner surface of the mandrel, and using insulations to accrue insulated boundary conditions within the system. However, traditional compression molding process, used in industry applications, was different from instrumented lab setting. The traditional process used convection oven which made it difficult to control the system boundary conditions. The convection oven setting was simulated and presented in **Figure 8.3**(f). In this numerical model, the heat was applied at the outer and the top mold surfaces only while the bottom surface was assumed to be insulated and the mandrel was simulated as a solid bar, i.e. no hole for cartridge. From the system temperature distributions, it was noticed that the heat penetrates through mandrel, top ring, and shell because they have high thermal conductivity. It was expected that temperature distributions of convection oven case could be similar to the lab setting with heating outside shell only; however, in the convection oven situation, mandrel played a significant role in conducting heat from its top surface to polymer bushing which made the system acquire different thermal behavior compared with all other lab setting scenarios. It is important to mention that the lab setting with top insulation, presented in **Figure 8.3**(c), was the better than the traditional industry method with convection oven because it was the fastest case to heat and approach system steady state. Thus, the local heating applied on the inside mandrel and outside shell of compression molding system accompanied with a good

insulation considered as best processing method compared with the traditional industry method which uses convection oven. This preference is attributed to reducing the heating time and approaching steady state everywhere throughout the system without introducing lower temperature spots in the modified heating method. It is important to mention that indicating any lower temperature area in the compression molding system can assist in driving thermal gradient throughout the molded polymer, and subsequently trigger the crystallinity and property variation throughout the produced product.

The results found from the numerical simulation established strong foundation to assist in designing and building lab compression molding system as well as provided an idea about the temperature profile differences between lab setting vs. traditional method of compression molding process. Those models predicted time required for heating the lab compression molding system to its melting temperature at different boundary conditions. In addition, it provided an overview about the effect of different external parameters and manufacturing errors on thermal system behavior. As the numerical models' results are validated experimentally, those models can substitute the expensive experimental setting required to estimate the processing time of compression molded polymers. This can enhance the industry to proceed with compression molding processing method for various thick high performance polymers applications.

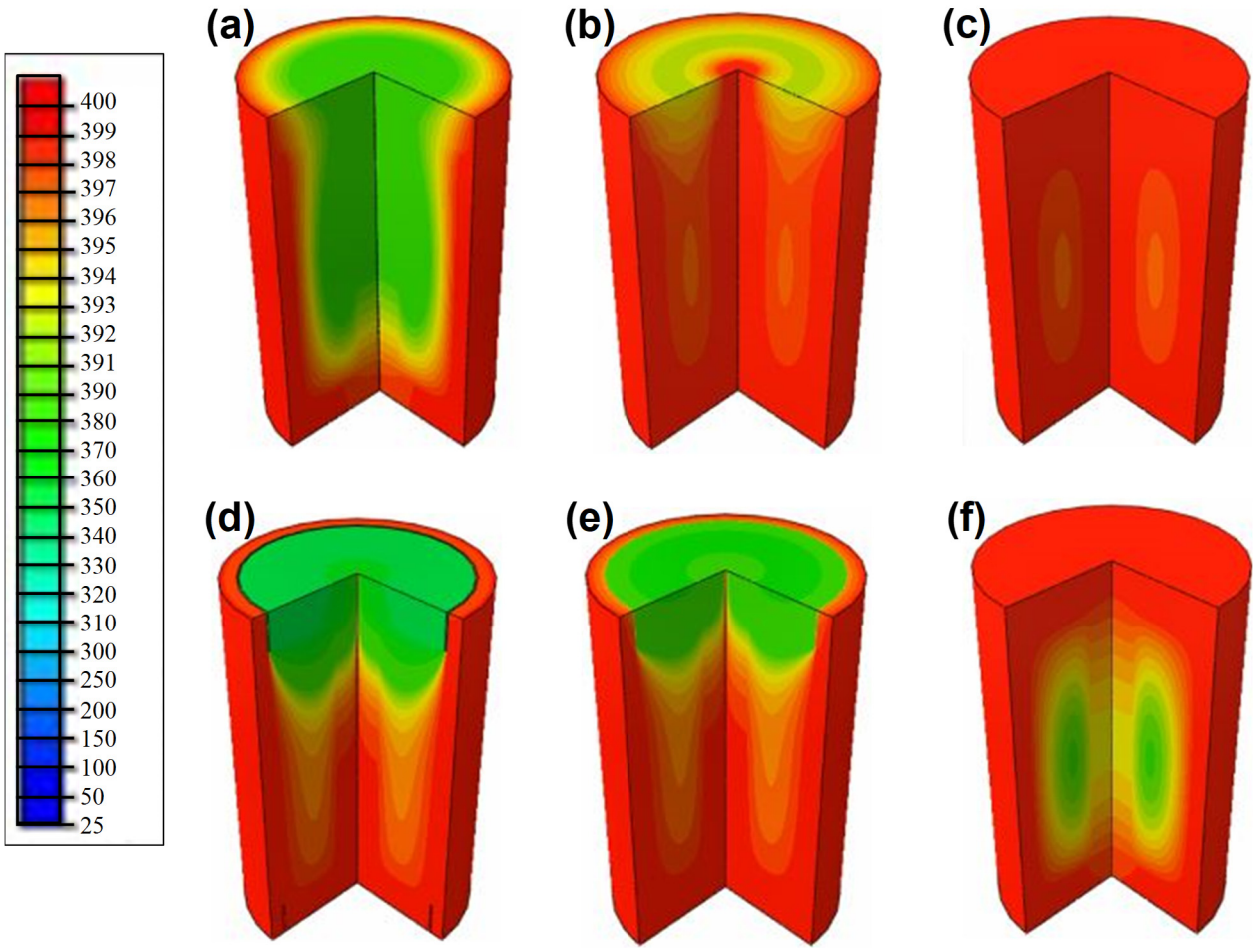

Figure 8.3. Temperature distributions after 5 hours for different cases of numerical compression molding models. (a) Heating outer shell to 400 ºC. (b-e) Heating outer shell and inner mandrel to 400 ºC with (b) Top convection surface, (c) Top insulated surface, (d) 1.27 mm gap between end-rings and shell, (e) extended gasket between end-rings and shell. (f) Heating outer shell and mold top surface with sold mandrel (simulate convection oven).

9 SUMMARY AND FUTURE WORK

9.1 Summary of Research

This research has probed manipulating thick, advanced performance polymers processed in an instrumented compression mold set with embedded thermocouples driven by a thermal control system. A combined experiment-modeling approach was used to optimize the design and the processing procedures. In this study, the pros and cons for adjusting external processing parameters were investigated. More importantly, the thick wall and long compression molded PEEK and CF/PEEK parts have been studied for the first time. Thermal profiles throughout the thick parts during the entire high pressure and high temperature process (HPHT) were investigated which can set a platform to study the tradeoffs between traditional molding process and manipulated process on temperature distributions throughout the produced parts and how that can drive the final product's morphology and properties. It was observed that adding carbon fibers to PEEK polymer assisted in accelerating the compression molding process and enhanced temperature distribution throughout the processed bushing.

This research introduces, for the first time, a novel "hybrid sealing" method for high pressure and high temperature processes. The novel hybrid seal consists of two layers of steel filled polytetrafluoroethylene PTFE composite with a sand layer sandwiched between them. This critical concept ensures providing the escape path for the air trapped inside the processed material. At the same time, the introduced novel HPHT hybrid sealing method prevents all leaking issues associated with the process caused by limited seal function, high applied pressure during the process, manufacturing imperfection, and other related factors. With this sealing method, higher pressure can be applied during the process to ensure eliminating all voids and trapped air inside

the produced parts. In addition, this new method can reduce seal cost by more than 80%. Thus, it can provide a huge shift in compression molding processing field.

The recent efforts to develop a comprehensive basis for understanding behavior of thick neat PEEK and CF/PEEK composites was addressed in this work. The importance of this potential new field of technology is dramatically growing as a result of the challenges imposed by rising the demand for advanced performance materials that have the ability to resist harsh environments. When thermal, pressure and corrosive conditions move to the extreme zones, polymer structure performance become problematic. Thus, involving advanced performance polymers in those applications was demanded. Polyaryletherketone (PAEK) polymers, specifically polyetheretherketone (PEEK) type, are the most popular and rapidly growing material for many applications in extremely harsh environments because they have desirable features such as low chemical reactivity, high modulus, high glass transition temperature, high corrosion resistance for caustic and acidic environments, and high crystalline melting temperature. However, most of the extreme applications require high performance polymer parts with thick wall and extended length. Producing such products is challenging because their semi-crystalline nature triggers property variation throughout the products. Thus, the overall performance and durability of resultant parts drop dramatically and become huge concern from engineering design and risk managements perspectives. As a first step towards developing those products and enhancing their service life, it is crucial to understand the fundamental mechanisms that cause the properties deterioration in those materials.

The current dissertation discussed the mechanisms associated with compromising the mechanical properties and the factors contributing to failure of thick long advance performance thermoplastics and composite products. In both neat PEEK and CF/PEEK, holding temperature at

crystallization provided the opportunity for material to develop its crystal structure to the maximum limit. After that, it became harder for the material to form more crystal structure. Instead, the material worked on adjusting the imperfection in their structure. Therefore, there was no huge influence on increasing crystallinity percentage by holding temperature at crystallization for further time; but there were improvements in crystallization variability ranges and the mechanical properties. These responses were clearly detected in neat PEEK over CF/PEEK because CF effect and interfacial areas influence were dominant over polymer structure matrix during mechanical tests. In addition, variabilities of free convection cooling for CF/PEEK bushing was already better than neat PEEK as a result of the CF effect in enhancing crystallization. Thus, involving CF minimized the processing time and influenced crystallinity distribution along traditional free convection cooling bushing by maximizing surface area and enhancing crystal structure formation. Holding temperature at crystallization for sufficient time during the process benefits thick products produced from neat polymer more than thick composite parts.

Multiple techniques were investigated in this study to evaluate the influence of manipulating the processing methodologies on material morphology distribution throughout thick and long products. DSC measurements highlighted enhancing crystallinity uniformity throughout thick parts by manipulating the manufacturing processes. However, it didn't distinguish an obvious increase in crystal structure formation after holding temperature at crystallization. While, WAXS technique was able to exhibit the crystalline structures improvement and evaluate their uniformity by comparing the patterns along bushing for different processes.

Moreover, POM microstructure images of both neat PEEK and CF/PEEK composites crystal structures supported DSC and WAXS results. All observations indicated that using the step

of holding temperature for sufficient time ensure the formation of uniform crystal structure throughout the bushing.

Although POM images of CF/PEEK provided evidence of disappearing spherulite crystal structure in the polymer composite bushing processed using the traditional free convection cooling method, DSC results exhibited some crystallinity percentages in the composite processed using this method. Two scenarios played significant role in forming CF/PEEK morphology during traditional convection cooling process of thick wall parts. On one hand, the main CF role in maximizing the surface area which assists in forming more crystal structure. On the other hand, the fact that CF minimized time required for cooling by enhancing material thermal conductivity and accelerating heat lost which could limit crystallization process. The outcomes of balancing those factors influenced the composite morphology behavior through initiating uniform crystal structures that were too small to be seen under POM. However, holding temperature at crystallization for sufficient time assisted in growing those crystal structure to become visible under microscope.

Polymer mechanical properties at room temperature and elevated temperature were investigated using Dynamic Mechanical Analysis DMA, compression, and 3-point bending tests. It was observed that controlling polymer process by holding temperature at crystallization for sufficient time influenced thick polymer morphology, and subsequently altered the product mechanical properties.

DMA technique was used to evaluate the effects of adjusting the compression molding processing procedure on polymer structure distribution and storage modulus along thick parts for various temperature range between 30 °C – 300 °C. The high sensitivity of this technique revealed the influence of holding temperature for 4 hours on producing uniform modulus throughout thick

part. The 4 hours hold assisted in enhancing the crystal structure within the sections that had lack in crystallinity; however, it introduced more than one crystal structure because the holding time was not enough to fully build the secondary crystal structure to become similar to primary structure. Increasing holding time assisted in developing the secondary structure to become similar to the primary structure, as exhibited by the DMA results. By advantage of higher crystal structure content obtained by holding temperature for sufficient time, material was able to retain higher storage modulus at elevated temperature compared with other strategies.

Compression and 3-point bending tests were used to explore compression modulus and bending modulus at room temperature and elevated temperature. It was concluded that four hours was the minimum time required for approaching a uniform compression modulus throughout the bushing. While 15 hours hold was the optimum time to increase the average modulus throughout the bushing. Moreover, flexural results for all processing strategies displayed minimal effects on bending modulus at room temperature. However, a noticeable increase in bending modulus was observed by holding at T_c when the samples were tested at 225ºC elevated temperature.

Although morphological images reflected huge changes in CF/PEEK structure formation obtained as a result of holding temperature for sufficient time, it was interesting to find out that those morphological changes had no effect on the modulus behavior of the material at room temperature and elevated temperature. This behavior was attributed to the CF interfacial area with the matrix which was dominant over polymer structure morphology manipulation effect. Thus, the composite compression behavior was monitored by CF influence rather than polymer matrix morphology.

This dissertation described reliable methods for developing numerical simulation models to predict the time required for compression molding heating process as well as simulate the

external parameters effects on thermal profile of compression molding process. The results found from the numerical FEA models established strong foundation for designing and building lab compression molding system. In addition, the models developed in this study provided an idea about the compression molding temperature profile differences between lab setting vs. traditional processing methods. Those models predicted time required for heating the lab compression molding system to its melting temperature using different boundary conditions. Moreover, it provided an overview about the influence of different external parameters and manufacturing errors on thermal system behavior. It was found that the predicted time required for heating the FEA compression molding system agreed with the experimental finding which validated the numerical models. Because the numerical results were confirmed experimentally, those models could substitute the expensive experimental setting required to estimate the processing time of various compression molded polymers. This can enhance the industry to proceed with compression molding processing method for various thick high performance polymers applications.

This work disclosed the dependence of the morphology and the mechanical properties of the thick parts on compression molding processing procedure and presented a protocol to identify that. Multiple processing strategies were applied to probe how altering the compression molding process can influence the microstructure and the properties of neat PEEK and CF/PEEK composites.

9.2 Concluding Remarks and Future Works

Manipulating the compression molding process of thick wall and tall advanced performance polymer (neat and composites) to enhance morphology and properties distributions throughout those products were investigated for the first time in this dissertation. This work is critical for potential future applications of high performance polymers and composites in aerospace, biomedical, and harsh environments.

The outcomes of this study revealed the optimum manufacturing processing procedures to manipulate thick polymer parts and produce products with uniform and enhanced properties. The studies conducted in this dissertation provide the groundwork for fundamental understanding on the effect of manipulating the compression molding process on thick wall and tall PEEK and CF/PEEK products.

To this end, there still be great scope for further investigations to be done in the following areas:

1- Reinforcement of other fillers such as glass fibers GF, polybenzimidazole PBI, and carbon nanotubes CNT towards PEEK polymer need to be considered to demonstrate the influence of those fillers on crystallinity and mechanical properties distribution throughout thick parts.

2- Various thick polyaryletherketone PAEK polymers family such as PEK and PEKK types are of interest to be investigated with and without fillers.

3- Different thick wall and tall polymers and composites products, such as polypropylene PP (isotactic polypropylene and syndiotactic polypropylene), are recommended to be explored under various processing conditions.

4- Thick wall and tall parts of neat PEEK and PEEK composites investigations will be directed to evaluate internal stresses in these products.
5- Developing the current numerical models to consider the cooling process and involving the crystal structure formation is highly recommended.
6- Influence of other manufacturing processing methods such as transfer molding on the structure-properties behavior of thick parts need to be explored. Manipulating those processes and set new protocols can assist in producing better parts and enhancing the production line of the thick wall and tall advanced performance polymer products.

The current study cannot cover all available materials as well as the factors that may impact their processing procedure and thus their field lifetimes. Research correlated with other polymers and composites as well as the influence of the additional factors will be left for future investigations.

REFERENCES

1. Denault, J. and M. Dumouchel, *Consolidation Process of PEEK/Carbon Composite for Aerospace Applications.* Advanced Performance Materials, 1998. **5**(1): p. 83-96.
2. Shekar, R.I., et al., *Properties of high modulus PEEK yarns for aerospace applications.* Journal of Applied Polymer Science, 2009. **112**(4): p. 2497-2510.
3. Mangalgiri, P., *Composite materials for aerospace applications.* Bulletin of Materials Science, 1999. **22**(3): p. 657-664.
4. Soutis, C., *Fibre reinforced composites in aircraft construction.* Progress in Aerospace Sciences, 2005. **41**(2): p. 143-151.
5. Grujicic, M., et al., *Structural-response analysis, fatigue-life prediction, and material selection for 1 MW horizontal-axis wind-turbine blades.* Journal of materials engineering and performance, 2010. **19**(6): p. 790-801.
6. Nijssen, R.P.L., *Fatigue life prediction and strength degradation of wind turbine rotor blade composites.* 2006.
7. Mahieux, C., *Cost effective manufacturing process of thermoplastic matrix composites for the traditional industry: the example of a carbon-fiber reinforced thermoplastic flywheel.* Composite structures, 2001. **52**(3): p. 517-521.
8. Dowson, P., M.S. Walker, and A.P. Watson, *Development of abradable and rub-tolerant seal materials for application in centrifugal compressors and steam turbines.* Sealing Technology, 2004. **2004**(12): p. 5-10.
9. Murari, A. and A. Barzon, *Comparison of new PEEK® seals with traditional helicoflex for ultra high vacuum applications.* Vacuum, 2003. **72**(3): p. 327-334.

10. Koike, H., et al., *Self-lubrication of PEEK polymer bearings in rolling contact fatigue under radial loads.* Tribology International, 2012. **49**: p. 30-38.

11. Boccaccini, A., et al., *Electrophoretic deposition of polyetheretherketone (PEEK) and PEEK/Bioglass® coatings on NiTi shape memory alloy wires.* Journal of materials science, 2006. **41**(24): p. 8152-8159.

12. Normand, B., et al., *Electrochemical impedance spectroscopy and dielectric properties of polymer: application to PEEK thermally sprayed coating.* Electrochimica acta, 2004. **49**(17): p. 2981-2986.

13. Kurtz, S.M. and J.N. Devine, *PEEK biomaterials in trauma, orthopedic, and spinal implants.* Biomaterials, 2007. **28**(32): p. 4845-4869.

14. Bakar, M.A., et al., *Tensile properties, tension–tension fatigue and biological response of polyetheretherketone–hydroxyapatite composites for load-bearing orthopedic implants.* Biomaterials, 2003. **24**(13): p. 2245-2250.

15. Barkarmo, S., et al., *Nano-hydroxyapatite-coated PEEK implants: A pilot study in rabbit bone.* Journal of Biomedical Materials Research Part A, 2013. **101**(2): p. 465-471.

16. Macuvele, D.L.P., et al., *Advances in ultra high molecular weight polyethylene/hydroxyapatite composites for biomedical applications: A brief review.* Materials Science and Engineering: C, 2017.

17. van Rijswijk, K., *Thermoplastic composite wind turbine blades: vacuum infusion technology for anionic polyamide-6 composites.* 2007.

18. Xin, H., D. Shepherd, and K. Dearn, *Strength of poly-ether-ether-ketone: Effects of sterilisation and thermal ageing.* Polymer Testing, 2013. **32**(6): p. 1001-1005.

19. Blundell, D. and B. Osborn, *The morphology of poly (aryl-ether-ether-ketone).* Polymer, 1983. **24**(8): p. 953-958.

20. Rae, P., E. Brown, and E. Orler, *The mechanical properties of poly (ether-ether-ketone)(PEEK) with emphasis on the large compressive strain response.* Polymer, 2007. **48**(2): p. 598-615.

21. Chivers, R. and D. Moore, *The effect of molecular weight and crystallinity on the mechanical properties of injection moulded poly (aryl-ether-ether-ketone) resin.* Polymer, 1994. **35**(1): p. 110-116.

22. El-Qoubaa, Z. and R. Othman, *Strain rate sensitivity of polyetheretherketone's compressive yield stress at low and high temperatures.* Mechanics of Materials, 2016. **95**: p. 15-27.

23. Bas, C., P. Battesti, and N. Alberola, *Crystallization and melting behaviors of poly (aryletheretherketone)(PEEK) on origin of double melting peaks.* Journal of applied polymer science, 1994. **53**(13): p. 1745-1757.

24. Incardona, S., et al., *Crystallization in J-1 polymer/carbon-fibre composites: bulk and interface processes.* Journal of materials science, 1993. **28**(18): p. 4983-4987.

25. Waddon, A., et al., *On the crystal texture of linear polyaryls (PEEK, PEK and PPS).* Journal of Materials Science, 1987. **22**(5): p. 1773-1784.

26. Fougnies, C., et al., *Morphological study and melting behavior of narrow molecular weight fractions of poly (aryl ether ether ketone)(PEEK) annealed from the glassy state.* Macromolecules, 1998. **31**(18): p. 6266-6274.

27. Mathot, V. and M. Pijpers, *Molecular structure, melting behavior, and crystallinity of 1-octene-based very low density polyethylenes (VLDPEs) as studied by fractionation and*

heat capacity measurements with DSC. Journal of applied polymer science, 1990. **39**(4): p. 979-994.

28. Krüger, K. and H. Zachmann, *Investigation of the melting behavior of poly (aryl ether ketones) by simultaneous measurements of SAXS and WAXS employing synchrotron radiation.* Macromolecules, 1993. **26**(19): p. 5202-5208.

29. Tseng, J.-W., et al., *Screw extrusion-based additive manufacturing of PEEK.* Materials & Design, 2018. **140**: p. 209-221.

30. Jia, J. and D. Raabe, *Crystallinity and Crystallographic Texture in Isotactic Polypropylene during Deformation and Heating.* arXiv preprint arXiv:0811.2412, 2008.

31. Liu, P., et al., *Influence of trace amount of well-dispersed carbon nanotubes on structural development and tensile properties of polypropylene.* Macromolecules, 2013. **46**(2): p. 463-473.

32. Liu, P., et al., *Hygrothermal behavior of polybenzimidazole.* Polymer, 2016. **93**: p. 88-98.

33. Jonas, A. and R. Legras, *Relation between PEEK semicrystalline morphology and its subglass relaxations and glass transition.* Macromolecules, 1993. **26**(4): p. 813-824.

34. Jonas, A.M., T.P. Russell, and D.Y. Yoon, *Synchrotron x-ray scattering studies of crystallization of poly (ether-ether-ketone) from the glass and structural changes during subsequent heating-cooling processes.* Macromolecules, 1995. **28**(25): p. 8491-8503.

35. Rueda, D., et al., *Crystallization kinetics and polymorphism in aromatic polyketones (PEKEKK) with different molecular weight.* Macromolecules, 1998. **31**(23): p. 8201-8208.

36. White, K., H.-J. Sue, and T. Bremner, *Rheological characterization and differentiation in PAEK materials*. 2011.

37. White, K.L., et al., *Rheological and thermal behaviors of commercial poly (aryletherketone) s.* Polymer Engineering & Science, 2013. **53**(3): p. 651-661.

38. Rueda, D., et al., *Aromatic polymers obtained by precipitation polycondensation. 3. Thermal behavior and microstructure of PEKEKK particles.* Macromolecules, 1996. **29**(22): p. 7016-7021.

39. Zolotukhin, M., et al., *Aromatic polymers obtained by precipitation polycondensation: 4. Synthesis of poly (ether ketone ketone) s.* Polymer, 1997. **38**(6): p. 1471-1476.

40. Hay, J., J. Langford, and J. Lloyd, *Variation in unit cell parameters of aromatic polymers with crystallization temperature.* Polymer, 1989. **30**(3): p. 489-493.

41. Velisaris, C.N. and J.C. Seferis, *CRYSTALLIZATION KINETICS OF POLYETHERETHERKETONE (PEEK) MATRICES.* Polymer Engineering and Science, 1986. **26**(22): p. 1574-1581.

42. Day, M., et al., *EFFECT OF MOLECULAR-WEIGHT ON THE CRYSTALLIZATION BEHAVIOR OF POLY(ARYL ETHER ETHER KETONE) - A DIFFERENTIAL SCANNING CALORIMETRY STUDY.* Polymer, 1991. **32**(7): p. 1258-1266.

43. Jonas, A. and R. Legras, *THERMAL-STABILITY AND CRYSTALLIZATION OF POLY(ARYL ETHER ETHER KETONE).* Polymer, 1991. **32**(15): p. 2691-2706.

44. MedellinRodriguez, F.J. and P.J. Phillips, *Bulk crystallization of poly(aryl ether ether ketone) (PEEK).* Polymer Engineering and Science, 1996. **36**(5): p. 703-712.

45. Chen, M. and J.Y. Chen, *Analysis of crystallization kinetics of poly(ether ether ketone).* Journal of Polymer Science Part B-Polymer Physics, 1998. **36**(8): p. 1335-1348.

46. Kemmish, D., *Update on the Technology and Applications of Polyaryletherketones: Manufacturing and Polymerisation Chemistry; 2 Characterisation; 3 Properties and*

Processing of Unfilled Polyaryletherketones; 4 Product Forms; 5 Competitive Materials; 6 Polyaryletherketone Blends; 7 Applications of Polyaryletherketones; 8 Medical Grades and their Applications; Abbreviations; Appendix; Index. 2010: ISmithers Rapra Pub.

47. Tung, C. and P. Dynes, *Morphological characterization of polyetheretherketone–carbon fiber composites.* Journal of applied polymer science, 1987. **33**(2): p. 505-520.

48. Jin, L., et al., *Crystallization behavior and morphological characterization of poly (ether ether ketone).* Polymer, 2014. **55**(20): p. 5255-5265.

49. Kumar, S., D.P. Anderson, and W.W. Adams, *Crystallization and morphology of poly (aryl-ether-ether-ketone).* Polymer, 1986. **27**(3): p. 329-336.

50. Bassett, D., R. Olley, and I. Al Raheil, *On crystallization phenomena in PEEK.* Polymer, 1988. **29**(10): p. 1745-1754.

51. Cebe, P., et al., *Wide-angle x-ray scattering study of heat-treated peek and peek composite.* Journal of Applied Polymer Science, 1987. **34**(6): p. 2273-2283.

52. Hsiao, B.S., et al., *Time-resolved X-ray study of poly (aryl ether ether ketone) crystallization and melting behaviour: 2. Melting.* Polymer, 1993. **34**(19): p. 3996-4003.

53. Marand, H., et al., *Influence of structural and topological constraints on the crystallization and melting behavior of polymers. 2. Poly (arylene ether ether ketone).* Macromolecules, 2000. **33**(9): p. 3392-3403.

54. Lee, Y. and R.S. Porter, *Double-melting behavior of poly (ether ether ketone).* Macromolecules, 1987. **20**(6): p. 1336-1341.

55. Hutchinson, J.M., *Physical aging of polymers.* Progress in Polymer Science, 1995. **20**(4): p. 703-760.

56. Huo, P. and P. Cebe, *Temperature-dependent relaxation of the crystal-amorphous interphase in poly (ether ether ketone).* Macromolecules, 1992. **25**(2): p. 902-909.

57. Holdsworth, P. and A. Turner-Jones, *The melting behaviour of heat crystallized poly (ethylene terephthalate).* Polymer, 1971. **12**(3): p. 195-208.

58. Cheng, S.Z., M. Cao, and B. Wunderlich, *Glass transition and melting behavior of poly (oxy-1, 4-phenyleneoxy-1, 4-phenylenecarbonyl-1, 4-phenylene)(PEEK).* Macromolecules, 1986. **19**(7): p. 1868-1876.

59. Jonas, A. and R. Legras, *Thermal stability and crystallization of poly (aryl ether ether ketone).* Polymer, 1991. **32**(15): p. 2691-2706.

60. Ostberg, G.M. and J.C. Seferis, *Annealing effects on the crystallinity of polyetheretherketone (PEEK) and its carbon fiber composite.* Journal of Applied Polymer Science, 1987. **33**(1): p. 29-39.

61. Wu, Z., et al., *Effect of thermal history on crystallization behavior of polyetheretherketone studied by differential scanning calorimetry.* Macromolecular Materials and Engineering, 1988. **164**(1): p. 21-34.

62. Arzak, A., J. Eguiazabal, and J. Nazabal, *Effect of annealing on the properties of poly (ether ether ketone).* Polymer Engineering & Science, 1991. **31**(8): p. 586-591.

63. Stolov, A.A., et al. *Effects of sterilization methods on key properties of specialty optical fibers used in medical devices*. in *Proc. SPIE*. 2013.

64. Gao, S.-L. and J.-K. Kim, *Cooling rate influences in carbon fibre/PEEK composites. Part 1. Crystallinity and interface adhesion.* Composites Part A: Applied science and manufacturing, 2000. **31**(6): p. 517-530.

65. Lustiger, A., F. Uralil, and G. Newaz, *Processing and structural optimization of PEEK composites.* Polymer composites, 1990. **11**(1): p. 65-75.

66. Ma, P.-C., et al., *Dispersion and functionalization of carbon nanotubes for polymer-based nanocomposites: A review.* Composites Part a-Applied Science and Manufacturing, 2010. **41**(10): p. 1345-1367.

67. Deng, F., T. Ogasawara, and N. Takeda, *Evaluating the orientation and dispersion of carbon nanotubes inside nanocomposites by a focused-ion-beam technique.* Materials Letters, 2007. **61**(29): p. 5095-5097.

68. Kumar, R., *Manufacturing of High Performance Polymer Nanocomposites Containing Carbon Nanotubes And Carbon Nanofibers Using Ultrasound Assisted Extrusion Process*. 2010, University of Akron.

69. Lee, G.-W., et al., *Carbon nanotube dispersion and exfoliation in polypropylene and structure and properties of the resulting composites.* Polymer, 2008. **49**(7): p. 1831-1840.

70. Bhattacharyya, A.R., et al., *Crystallization and orientation studies in polypropylene/single wall carbon nanotube composite.* Polymer, 2003. **44**(8): p. 2373-2377.

71. Li, L., et al., *Structure and crystallization behavior of Nylon 66/multi-walled carbon nanotube nanocomposites at low carbon nanotube contents.* Polymer, 2007. **48**(12): p. 3452-3460.

72. Jin, J., M. Song, and F. Pan, *A DSC study of effect of carbon nanotubes on crystallisation behaviour of poly(ethylene oxide).* Thermochimica Acta, 2007. **456**(1): p. 25-31.

73. Diez-Pascual, A.M., et al., *The influence of a compatibilizer on the thermal and dynamic mechanical properties of PEEK/carbon nanotube composites.* Nanotechnology, 2009. **20**(31).

74. Dobreva, A. and I. Gutzow, *ACTIVITY OF SUBSTRATES IN THE CATALYZED NUCLEATION OF GLASS-FORMING MELTS .1. THEORY.* Journal of Non-Crystalline Solids, 1993. **162**(1-2): p. 1-12.

75. Dobreva, A. and I. Gutzow, *ACTIVITY OF SUBSTRATES IN THE CATALYZED NUCLEATION OF GLASS-FORMING MELTS .2. EXPERIMENTAL-EVIDENCE.* Journal of Non-Crystalline Solids, 1993. **162**(1-2): p. 13-25.

76. Knör, N., R. Walter, and F. Haupert, *Mechanical and thermal properties of nano-titanium dioxide-reinforced polyetheretherketone produced by optimized twin screw extrusion.* Journal of Thermoplastic Composite Materials, 2011. **24**(2): p. 185-205.

77. Hsiung, C.M., M. Cakmak, and J.L. White, *Crystallization phenomena in the injection molding of poly ether ether ketone and its influence on mechanical properties.* Polymer Engineering & Science, 1990. **30**(16): p. 967-980.

78. Howell, D.D. and S. Fukumoto, *Compression molding of long chopped fiber thermoplastic composites.* CAMX, October, 2014.

79. Capone, C., et al., *Thermal and mechanical degradation during polymer extrusion processing.* Polymer Engineering & Science, 2007. **47**(11): p. 1813-1819.

80. Vlachopoulos, J. and D. Strutt, *Polymer processing.* Materials science and technology, 2003. **19**(9): p. 1161-1169.

81. IMIHEZRI, S., S. SAPUAN, and E. ZAINUDDIN, *A review of the effect of moulding parameters on the performance of polymeric composite injection moulding.* Turkish Journal of Engineering and Environmental Sciences, 2006. **30**(1): p. 23-34.

82. Blundell, D., *On the interpretation of multiple melting peaks in poly (ether ether ketone).* Polymer, 1987. **28**(13): p. 2248-2251.

83. Shen, S.B. and H. Ishida, *Dynamic mechanical and thermal characterization of high-performance polybenzoxazines.* Journal of Polymer Science Part B: Polymer Physics, 1999. **37**(23): p. 3257-3268.

84. Krishnaswamy, R. and D. Kalika, *Dynamic mechanical relaxation properties of poly (ether ether ketone).* Polymer, 1994. **35**(6): p. 1157-1165.

85. Liu, P., *Influence of Solid Inclusion Phase on the Mechanical Behavior of Thermoplastic Polymer Composite and Blend*. 2016, Texas A & M University.

86. Hart, A., *Mann-Whitney test is not just a test of medians: differences in spread can be important.* BMJ: British Medical Journal, 2001. **323**(7309): p. 391.

87. Holman, J., *Heat Transfer. 10th*. 2010, Boston, MASS. McGraw-Hill.